TECHNISCHE UNIVERSITÄT MÜNCHEN

Fakultät für Medizin

Institut für Allgemeine Pathologie
und Pathologische Anatomie

(Direktor: Prof. Dr. W. Weichert)

Characterization of Pancreatic Stellate Cells in Pancreatic Ductal Adenocarcinoma and Cases of Chronic Pancreatitis of Various Etiologies

Lena Julia Häberle

Vollständiger Abdruck der von der Fakultät für Medizin der Technischen Universität München zur Erlangung des akademischen Grades eines Doktors der Medizin genehmigten Dissertation.

Vorsitzender: Prof. Dr. Ernst J. Rummeny
Prüfer der Dissertation: 1. Prof. Dr. Irene Esposito
                            2. Prof. Dr. Bernhard Holzmann

Die Dissertation wurde am 12.12.2016 bei der Technischen Universität München eingereicht und durch die Fakultät für Medizin am 08.11.2017 angenommen.

Index

1 Abbreviations

α-CB	α-Crystallin B
α-SMA	α-Smooth muscle actin
5-FU	5-Fluoruracil
AIP	Autoimmune pancreatitis
AIP1	Autoimmune pancreatitis type 1
AIP2	Autoimmune pancreatitis type 2
APC	Adenomatous polyposis coli
APS	Ammonium persulfate
ASI	Activated stroma index
BCA	Bicinchoninic acid
BDNF	Brain-derived neurotrophic factor
BRCA1	Breast cancer 1, early onset
BRCA2	Breast cancer 2, early onset
BSA	Bovine serum albumin
CCK-A	Cholecystokinin A
CD34	Cluster of differentiation 34
CD4	Cluster of differentiation 4
CD56	Cluster of differentiation 56
CFTR	Cystic fibrosis transmembrane conductance regulator
CP	Chronic pancreatitis
CT	Computed tomography
Da	Dalton (1 Dalton = 1 g/mol)
DAB	Diaminobenzidine
DMEM	Complete Dulbecco's Modified Eagle's Medium
DMSO	Dimethyl sulfoxide
DNA	Deoxyribonucleic acid
ECM	Extracellular matrix
EDTA	Ethylenediaminetetraacetic acid
EGTA	Ethylene glycol-bis(β-aminoethyl ether)-N,N,N',N'-tetraacetic acid
EMT	Epithelial-mesenchymal transition
ERCP	Endoscopic retrograde cholangiopancreatography
EtBr	Ethidiumbromide
EUS	Endoscopic ultrasound

Abbreviations

FAP	Familial adenomatous polyposis
FBOC	Familial breast and ovarian cancer
FBS	Fetal bovine serum
FGF-2	Fibroblast growth factor 2
FOLFIRINOX	Folinic acid, 5-fluoruracil, irinotecan and oxaliplatin chemotherapy regimen
FPC	Familial pancreatic cancer
GAPDH	Glyceraldehyde 3-phosphate dehydrogenase
GEL(s)	Granulocytic epithelial lesion(s)
GFAP	Glial fibrillary acidic protein
HE, H&E	Hematoxilin & Eosin stain
HNPCC	Hereditary nonpolyposis colorectal cancer
HRP	Horseradish peroxidase
(h)rs	Hour(s)
HSC(s)	Hepatic stellate cell(s)
IF	Immunofluorescence
IgG4	Immunoglobulin G4
IHC	Immunohistochemistry
IL-1	Interleukin 1
IL-6	Interleukin 6
IL-10	Interleukin 10
KCl	Potassium chloride
mA	Milliampere
MDCT	Multidetector computed tomography
min(s)	Minute(s)
mL	Milliliter
MLH1	MutL homolog 1
MMP	Matrix metalloprotease
MRCP	Magnet resonance cholangiopancreatography
MRI	Magnet resonance imaging
mRNA	Messenger ribonucleic acid
MSH2	MutS homolog 2
MSH6	MutS homolog 6
Nab-paclitaxel	Nanoparticle albumin bound paclitaxel
NaCl	Sodium chloride
N-CAM	Neural cell adhesion molecule

Abbreviations

NGF	Nerve growth factor
NGFR	Nerve growth factor receptor
NP-40	Tergitol-type NP-40
dNTP	Deoxynucleotide triphosphates
NT-3	Neurotrophin-3
NT-4	Neurotrophin-4
PBS	Phosphate-buffered saline
PCC(s)	Pancreatic cancer cell(s)
PCR	Polymerase chain reaction
PDAC	Pancreatic ductal adenocarcinoma
PDGF	Platelet-derived growth factor
PEGPH20	PEGylated human recombinant PH20 hyaluronidase
PMS2	PMS1 homolog 2
PRSS1	Protease, serine 1
PSC(s)	Pancreatic stellate cell(s)
ROI	Region of interest
ROS	Reactive oxygen species
rpm	Rounds per minute
RT	Room temperature
SDS-PAGE	Sodium dodecyl sulfat-polyacrylamide gel electrophoresis
sec(s)	Second(s)
sHSP(s)	Small heat-shock protein(s)
SPARC	Secreted protein acidic and rich in cysteine
SPINK1	Serine protease inhibitor, Kazal type 1
Taq polymerase	Thermus aquaticus polymerase
TBS	Tris-buffered saline
TBS-T	Tris-buffered saline with Tween 20
TEMED	Tetramethylethylenediamine
TGF-β	Transforming growth factor β
TNF-α	Tumor necrosis factor α
TRIS	Tris(hydroxymethyl)aminomethane
TrkA	Topomyosin receptor kinase A
TrkB	Topomyosin receptor kinase B
TrkC	Topomyosin receptor kinase C
TTBS	Tris-buffered saline and tween 20

Abbreviations

UV	Ultraviolet
V	Volt
VDR	Vitamin D receptor
WB	Western blot
WHO	World Health Organization
YFP	Yellow fluorescent protein

2   Introduction

2.1   Stromal reaction

The stroma, which consists of both fibrous proteins and proteoglycans, is the supporting connective tissue of an organ. However, its significance runs much deeper than simply providing a framework for tissue architecture.

The term "stromal reaction" or "fibrosis" refers to the excessive production and deposition of collagen I and other extracellular matrix (ECM) components by activated cells of the stroma. The stromal reaction is a response to tissue damage of any origin. It can occur in the context of repair after tissue necrosis, persistent chronic inflammation or cancer. A stromal reaction as consequence of tissue repair can be referred to as *scar*, while the stromal reaction accompanying cancer is called *desmoplasia*. The term *sclerosis* describes mature paucicellular connective tissue rich in collagen, while the term *cirrhosis* is bound to the additional formation of regenerative nodules.

2.1.1   Production of connective tissue in physiological wound healing

The production of connective tissue per se is an integral part of physiological wound healing. After primary hemostasis, which is facilitated by activated platelets, the inflammatory phase of wound healing follows, where neutrophils and later on also macrophages perform phagocytosis. The release of PDGF and TGF-β from macrophages leads to migration and activation of fibroblasts, which begin to synthesize and deposit ECM proteins during the proliferative phase of wound healing. The newly synthesized ECM is then further organized in the phase of remodeling (Broughton et al., 2006).

The control of the ECM production and the proper progress of tissue organization are crucial to keep the process within physiological boundaries.

2.1.2   Fibrosis in chronic inflammatory diseases

Chronic inflammation is a persistent immune reaction characterized by the co-existence of inflammation, ECM deposition and remodeling processes. While acute inflammation typically resolves rapidly, chronic inflammation is characterized by a persistent stimulus that continuously triggers the proliferation of stromal cells and their production and synthesis of ECM, leading to an imbalance between anti- and pro-fibrotic processes in favor of the latter. Therefore, fibrosis is a crucial factor in a variety of chronic inflammatory diseases, such as idiopathic pulmonary fibrosis, kidney fibrosis due

to glomerulonephritis or diabetic nephropathy, hepatic fibrosis or cirrhosis triggered by chronic hepatitis and pancreatic fibrosis in chronic pancreatitis (Klöppel et al., 2004; Ueha et al., 2012). Fibrosis results in the loss and replacement of functional tissue and eventually leads to organ failure. The process of fibrosis was considered completely irreversible for a long time and the possibility of reversing fibrosis therapeutically, at least to some extent, is still being debated controversially (Paz & Shoenfeld, 2010).

2.1.3 Desmoplasia in malignant diseases

While chronic inflammation itself is an established risk factor for the development of cancer (Balkwill & Mantovani, 2001; Coussens & Werb, 2002), the stromal reaction can provide another link between the two processes. Just like chronic inflammatory diseases, malignant tumors can trigger the production of excessive amounts of ECM proteins. Originally thought to act as a barrier of the body against cancer invasion, the dense stroma surrounding tumors is now thought to create a tumor-supportive microenvironment (Erkan et al., 2010), although controversial data exist (Ozdemir et al., 2014; Rhim et al., 2014). A desmoplastic stromal reaction is especially relevant in breast cancer (Conklin & Keely, 2012; Walker, 2001), prostate cancer (Dakhova et al., 2014; Tuxhorn et al., 2002) and pancreatic cancer (Erkan et al., 2007; Esposito et al., 2006; Paron et al., 2011).

2.2 Chronic pancreatitis

2.2.1 Subtypes

Chronic pancreatitis is an inflammatory disease characterized by a progressive destruction of the secretory parenchyma of the pancreas and its replacement with fibrous tissue. These irreversible morphological changes result in a loss of exocrine and endocrine functions of the pancreas. There are various subtypes of chronic pancreatitis derived from different etiologies. These different subtypes display varying histological changes, for example distinctive patterns of fibrosis.

2.2.1.1 Alcohol-induced chronic pancreatitis

Although initially thought to account for as much as 70 % of cases of chronic pancreatitis (Amann et al., 1996), newer studies suggest that only 44 % of chronic pancreatitis cases in the United States are alcohol-induced (Yadav & Whitcomb, 2010). There are several theories about the pathogenesis of alcohol-induced chronic pancreatitis. The *protein plug* or *ductal hypothesis* suggests that chronic

ethanol consumption leads to an increased concentration of proteins in the pancreatic juice, which results in precipitation of calcifying protein deposits in pancreatic ducts. These protein plugs cause duct obstruction and damage of the duct-lining epithelium, which then leads to acinar atrophy and inflammation upstream of the obstruction, eventually creating a **periductal** fibrosis (Sarles, 1986). A different theory, known as *necrosis-fibrosis sequence*, postulates that alcohol-induced chronic pancreatitis is a result of recurrent episodes of severe acute (necrotizing) pancreatitis. It is suggested that a focal autodigestive necrosis of interstitial fat cells leads to an inflammatory reaction as well as hemorrhage, eventually resulting in fibrosis (Klöppel et al., 2004). Since the initial necrosis is located in the interstitial spaces surrounding the lobules, an **inter- or perilobular** pattern of fibrosis results. When interlobular ducts are subsequently affected, the fibrosis leads to duct strictures, precipitation of proteins in the duct and, finally, duct obstruction. This eventually leads to acinar atrophy and **intralobular** fibrosis in the incompletely drained regions upstream of the obstruction (Klöppel et al., 2004). The *toxic metabolite* or *acinar theory* hypothesizes that chronic consumption of ethanol induces a fatty degeneration of acinar cells, thus resulting in acinar atrophy and pancreatic fibrosis (Bordalo et al., 1984; Noronha et al., 1981). Similarly, the *oxidative stress hypothesis* speculates that ethanol-induced excess free radicals induce acinar degeneration, which then triggers an inflammatory response and leads to fibrosis (Braganza, 1983).

2.2.1.2   Autoimmune pancreatitis

Autoimmune pancreatitis type 1 (AIP type 1) is believed to be the pancreatic manifestation of an IgG4-related systemic, probably autoimmune disease, which can be associated with extrapancreatic lesions like sclerosing cholangitis, sclerosing sialadenitis and retroperitoneal fibrosis (Chari et al., 2010; Esposito et al., 2008). The histopathological appearance of AIP type 1 is characterized by an extensive infiltration of IgG4-positive plasma cells and CD4-positive lymphocytes, a lymphoplasmacellular perivenular infiltration, which often leads to an obstructive phlebitis, and a storiform or swirling fibrosis (Okazaki et al., 2014). The initial lymphoplasmacellular infiltration and the resulting fibrosis focus on medium-sized ducts, which become obstructed in the process. It has been proposed that the inflammation subsequently expands, leading to a **periductal**, then **interlobular** and finally also **intralobular** fibrosis pattern. The result is a **storiform** fibrosis pattern (Klöppel et al., 2004).

Autoimmune pancreatitis type 2 (AIP type 2), on the other hand, exclusively affects the pancreas. A distinctive feature of AIP type 2 are so-called granulocytic epithelial lesions (GELs), characterized by the destruction of duct epithelium by infiltrating neutrophile granulocytes. Like in AIP type 1, a storiform fibrosis and a prominent lymphoplasmacellular infiltrate may occur. However, IgG4-positive plasma cells are scarce, if present at all, in AIP type 2 (Klöppel, 2013).

The storiform fibrosis and the fact that the disease is often limited to a marked out area of the pancreas can lead to a tumorous appearance of AIP, causing it to macroscopically mimic PDAC (Klöppel, 2013).

2.2.1.3 Hereditary pancreatitis

Hereditary pancreatitis is caused by a dysfunctional regulation of the enzyme trypsin. In 60-100 % of families with hereditary pancreatitis, an autosomal-dominant mutation in the *PRSS1* (protease, serine 1) gene can be found (LaRusch & Whitcomb, 2011). *PRSS1* codes for cationic trypsinogen (trypsin-1), which is normally cleaved into its active form trypsin in the small intestine and subsequently also activates other pancreatic enzymes. A gain-of-function mutation of *PRSS1* results either in a prematurely activated or in a degradation-resistant form of trypsin, leading to autodigestion and inflammation of the pancreatic tissue (Halangk et al., 2002).

Aside from *PRSS1*, there are other mutations linked to chronic pancreatitis. For example, a loss-of-function mutation in *SPINK1* (serine peptidase inhibitor, Kazal type 1) encoding for a trypsin inhibitor, and a loss-of-function mutation in *CFTR* (cystic fibrosis transmembrane conductance regulator), which codes for the cystic fibrosis transmembrane conductance protein, can lead to autosomal-recessive forms of pancreatitis (Midha et al., 2010). It has been suggested that the autodigestive necrosis and inflammation that lead to hereditary pancreatitis most likely occur in the duct lumen first and eventually affect the surrounding interstitial tissue, resulting in a mostly **periductal** and, to a lesser extent, **intralobular** pattern of fibrosis (Klöppel et al., 2004)

2.2.1.4 Others

There are several subtypes of chronic pancreatitis aside from alcoholic, autoimmune or hereditary chronic pancreatitis.

The TIGAR-O classification system of chronic pancreatitis suggests several "risk modifiers", which are again divided into the six main sections *toxic-metabolic* (T), *idiopathic* (I), *genetic* (G), *autoimmune* (A), *recurrent and severe acute pancreatitis* (R) and *obstructive* (O) (Etemad & Whitcomb, 2001) (table 1).

Table 1. TIGAR-O classification system of chronic pancreatitis, modified after Etemad &
Whitcomb, 2001.

Toxic-metabolic	Alcoholic
	Tobacco smoking
	Hypercalcemia
	Hyperlipidemia (rare and controversial)
	Chronic renal failure
	Medications
	Toxins
Idiopathic	Early onset
	Late onset
	Tropical
	Other
Genetic	Autosomal-dominant: Cationic trypsinogen mutations (codon 29 and 122 mutations)
	Autosomal-recessive/modifier genes
	➤ CFTR mutations
	➤ SPINK1 mutations
	➤ Cationic trypsinogen mutations (codon 16, 22 and 23 mutations)
	➤ α_1-Antitrypsin deficiency (possible)
Autoimmune	Isolated autoimmune pancreatitis
	Syndromic autoimmune pancreatitis
	➤ Chronic pancreatitis associated with Sjögren syndrom
	➤ Chronic pancreatitis associated with inflammatory bowel disease
	➤ Chronic pancreatitis associated with primary biliary cirrhosis
Recurrent and severe acute pancreatitis	Postnecrotic (severe acute pancreatitis)
	Recurrent acute pancreatitis
	Vascular/ischemic
	Postirradiation
Obstructive	Pancreas divisum
	Sphincter of Oddi disorders (controversial)
	Duct obstruction (e.g. tumors)
	Preampullary duodenal wall cysts
	Posttraumatic pancreatic duct scars

2.2.2 Epidemiology and risk factors

Chronic pancreatitis of any cause has an incidence of 5-12/100,000/year in the United States. For reasons yet to be determined, the risk of developing chronic pancreatitis is about 2- to 3-fold higher in the black population than in the white population (Yadav & Lowenfels, 2013).

Alcoholic pancreatitis typically occurs in patients in their 4th and 5th decade of age and mostly affects men (Layer et al., 1994). While patients with AIP type 1 showed an average age of 61.4 years at diagnosis in a study from 2012, patients with AIP type 2 were diagnosed at an average of 39.9 years. In the same study, a male to female ratio of almost 4:1 was found in AIP type 1, whereas AIP type 2 showed relatively equal gender distribution (Hart et al., 2013). Hereditary pancreatitis usually manifests at the young age of approximately 10 years (Rosendahl et al., 2007).

As alcohol-induced chronic pancreatitis is by far the most common form of the disease, naturally, alcohol is the single most common risk factor for chronic pancreatitis (Coté et al., 2011). On the other hand, it is important to note that the absolute risk of developing pancreatitis among patients suffering from alcoholism ranges between only 2 and 5 % (Lankisch et al., 2002), strongly implying the importance of other predisposing factors besides alcohol. Smoking also increases the risk of chronic pancreatitis, both independently and as a cofactor of alcoholism (Andriulli et al., 2010). The role of dietary factors in the development of chronic pancreatitis is unclear and needs to be further elucidated.

2.2.3 Diagnostics and therapy

Severe recurrent or constant pain, which usually begins in the epigastrium and will often radiate to the back, is the main symptom of chronic pancreatitis. The progressive loss of exocrine and endocrine pancreatic function can further lead to food malabsorption, resulting in bloating, steatorrhea and diarrhea, as well as the development of diabetes mellitus (Banks et al., 2010).

Aside from AIP type 1, where serology will show elevated levels of γ-globulins (especially IgG4) and various auto-antibodies, the diagnostics of chronic pancreatitis focus mainly on structural changes of the pancreatic ducts. Imaging techniques include endoscopic retrograde cholangiopancreatography (ERCP), magnetic resonance cholangiopancreatography (MRCP), multidetector CT (MDCT), MRI and endoscopic ultrasound (EUS). Few centers worldwide are able to perform a secretory test that can objectify the exocrine function of the pancreas: A reduced level of bicarbonate in duodenal aspirates collected after stimulation with i.v. secretin points to a decreased pancreatic function. However, the only way to definitely confirm the diagnosis is a histopathological examination of biopsies or resected specimens (Braganza et al., 2011).

A main focus of the conservative treatment of chronic pancreatitis is the management of pain. For this purpose, analgesics should be used according to the WHO analgesic ladder originally developed for the treatment of cancer pain (Braganza et al., 2011; WHO, 1990). Moreover, it has been shown that patients can benefit from treatment with orally substituted pancreatic enzymes, subcutaneous somatostatin analogon octreotide and the CCK-A receptor antagonist loxiglumid. New-onset diabetes mellitus should be treated with simple insulin regimens (Braganza et al., 2011).

Unlike all other forms of chronic pancreatitis, both type 1 and type 2 AIP are responsive to steroid treatment (Hart et al., 2013).

Complications like severe pain that cannot be controlled conservatively, stenoses of the common bile duct or the duodenum as well as pseudocysts that are not connected to the pancreatic duct can require endoscopic dilatation, stenting or drainage as well as surgical drainage or resection in order to relieve symptoms and preserve functional tissue (Braganza et al., 2011).

2.2.4 Role of stromal reaction in chronic pancreatitis

A prominent fibrosis, which consists of cellular elements (pancreatic stellate cells (PSCs), fibroblasts, immune cells) as well as ECM proteins (e.g. collagen I, collagen III, fibronectin), growth factors and cytokines, is a histopathological hallmark of all types of chronic pancreatitis.

Fibrosis is a main problem in chronic pancreatitis, because it results in a gradual loss of functional tissue, which inevitably leads to exocrine and endocrine insufficiency of the pancreas. This replacement of normal pancreas tissue with fibrosis is irreversible, making chronic pancreatitis an incurable disease at present (He et al., 2009). Moreover, pancreatic fibrosis on the basis of chronic pancreatitis is also a risk factor for the development of pancreatic cancer (Raimondi et al., 2010). The chronic inflammatory response leads to an enhanced release of potentially DNA damaging reactive oxygen species (ROS) and reactive nitrogen intermediates on one hand as well as growth factors and cytokines on the other hand (Ling et al., 2014). The consequently stimulated proliferation of parenchymal cells naturally comes with an increased risk of accumulating somatic mutations. It has further been shown that 107 genes are similarly expressed in the stromal reaction of chronic pancreatitis and PDAC, additionally highlighting the stroma as a crosslink between chronic pancreatitis and cancer (Binkley et al., 2004).

2.3 Pancreatic ductal adenocarcinoma

2.3.1 Epidemiology and risk factors

Pancreatic cancer, of which PDAC accounts for 90 % of cases (Cascinu et al., 2010), ranks 9th in the incidence of solid cancers in men and 7th in the incidence of solid cancers in women, respectively, but 4th for cancer-related deaths in both men and women in the United States (Siegel et al., 2016). These facts illustrate the poor prognosis for which PDAC is notorious. Despite the overall progress made in cancer research and therapy, the 5-year survival rate of PDAC has seen very minimal improvement and is still at only 8 % (Siegel et al., 2016), underlining the desperate need for new approaches in diagnostics and therapy of this particular type of cancer.

PDAC only rarely occurs before the age of 55 and the median age of onset is 71 years. Men show slightly higher incidence rates for PDAC than women and incidence rates are considerably higher in the black population than in all other racial groups (Yadav & Lowenfels, 2013).

Besides age and race, various other risk factors for PDAC have been described, including lifestyle factors like alcohol abuse (Gapstur et al., 2011), a diet high in red meats (Stolzenberg-Solomon et al., 2007), obesity (de Gonzalez et al., 2003) and, most importantly, tobacco smoking (Bosetti et al., 2012). Furthermore, the risk to develop PDAC is approximately 2-fold increased in patients suffering from longstanding diabetes mellitus (Yadav & Lowenfels, 2013). Importantly, chronic pancreatitis is a risk factor for PDAC: While patients with chronic pancreatitis in general have a pooled relative risk of 13.3, the pooled relative risk in patients suffering from hereditary chronic pancreatitis is as high as 69 (Raimondi et al., 2010). Besides hereditary pancreatitis, various other inherited syndromes, such as familial breast and ovarian cancer (FBOC; *BRCA1* and *BRCA2* mutations), familial adenomatous polyposis (FAP; *APC* mutations) or hereditary nonpolyposis colorectal cancer (HNPCC; *MLH1*, *MSH2*, *MSH6* and *PMS2* mutations), are also associated with an increased risk of PDAC. Moreover, a familial pancreatic cancer syndrome (FPC) has been proposed, but the major underlying gene defect has not been identified so far (Bartsch et al., 2012).

2.3.2 Diagnostics and therapy

PDAC is an aggressive and lethal malignancy especially due to its tendency for early local invasion, including retroperitoneal infiltration and perineural invasion, as well as early metastasis. However, symptoms usually occur at an advanced tumor stage, making diagnosis significantly more challenging. Symptoms are mostly non-specific and can include back pain, abdominal pain, digestive problems, weight loss and new-onset diabetes mellitus. Painless jaundice can occur in cases of tumors that

obstruct the bile duct (Herold, 2013). The suspected diagnosis is usually substantiated and further defined using spiral CT, ERCP, MRCP, EUS or, in selected cases, MRI or laparoscopy. Histopathological confirmation of the diagnosis is recommended in patients not eligible for surgery or patients that need preoperative treatment (Cascinu et al., 2010).

As PDAC is virtually resistant to radio- and chemotherapy, complete surgical resection remains the only possibility for curative therapy at this point. However, only 10-15 % of patients are eligible for potentially curative resection at the time of diagnosis (Beger et al., 2003). At the moment, the nucleoside analog gemcitabine and the tyrosine kinase inhibitor erlotinib are the only two agents approved for systemic treatment of advanced and metastatic pancreatic cancer, albeit their benefits are only marginal. Gemcitabine was shown to prolong median survival from 4.4 to 5.6 months (Burris et al., 1997). The addition of erlotinib to gemcitabine treatment prolongs median survival slightly from 5.9 to 6.2 months (Moore et al., 2007). In 2011, a phase III randomized trial was able to show that the FOLFIRINOX regimen, a four-drug combination of 5-FU, leucovorin, oxaliplatin and irinotecan, can achieve a median survival of 11.1 months versus 6.8 months with gemcitabine treatment. However, the FOLFIRINOX regimen comes with significant toxicity and is therefore limited to patients in good general condition (Conroy et al., 2011). More recently, the addition of nab-paclitaxel (nanoparticle albumin bound paclitaxel) to gemcitabine therapy was demonstrated to prolong median survival from 6.7 to 8.5 months compared to gemcitabine monotherapy with manageable toxicity (Goldstein et al., 2015; Von Hoff et al., 2013).

2.3.3 Role of stromal reaction in PDAC

An excessive stromal reaction is the histopathological hallmark of PDAC. The resulting abundant mass of dense stroma leaves the PDAC tumor mass poorly vascularized and perfused and therefore acts as a physical barrier to drug delivery (Oberstein & Olive, 2013). Depleting the stroma can significantly increase the delivery and efficacy of the chemotherapeutic agent gemcitabine in a PDAC mouse model (Olive et al., 2009) and selective stromal depletion coupled with chemotherapy is giving encouraging results in patients (Bhaw-Luximon & Jhurry, 2015). Furthermore, the stroma creates tumor hypoxia, which is generally associated with therapy resistance and poor prognosis (Harris, 2002). On top of these mere physical aspects, the stromal reaction also creates a complex microenvironment that is supportive to tumor cells. Aside from the impact of PSCs on pancreatic carcinogenesis (see 2.4.4), ECM proteins themselves seem to have growth- and survival-promoting effects on pancreatic cancer cells (PCCs) (Edderkaoui et al., 2005; Erkan et al., 2007; Vaquero et al., 2003; Vaquero et al., 2004). Moreover, it has also been shown that the resistance of PCC lines to chemotherapeutic agents is

increased when they are cultured in the presence of ECM proteins (Armstrong et al., 2004; Berchtold et al., 2015; Miyamoto et al., 2004).

However, it is important to note that there are also data suggesting that the tumor stroma can play a protective role in PDAC (Ozdemir et al., 2014; Rhim et al., 2014).

Taken together, it can be said the stromal reaction indisputably takes an active part in pancreatic carcinogenesis.

2.4 Pancreatic stellate cells

2.4.1 Phenotype and function

PSCs were first described in 1982 (Watari & Hotta, 1982) and were isolated and cultured in 1998 (Apte et al., 1998; Bachem et al., 1998), which accounts for the fact that these cells are still not thoroughly characterized regarding their origin, function and immunophenotype.

PSCs are resident cells of the exocrine pancreas and comprise about 4-7 % of the total pancreatic tissue. They are located alongside pancreatic acinar cells as well as small ducts and blood vessels (Apte et al., 1998). In healthy pancreatic tissue, PSCs exist in a quiescent state distinguished by an angular shape and an abundance of cytoplasmic lipid droplets containing vitamin A, which can be visualized using its autofluorescence when exposed to UV light at 328 nm (Apte et al., 1998). Although the main function of PSCs as vitamin-A storing cells in the healthy pancreas is not completely clear yet, they seem to regulate the ECM-turnover in order to ensure the maintenance of a normal stroma composition. For this purpose, they synthesize extracellular matrix proteins (Haber et al., 1999) as well as matrix metalloproteinases and tissue inhibitors of matrix metalloproteinases (Phillips et al., 2003). Upon tissue injury, for example in the course of chronic pancreatitis or PDAC, but also during cultivation, PSCs transform into a myofibroblast-like phenotype. This phenotype appears star-shaped with long cytoplasmic projections and no longer contains lipid droplets (Apte et al., 1998) (figure 1). In their activated state, PSCs show an increase in proliferation, migration (Omary et al., 2007), synthesis of ECM proteins, matrix metalloproteinases and their inhibitors (Apte et al., 2004) as well as in the secretion of cytokines and growth factors (Omary et al., 2007).
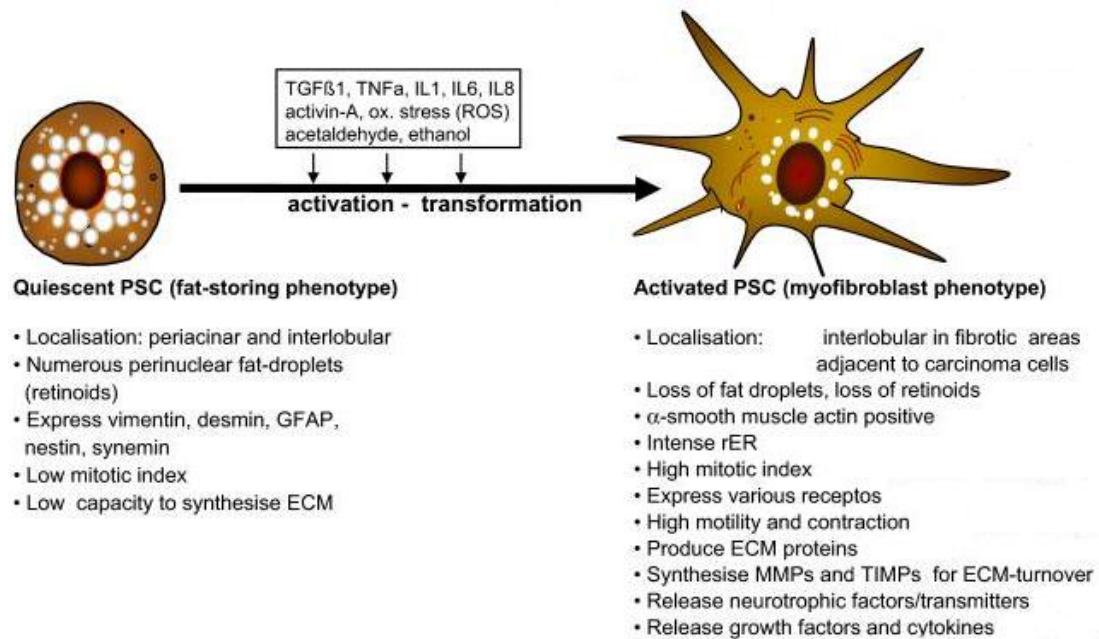
Figure 1. Activation of PSCs, modified after Erkan et al., 2012.

Several markers have been described to identify PSCs. These include desmin, vimentin, nestin and glial fibrillary acidic protein (GFAP) (Apte et al., 1998) as well as nerve growth factor receptor (NGFR) and CD34 (Habisch et al., 2010). Alpha-smooth muscle actin (α-SMA) has been proposed as a marker for activated PSCs (Apte et al., 1998). However, it is now thought to be more of a marker for transdifferentiation into an activated phentotype than a marker for activated PSCs per se (Krizhanovsky et al., 2008). A reliable panel of markers to distinguish PSCs from other subtypes of stromal cells (myofibroblasts, fibroblasts) – in analogy to what has been already shown in hepatic stellate cells (see 2.4.2) – is not yet available.

2.4.2 Similarities with hepatic stellate cells

Unlike their pancreatic counterparts, hepatic stellate cells (HSCs) were first described significantly earlier, in 1876, by Karl Wilhelm von Kupffer (Haubrich, 2004). HSCs are fat-storing cells of the liver that are located in the perisinusoidal space (space of Disse) between the basolateral aspects of hepatocytes and sinusoidal endothelial cells (Ito, 1951). They share a very similar cytoskeletal phenotype with PSCs and can also transform from a quiescent vitamin-A-rich cell type into a contractile myofibroblast-like phenotype, which synthesizes an excessive amount of ECM proteins like collagen I and III (Friedman, 1993). The crucial role of HSCs in liver fibrosis has long been established (Gressner & Bachem, 1995). Beyond this well-known role in liver injury and repair, a variety of other possible functions have been discussed, such as, for example, a role in immunoregulation (Maher, 2001). Aside

from the previously mentioned similarities between HSCs and PSCs in morphology and function, a direct transcriptome analysis between HSCs and PSCs showed that only 29 genes are differently expressed between the two cell types, while they both differ significantly from skin fibroblasts (Buchholz et al., 2005). Taken together, these findings have led to the hypothesis that HSCs and PSCs might share a common precursor cell (Buchholz et al., 2005). However, even the origin of the well-characterized HSCs has been a subject of much debate. While a **neuroectodermal** origin of HSCs has been proposed due to the expression of previously mentioned neural crest markers like GFAP, a cell lineage analysis using transgenic mice expressing yellow fluorescent protein (YFP) in all neural crest cells and their derivatives failed to support this hypothesis (Cassiman et al., 2006). Findings like the expression of CD34 and cytokeratin-7/8 in HSCs of the human fetal liver suggest an **endodermal** origin of HSCs (Suskind & Muench, 2004). On the other hand, results of cell lineage tracing using MesP1-Cre mice point to an origin from the **mesodermal** septum transversum mesenchyme, which grows to form the mesothelium lining the liver (Asahina et al., 2009). Bone-marrow derived cells are also thought to be able to contribute to HSCs (Miyata et al., 2008). Another highly debated question is whether HSCs can arise from hepatic epithelial cells that undergo epithelial-mesenchymal transition (EMT) upon liver injury (Sicklick et al., 2006). Unfortunately, even less is known about the origin of PSCs. While HSCs, despite their striking expression of neural markers, do not seem to derive from the neural crest, lineage tracing techniques similar to the ones used in HSCs by Cassiman and colleagues (Cassiman et al., 2006) have not been used in PSCs yet. Therefore, this possibility cannot be ruled out completely at this time, especially as PSCs also express many of these neural proteins (see 2.4.1). Multipotent precursor cells that can differentiate into PSCs have been found in the adult mouse pancreas (Seaberg et al., 2004). This suggests that PSCs could derive from a local precursor specific to the pancreas and not share a common origin with HSCs after all. As described for HSCs, rat bone marrow cells home to the pancreas and transform into PSCs during chronic pancreatitis, even though they only contribute partly to the total PSC population (Sparmann et al., 2010).

Several HSC markers have been found so far, some of which have already been suggested as PSCs markers as well (see 2.4.1). HSC markers include desmin, vimentin and α-smooth muscle actin (α-SMA) as well as neural markers like nestin, glial fibrillary acidic protein (GFAP), nerve growth factor (NGF), brain-derived neurotrophic factor (BDNF), neurotrophin-3 (NT-3), neurotrophin-4 (NT-4), nerve growth factor receptor (NGFR, p75), TrkB neurotrophic receptor, TrkC neurotrophic receptor, neural cell adhesion molecule (N-CAM, CD56), synaptophysin and α-crystallin B (Cassiman et al., 2002) . The use of these markers has been proven useful to distinguish HSCs from other subtypes of hepatic myofibroblasts, such as portal/septal and interface myofibroblasts (Cassiman et al., 2002).

2.4.3   Role of pancreatic stellate cells in chronic pancreatitis

PSCs are the principal source of the fibrosis that accompanies all types of chronic pancreatitis and that eventually leads to the loss of functioning pancreatic tissue (Apte & Wilson, 2003). Alpha-SMA-positive cells have been observed in the fibrotic areas of tissue sections from patients with chronic pancreatitis from various etiologies. Using dual staining techniques, it could be shown that only these α-SMA-positive cells express procollagen mRNA, strongly suggesting that activated PSCs are the main contributors to collagen in chronic pancreatitis fibrosis (Haber et al., 1999).

As alcohol abuse is the main cause of chronic pancreatitis, it is no surprise that alcohol can activate PSCs. An activation of PSCs facilitated directly by ethanol, its metabolite acetaldehyde and the oxidative stress caused by these two substances has been shown (Apte et al., 2000). Moreover, there is a necroinflammatory pathway, in which PSCs are activated by cytokines that are released upon alcohol exposure (Apte & Wilson, 2003). The cytokines that are able to activate PSCs include TNF-α as well as IL-1, IL-6 and IL-10, which are known to be upregulated during acute pancreatitis, and it is hypothesized that recurrent attacks of acute pancreatitis (which are, according to the *necrosis-fibrosis sequence*, the origin of chronic alcohol-induced pancreatitis; see 2.2.1.1) might lead to a permanent activation of PSCs, mediated by constant exposure to the mentioned cytokines (Mews et al., 2002).

2.4.4   Role of pancreatic stellate cells in pancreatic ductal adenocarcinoma

PSCs are the main contributors of ECM proteins in PDAC desmoplasia. Not only do stromal areas in tissue sections of patients with PDAC stain positive for PSC markers including α-SMA, indicating the presence of PSCs in their activated state, but PSCs in PDAC also co-localize with procollagen mRNA expression, implying that PSCs are responsible for the production of collagen I in PDAC stroma (Apte et al., 2004). In addition, PSCs have also been identified as the source of tenascin C and collagen V, two ECM proteins that are increasingly expressed in the progression of pancreatic dysplasia to PDAC (Berchtold et al., 2015; Esposito et al., 2006).

While the fact that PSCs are the main source of desmoplastic stroma underscores their importance in PDAC (see 2.3.1), it has been shown that it is not necessarily the amount of synthesized stroma per se, but mostly the number of activated PSCs that is crucial for the prognosis of PDAC patients. In 2008, Erkan and colleagues proposed the *activated stroma index (ASI)*, an α-SMA/collagen staining ratio, as a novel prognostic marker for PDAC and showed that a high ASI, respectively a high number of activated PSCs and a low amount of collagen, was associated with a poor prognosis (Erkan et al., 2008). This strongly indicates that the importance of the stromal reaction does not only lie within the sheer physical mass of fibrosis, but rather in its biological activity. Supporting this, several *in vitro* and *in vivo*

studies have shown that PSCs interact reciprocally with PCCs. *In vitro*, PCCs are able to increase proliferation and ECM synthesis (Bachem et al., 2005) as well as migration (Vonlaufen et al., 2008) of PSCs. The effect of PCCs on PSC proliferation could be reduced by adding anti-PDGF, indicating that PDGF is the mediating factor of PSC proliferation induced by PCCs. In a similar manner, the effect of PCCs on ECM synthesis by PSCs could be inhibited by adding anti-PDGF, anti-FGF-2 and anti-TGF-β1, indicating that these factors mediate the PCCs-induced effects on ECM synthesis by PCCs (Bachem et al., 2005). Vice versa, PSCs also have effects on PCCs: PSCs increase PCC proliferation, migration and invasion and inhibit tumor cell apoptosis (Vonlaufen et al., 2008). Vonlaufen and colleagues were also able to show in their study that mice injected with a mixture of PCCs and PSCs developed larger primary tumors as well as an increased number of metastases than mice injected with PCCs alone (Vonlaufen et al., 2008). In a sex mismatch study, in which male PSCs mixed with female PCCs were injected into the pancreas of female mice, male PSCs could be detected in multiple metastatic sites, indicating that PSCs may accompany PCCs during metastatic spread (Xu et al., 2010).

3 Aim of the study

The primary aim of this study was a detailed morphological and immunophenotypical characterization of PSCs in PDAC and chronic pancreatitis by means of immunohistochemistry and immunofluorescence.

A similar approach has previously been used for the characterization of HSCs (Cassiman et al., 2002), which are known to share similarities with their pancreatic counterparts. A further aim of the study was therefore to compare PSCs with HSCs and ascertain similarities and differences between the two cell types.

4 Material and Methods

4.1 Material

4.1.1 Reagents

Product	Company
3,3'-Diaminobenzidine (DAB)	Medac GmbH, Wedel, GER
Acetic acid	Merck KGaA, Darmstadt, GER
Acrylamide/bis solution 40 %, 37.5:1	Bio-Rad Laboratories GmbH, Munich, GER
Adefofix fixing concentrate	Adefo-Chemie, Dietzenbach, GER
Adefofur developing concentrate	Adefo-Chemie, Dietzenbach, GER
Agarose LE for gel electrophoresis	Biozym Scientific GmbH, Hessisch Oldendorf, GER
Alcian blue 1 %	MORPHISTO® Evolutionsforschung und Anwendung GmbH, Frankfurt am Main, GER
Ammonium persulfate (APS)	Sigma-Aldrich Chemie GmbH, Steinheim, GER
Amphotericin B	Biochrom AG, Berlin, GER
Antibody diluent Dako REAL™	Dako Deutschland GmbH, Hamburg, GER
Biotin-labeled goat anti-rabbit IgG	KPL, Inc., Gaithersburg, MD, USA
Biozym LE agarose	Biozym Scientific GmbH, Hessisch Oldendorf, GER
Bovine serum albumin (BSA)	Sigma-Aldrich Chemie GmbH, Steinheim, GER
Brilliant-croceine-fuchsine-acid solution	MORPHISTO® Evolutionsforschung und Anwendung GmbH, Frankfurt am Main, GER
Bromophenol blue	Sigma-Aldrich Chemie GmbH, Steinheim, GER
Citric acid	Merck KGaA, Darmstadt, GER
Complete protease inhibitor cocktail tablets (PrI)	Roche Diagnostics, Mannheim, GER
Dako wash buffer 10X	Dako Deutschland GmbH, Hamburg, GER
Deoxycholic acid	Sigma-Aldrich Chemie GmbH, Steinheim, GER
Dimethylsulfoxid (DMSO)	Sigma-Aldrich Chemie GmbH, Steinheim, GER
DNA loading dye 6X	Thermo Fisher Scientific, Schwerte, GER
dNTP Set, 100 mM solutions	Invitrogen™, Darmstadt, GER
Dulbecco's Modified Eagle Medium (D-MEM) (1X), liquid, high glucose 4.5 g/L	Gibco®, Darmstadt, GER

Dulbecco's Modified Eagle Medium (D-MEM) (1X), liquid, low glucose 1 g/L	Gibco®, Darmstadt, GER
ECL™ anti-mouse IgG	GE Healthcare, Munich, GER
ECL™ anti-rabbit IgG	GE Healthcare, Munich, GER
EnVision™ anti-rabbit	Dako Deutschland GmbH, Hamburg, GER
Eosin	Sigma-Aldrich Chemie GmbH, Steinheim, GER
Ethanol	Merck KGaA, Darmstadt, GER
Ethidium bromide	Amresco, Solon, OH, USA
Ethylene glycol tetraacetic acid (EGTA)	Sigma-Aldrich Chemie GmbH, Steinheim, GER
Ethylenediaminetetraacetic acid (EDTA)	Sigma-Aldrich Chemie GmbH, Steinheim, GER
F12 nutrient mixture, L-glutamin	Gibco®, Darmstadt, GER
Fetal bovine serum (FBS)	Gibco®, Darmstadt, GER
Formalin	Staub & Co. GmbH, Munich, GER
GeneRuler™ 1 kb DNA ladder	Thermo Fisher Scientific, Schwerte, GER
GeneRuler™ 100 bp DNA ladder	Thermo Fisher Scientific, Schwerte, GER
Glycerin	Merck KGaA, Darmstadt, GER
Glycine	Sigma-Aldrich Chemie GmbH, Steinheim, GER
Goat serum (normal goat serum)	Abcam, Cambridge, UK
Hemalaun, Mayer's	AppliChem GmbH, Darmstadt, GER
HistoMark® biotin streptavidin-HRP systems	KPL Inc., Gaithersburg, MD, USA
Hoechst 33342	Sigma-Aldrich Chemie GmbH, Steinheim, GER
Hydrogen chloride (HCl)	neoLab, Heidelberg, GER
Iron(III) chloride 1 %	MORPHISTO® Evolutionsforschung und Anwendung GmbH, Frankfurt am Main, GER
Isopropanol	Merck KGaA, Darmstadt, GER
Matrigel™	BD Bioscience, Heidelberg, GER
Methanol	Merck KGaA, Darmstadt, GER
Nonfat dry milk	Carl-Roth GmbH & Co. KG, Karlsruhe, GER
Nonidet-P40	Sigma-Aldrich Chemie GmbH, Steinheim, GER
Oil Red O solution	Sigma-Aldrich Chemie GmbH, Steinheim, GER
Opti-MEM® reduced serum media	Gibco®, Darmstadt, GER

Penicillin-streptomycin, liquid	Gibco®, Darmstadt, GER
Pertex mounting medium for IHC	Medite GmbH, Burgdorf, GER
Phosphate buffered saline (PBS)	GE Healthcare, Munich, GER
Phosphotungstic acid 2 %	MORPHISTO® Evolutionsforschung und Anwendung GmbH, Frankfurt am Main, GER
PhosSTOP phosphatase inhibitor cocktail tablets (PhI)	Roche Diagnostics, Mannheim, GER
Ponceau S dye	Sigma-Aldrich Chemie GmbH, Steinheim, GER
Potassium chloride (KCl)	Sigma-Aldrich Chemie GmbH, Steinheim, GER
Pre-stained protein ladder plus, PageRuler™	Thermo Fisher Scientific, Schwerte, GER
Pre-stained protein ladder, PageRuler™	Thermo Fisher Scientific, Schwerte, GER
Pronase E	Merck Millipore, Darmstadt, GER
Safron du Gâtinais solution	MORPHISTO® Evolutionsforschung und Anwendung GmbH, Frankfurt am Main, GER
Sodium chloride (NaCl)	Merck KGaA, Darmstadt, GER
Sodium dodecyl sulfate 20 % (w/v) solution (SDS)	AppliChem GmbH, Darmstadt, GER
Taq DNA polymerase BioTherm™	Ares Bioscience GmbH, Koeln, GER
Tetramethylethylenediamine (TEMED)	Bio-Rad Laboratories GmbH, Munich, GER
Triton X-100	Merck KGaA, Darmstadt, GER
Trizma® base (TRIS base)	Sigma-Aldrich Chemie GmbH, Steinheim, GER
Trypan blue solution 0.4 %	Sigma-Aldrich Chemie GmbH, Steinheim, GER
Trypsin, 0.05 % with EDTA	PAA Laboratories GmbH, Coelbe, GER
Vectashield mounting medium for fluorescence	Vectashield, Loerrach, GER
Ventana Bluing Reagent	Ventana Medical Systems, Inc., Basel, CH
Ventana Cell Conditioning 1 (CC1)	Ventana Medical Systems, Inc., Basel, CH
Ventana EZ Prep™ 10X	Ventana Medical Systems, Inc., Basel, CH
Ventana Liquid Coverslip (LCS)	Ventana Medical Systems, Inc., Basel, CH
Ventana Reaction Buffer 10X	Ventana Medical Systems, Inc., Basel, CH
Ventana ultraView™ Copper	Ventana Medical Systems, Inc., Basel, CH
Ventana ultraView™ DAB Chromogen	Ventana Medical Systems, Inc., Basel, CH
Ventana ultraView™ DAB H_2O_2	Ventana Medical Systems, Inc., Basel, CH
Ventana ultraView™ HRP Universal Multimer	Ventana Medical Systems, Inc., Basel, CH

Ventana ultraView™ Inhibitor	Ventana Medical Systems, Inc., Basel, CH
Verhoeff's solution A, B and C	MORPHISTO® Evolutionsforschung und Anwendung GmbH, Frankfurt am Main, GER
Water, aqua ad iniectabilia	AlleMan Pharma GmbH, Rimbach, GER
Xylol	Merck KGaA, Darmstadt, GER
B-Mercaptoethanol	Sigma-Aldrich Chemie GmbH, Steinheim, GER

4.1.2 Consumables

Product	Company
AmershamHybond™ ECL™ nitrocellulose membrane	GE Healthcare Lifescience, Freiburg, GER
AmershamHyperfilm ECL	GE Healthcare Lifescience, Freiburg, GER
Cell scraper	SARSTEDT AG & Co., Nuembrecht, GER
Corning®DeckWorks® pipette tips, 10 µL	Sigma-Aldrich Chemie GmbH, Steinheim, GER
Corning®DeckWorks® pipette tips, 1000 µL	Sigma-Aldrich Chemie GmbH, Steinheim, GER
Corning®DeckWorks® pipette tips, 20 µL	Sigma-Aldrich Chemie GmbH, Steinheim, GER
Corning®DeckWorks® pipette tips, 200 µL	Sigma-Aldrich Chemie GmbH, Steinheim, GER
Coverslips for microscopic slides, 24 x 50 mm	Engelbrecht, Edermuende, GER
Coverslips, round, 12 mm diameter	Thermo Fisher Scientific, Schwerte, GER
Cryotubes	A. Hartenstein, Wuerzburg, GER
Microscope slides	Thermo Fisher Scientific, Schwerte, GER
PCR tube strips 0.2 mL	Eppendorf AG, Hamburg, GER
Pipettes, Pasteur glass 3.2 mL	Carl-Roth GmbH & Co. KG, Karlsruhe, GER
Pipettes, serological CELLSTAR® 2 mL	Greiner Bio-One, Frickenhausen, GER
Pipettes, serological CELLSTAR® 5 mL	Greiner Bio-One, Frickenhausen, GER
Pipettes, serological CELLSTAR® 10 mL	Greiner Bio-One, Frickenhausen, GER
Pipettes, serological CELLSTAR® 25 mL	Greiner Bio-One, Frickenhausen, GER
Reaction tubes 1.5 mL	Eppendorf AG, Hamburg, GER
Reaction tubes 2 mL	Eppendorf AG, Hamburg, GER
Reaction tubes Falcon™ blue max 15 mL	BD Bioscience, Heidelberg, GER
Reaction tubes Falcon™ blue max 50 mL	BD Bioscience, Heidelberg, GER

Safe seal microtubes	Eppendorf AG, Hamburg, GER
Syringe, single-use 20 mL	B. Braun Melsungen AG, Melsungen, GER
Tissue culture dish	TPP, Trasadingen, CH
Tissue culture flasks (25 cm^2, 75 cm^2)	TPP, Trasadingen, CH
Tissue culture test plates (96-well, 24-well, 6-well)	TPP, Trasadingen, CH
Wide Mini-Sub cell GT electrophoresis system	Bio-Rad Laboratories GmbH, Munich, GER

4.1.3 Equipment

Product	Company
Accu-jet® pro	Brand GmbH + CO KG, Wertheim, GER
Asys Expert Plus microplate reader	Biochrom AG, Berlin, GER
Axio Observer Z1	Carl Zeiss AG, Jena, GER
Axiocam ICm1	Carl Zeiss AG, Jena, GER
Axiovert 135	Carl Zeiss AG, Jena, GER
Axiovert 25	Carl Zeiss AG, Jena, GER
BenchMark XT automated IHC/ISH slide staining system	Ventana Medical Systems, Inc., Basel, CH
Cat SRX 101 A development machine	Konica Minolta, Langenhagen, GER
Centrifuge 5415D	Eppendorf AG, Hamburg, GER
Centrifuge 5417R	Eppendorf AG, Hamburg, GER
DakoAutostainer universal staining system	Dako Deutschland GmbH, Hamburg, GER
Ebox VX2 gel documentation system	Peqlab Biotechnology GmbH, Erlangen, GER
Electrophoresis transfer cell mini Trans-Blot®	Bio-Rad Laboratories GmbH, Munich, GER
Eppendorf Mastercycler gradient	Eppendorf AG, Hamburg, GER
Eppendorf research pipettes	Eppendorf AG, Hamburg, GER
Filter set 38 Endow GFP shift free	Carl Zeiss AG, Jena, GER
Filter set 43 Cy3, d=25 shift free	Carl Zeiss AG, Jena, GER
Filter set DAPI	Carl Zeiss AG, Jena, GER
Filter set 38 Endow GFP	Carl Zeiss AG, Jena, GER
Filter set 43 Cy3	Carl Zeiss AG, Jena, GER

Freezer -20 °C Liebherr comfort	Liebherr GmbH, Biberach an der Riss, GER
Freezer -20 °C, economic froster	Bosch GmbH, Stuttgart, GER
Freezer -80 °C HFC86-360	Heraeus Instruments, Osterode, GER
Freezer -80 °C Sanyo ultra-low temperature chest freezer MDF-594	Panasonic, San Diego, USA
Freezing container NALGENE™ Cryo 1 °C	Thermo Fisher Scientific, Schwerte, GER
Fridge +4 °C Liebherr premium	Liebherr GmbH, Biberach an der Riss, GER
GFL incubation waterbath	GFL GmbH, Burgwedel, GER
Glass coverslipper Promounter RCM2000	Medite GmbH, Burgdorf, GER
Hereus Hera Safe CO_2 incubator	Thermo Fisher Scientific, Schwerte, GER
Heating block Thermomixer® comfort 1.5 mL	Eppendorf AG, Hamburg, GER
Heating block ThermoStat plus 1.5 mL	Eppendorf AG, Hamburg, GER
Heating oven type BE400	Memmert, Schwabach, GER
Heating plate HP 30 digital IKATHERM	IKA®-Werke GmbH & CO. KG, Staufen, GER
Heracell 150i CO2 incubator	Thermo Fisher Scientific, Schwerte, GER
Hood Uniflow UVUB 1800	UniEquip, Planegg, GER
Hotplate stirrer IKAMAG® RCT	IKA® Werke GmbH und Co. KG, Staufen, GER
Ice machine	ZIEGRA Eismaschinen GmbH, Hannover, GER
IKA® MS1 minishaker	IKA® Werke GmbH und Co. KG, Staufen, GER
Ikamage® RCT magnetic stirrer	IKA® Werke GmbH und Co. KG, Staufen, GER
Lab centrifuge 4K15	Sigma-Aldrich Chemie GmbH, Steinheim, GER
Laboratory balance BP 310 S	Sartorius AG, Goettingen, GER
Leitz Labovert FS	Leica Microsystems GmbH, Wetzlar, GER
Liquid Nitrogen tank MVE TEC 3000 (1500 series)	Chart MVE BioMedical GmbH, Wuppertal, GER
Magnetic stir bars, various sizes	NeoLab, Heidelberg, GER
Magnetic stirrer MR2000	Heidolph Instruments, Schwabach, GER
Microm HM 335 E	Thermo Fisher Scientific, Schwerte, GER
Microtome blade	pfm medical AG, Koeln, GER
Microwave Privileg 1034HGD	Otto, Hamburg, GER
Miniprotean system 3 cell	Bio-Rad Laboratories GmbH, Munich, GER

Mini-PROTEAN® Tetra electrophoresis system	Bio-Rad Laboratories GmbH, Munich, GER
Mitsubishi P95 printer	Mitsubishi Electric, Ratingen, GER,
Neubauer counting chamber	Carl-Roth GmbH & Co. KG, Karlsruhe, GER
pH meter (pH 211)	HANNA Instruments GmbH, Kehl am Rhein, GER
Pipettor pipetus®	Hirschmann Laborgeraete, Eberstadt, GER
Power supply PowerPac 300	Bio-Rad Laboratories GmbH, Munich, GER
PowerPac Basic Power Supply	Bio-Rad Laboratories GmbH, Munich, GER
Pressure cooker	WMF, Geislingen/Steige, GER
Rocker table Rocky®	Froebel Labortechnik, Lindau, GER
Scales Sartorius universal	Sartorius AG, Goettingen, GER
Stuart Scientific SD rocking platform STR	Keison products, Chelmsford, UK
Thermomixer compact	Eppendorf AG, Hamburg, GER
Vortexer MS1 minishaker	IKA®-Werke GmbH & CO. KG, Staufen, GER
Vortexer VF 2	IKA®-Werke GmbH & CO. KG, Staufen, GER
Wide mini subset GT electrophoresis system	Bio-Rad Laboratories GmbH, Munich, GER

4.1.4 Kits

Senescence β-Galactosidase Staining Kit	Cell Signaling Technology, Danvers, MA, USA
Pierce® BCA Protein Assay Kit	Perbio Science Deutschland GmbH, Bonn, GER
SuperSignal® West Pico Chemiluminescent Substrate	Thermo Fisher Scientific, Schwerte, GER

4.1.5   Tissue samples

Sample	Diagnosis
1	Autoimmune pancreatitis type 2
2	Autoimmune pancreatitis type 2
3	Autoimmune pancreatitis type 1
4	Autoimmune pancreatitis type 1
5	Hereditary pancreatitis
6	Alcoholic chronic pancreatitis
7	Alcoholic chronic pancreatitis
8	Alcoholic chronic pancreatitis
9	Alcoholic chronic pancreatitis
10	Alcoholic chronic pancreatitis
11	PDAC of the pancreatic head, G2
12	PDAC of the pancreatic head, G3
13	PDAC of the pancreatic head, G1
14	PDAC of the pancreatic head, G2
15	PDAC of the pancreatic head, G2
16	PDAC of the pancreatic body and tail, G2
17	PDAC of the pancreatic tail, G2
18	PDAC of the pancreatic tail, G2
19	PDAC of the pancreatic tail, G2
20	PDAC of the pancreatic tail, G2
21	Autoimmune pancreatitis type 1
22	Autoimmune pancreatitis type 2
23	Normal pancreas tissue

4.1.6 Cell lines

M1134 (PSCs)

Organism	Human
Tissue	Chronic pancreatitis
Origin	Isolated (via outgrowth method) and kindly provided by AG Erkan, Department of Surgery, Klinikum rechts der Isar
Culture properties	Adherent, cell culture medium

M1198 (PSCs)

Organism	Human
Tissue	Pancreatic ductal adenocarcinoma
Origin	Isolated (via outgrowth method) and kindly provided by AG Erkan, Department of Surgery, Klinikum rechts der Isar
Culture properties	Adherent, cell culture medium

M1223 (PSCs)

Organism	Human
Tissue	Chronic pancreatitis
Origin	Isolated (via outgrowth method) and kindly provided by AG Erkan, Department of Surgery, Klinikum rechts der Isar
Culture properties	Adherent, cell culture medium

M1245 (PSCs)

Organism	Human
Tissue	Pancreatic ductal adenocarcinoma
Origin	Isolated (via outgrowth method) and kindly provided by AG Erkan, Department of Surgery, Klinikum rechts der Isar
Culture properties	Adherent, cell culture medium

M151 (PSCs)

Organism	Human
Tissue	Chronic pancreatitis
Origin	Isolated (via outgrowth method) and kindly provided by AG Erkan, Department of Surgery, Klinikum rechts der Isar
Culture properties	Adherent, cell culture medium

M1248 (HSCs)

Organism	Human
Tissue	Chronic hepatitis
Origin	Isolated (via outgrowth method) and kindly provided by AG Erkan, Department of Surgery, Klinikum rechts der Isar
Culture properties	Adherent, cell culture medium

U251

Organism	Human
Tissue	Glioblastoma
Origin	ATCC: The Global Bioresource Center
Culture properties	Adherent, cell culture medium

4.1.7 Antibodies

Primary antibodies:

Product	Application /Dilution	Company	Reaction pattern/Expression in IHC
Anti-α-crystallin B (rabbit polyclonal)	IHC (1:200) IF (1:100)	Enzo Life Sciences GmbH, Loerrach, GER	Intracytoplasmic; α-crystallin A expression is restricted to the lens, while α-crystallin B is expressed in many tissues, especially peripheral nerves
Anti-α-SMA (mouse monoclonal; clone HHF35)	IHC (1:100)	Dako Deutschland GmbH, Hamburg, GER	Intracytoplasmic; expressed in smooth muscle, myoepithelial cells, myofibroblasts, activated stellate cells
Anti-α-SMA (mouse monoclonal; clone 1A4)	IF (1:100)	Abcam, Cambridge, UK	(not used for IHC)
Anti-α-SMA (rabbit polyclonal)	WB (1:2000)	Abcam, Cambridge, UK	(not used for IHC)
Anti-α-tubulin (mouse monoclonal; clone B-5-1-2)	WB (1:10000)	Sigma Aldrich, St. Louis, MO, USA	(not used for IHC)
Anti-CD34 (mouse monoclonal; clone QBEnd/10)	IHC (1:200)	Cell Marque, Rocklin, CA, USA	Intracytoplasmic; expressed in hematopoetic cells and vascular-associated tissue
Anti-CD56 (rabbit monoclonal; clone MRQ-42)	IHC (1:4)	Cell Marque, Rocklin, CA, USA	Intracytoplasmic; expressed in neurons, glia, neuroendocrine tissue (such as islets of the pancreas), skeletal muscle
Anti-desmin (mouse monoclonal; clone 33)	IHC (1:100)	BioGenex, San Ramon, CA, USA	Intracytoplasmic; expressed in skeletal muscle, smooth muscle and cardiac muscle
Anti-GAPDH (polyclonal)	WB (1:5000)	Santa Cruz, Heidelberg, GER	(not used for IHC)
Anti-NGF (rabbit polyclonal)	IHC (1:50) IF (1:100)	Abcam, Cambridge, UK	Intracytoplasmic; neural tissue
Anti-NGFR (rabbit polyclonal)	IHC (1:50) IF (1:25)	Santa Cruz, Heidelberg, GER	Intracytoplasmic and intranuclear; neural tissue
Anti-NT-3 (rabbit polyclonal)	IHC (1:100) IF (1:25)	Santa Cruz, Heidelberg, GER	Intracytoplasmic; neural tissue
Anti-SPARC (mouse monoclonal; clone ON1-1)	IHC (1:500)	Invitrogen™, Darmstadt, GER	Intracytoplasmic; glia, stromal cells, ECM
Anti-synaptophysin (rabbit polyclonal)	IHC (ready to use)	Roche Diagnostics, Mannheim, GER	Intracytoplasmic; pancreatic islets, peripheral nerves
Anti-tenascin C (mouse monoclonal; clone 49)	IHC (1:10)	Leica Biosystems, Wetzlar, GER	Intracytoplasmic; PSCs, ECM
Anti-TrkC (rabbit polyclonal)	IHC (1:500) IF (1:500)	Abcam, Cambridge, UK	Intracytoplasmic; neural tissue

Secondary antibodies:

Product	Application/Dilution	Company
Alexa Fluor 488 goat anti-mouse IgG (goat polyclonal)	IF (1:200)	Life Technologies GmbH, Darmstadt, GER
Alexa Fluor 546 goat anti-rabbit IgG (goat polyclonal)	IF (1:200)	Life Technologies GmbH, Darmstadt, GER
Biotin-labeled goat anti-mouse IgG (goat polyclonal)	IHC (ready to use)	KPL, Inc., Gaithersburg, MD, USA
Biotin-labeled goat anti-rabbit IgG (goat polyclonal)	IHC (ready to use)	KPL, Inc., Gaithersburg, MD, USA
ECL™ anti-mouse IgG (sheep polyclonal)	WB (1:2000)	GE Healthcare, Munich, GER
ECL™ anti-rabbit IgG (sheep polyclonal)	WB (1:2000)	GE Healthcare, Munich, GER
EnVision™ anti-rabbit (goat polyclonal)	IHC (ready to use)	Dako Deutschland GmbH, Hamburg, GER
Ventana ultraView™ HRP Universal Multimer (goat polyclonal)	IHC (ready to use)	Ventana Medical Systems, Inc., Basel, CH

4.1.8 Buffers

Blotting buffer

TRIS base	48 mM
Glycine	39 mM
SDS	0.025 %
Methanol	20 %

Citrate buffer

Citric acid	10 mM
pH 6	

Laemmli 5X

TRIS	312.5 mM
Glycerol	40 %
SDS	10 %
Bromophenol blue	0.005 %
β-Mercaptoethanol	20 %

Ponceau S

Ponceau S	0.1 %
Acetic acid	1 %

RIPA buffer

TRIS pH 7.4	20 mM
NaCl	150 mM
EDTA	1 mM
EGTA	1 mM
NP-40	1 %
Deoxycholic acid	0.5 %

Running buffer

TRIS base	12.5 mM
Glycine	9.6 mM
SDS	0.05 %

Running gel buffer 4X

TRIS-HCl	1.5 M
pH 8.8	

Stacking gel buffer 4X

TRIS-HCl	0.5 M
pH 6.8	

Stripping buffer

MetOH	10 %
Acetic acid	10 %

TBS 10X for Immunofluorescence

TRIS base	500 mM
NaCl	1380 mM
KCl	27 mM
pH 7.6	

TBS 10X for Western Blot

TRIS base	200 mM
NaCl	1360 mM
pH 7.6	

4.1.9 Software

Product	Company
Adobe Acrobat 9 Pro	Adobe Systems GmbH, Munich, GER
Aperio ImageScope	Leica Biosystems, Wetzlar, GER
AxioVision	Carl Zeiss AG, Jena, GER
Definiens Tissue Studio	Definiens AG, Munich, GER
GIMP 2.8	The GIMP Development Team; http://www.gimp.org/
Image J	National Institutes of Health, Bethesda, MD, USA
Microsoft Office 2007, 2010	Microsoft, Redmond, WA, USA
OlyVIA	Olympus Deutschland GmbH, Hamburg, GER
GraphPad Prism 7	GraphPad Software, Inc., La Jolla, CA, USA
R	R Development Core Team; http://www.r-project.org

4.1.10 Primer pairs

Primers for mycoplasma test:

Primer supermix 1

Name	Sequence	Concentration in supermix
Myco-Fwd 1	5'-ACA CCA TGG GAG TTG GTA AT-3'	5 µM
Myco-Fwd 1t	5'-ACA CCA TGG GAG CTG GTA AT-3'	5 µM
Myco-Rev 1tt	5'-CTT CTT CGA CTT TCA GAC CCA AGG CAT-3'	2.5 µM
Myco-Rev 1	5'-CTT CAT CGA CTT TCA GAC CCA AGG CAT-3'	2.5 µM
Myco-Rev 1cat	5'-CCT CAT CGA CTT TCA GAC CCA AGG CAT-3'	2.5 µM
Myco-Rev 1ac	5'-CTT CAT CGA CTT CCA GAC CCA AGG CAT-3'	2.5 µM

Primer supermix 2

Name	Sequence	Concentration in supermix
Myco-Fwd 2a	5'-ATT CTT TGA AAA CTG AAT-3'	2.5 µM
Myco-Fwd 2	5'-GTT CTT TGA AAA CTG AAT-3'	2.5 µM
Myco-Fwd 2cc	5'-GCT CTT TCA AAA CTG AAT-3'	2.5 µM
Myco-Rev 2ca	5'-GCA TCC ACC ACA AAC TCT-3'	2.5 µM
Myco-Rev 2	5'-GCA TCC ACC AAA AAC TCT-3'	2.5 µM
Myco-Rev 2at	5'-GCA TCC ACC AAA TAC TCT-3'	2.5 µM

4.2 Methods

4.2.1 Tissue collection

Tissue samples were obtained from patients who underwent pancreatic resection due to either pancreatic ductal adenocarcinoma or chronic pancreatitis at the Department of Surgery of the Ruprecht-Karls-Universitaet Heidelberg. Tissue samples were fixed in 4 % formalin and subsequently embedded in paraffin.

4.2.2 Ethic vote

Written informed consent was obtained from all patients.

The use of human tissue samples was approved by the local ethics committee at the Ruprecht-Karls-Universitaet Heidelberg.

4.2.3 Hematoxylin & Eosin stain

Sections of formalin-fixed, paraffin-embedded tissues mounted on microscope slides were deparaffinized in xylol and rehydrated in a descending alcohol series. Sections were then rinsed in distilled water and stained with hematoxylin for 5 minutes. The slides were rinsed in running tap water for 5 minutes to obtain differentiation. Afterwards, slides were stained with eosin for 5 minutes. The slides were rinsed in running tap water again and dehydrated in an ascending alcohol series. To protect the tissue, coverslips were placed onto slides with a drop of mounting medium.

4.2.4 Movat's pentachrome stain

In order to be able to assess the composition of the stroma, tissues were stained with Movat's pentachrome stain, which dyes nuclei and elastic fibers black, collagen and reticular fibers yellow, mucin and ground substance blue and fibrin and muscle tissue red.

All steps were conducted at room temperature. Sections of formalin-fixed, paraffin-embedded tissues mounted on microscope slides were deparaffinized in xylol and rehydrated in a descending alcohol series. After being further hydrated in running distilled water, slides were pre-treated with 3 % acetic acid for 30 seconds. Afterwards, they were stained with 1 % Alcian blue solution for 30 minutes. After being washed in running tap water for 2 minutes, nuclei were stained with Verhoeff's stock solution (Verhoeff's solution A, B and C diluted 3:2:1) for 8 minutes. Following this, slides were submerged in 1 % iron(III) chloride for 1 minute to obtain differentiation. After being washed with tap water for 10 minutes, cytoplasm was stained with brilliant-croceine-fuchsine-acid solution for 6 minutes. Subsequently, slides were dipped in 1 % acetic acid for 30 seconds and thereafter submerged in 2 % phosphotungstic acid for 15 minutes for differentiation. Slides were then placed in 1 % acetic acid once again for 1 minute and afterwards dehydrated twice with 99 % ethanol for 3 and then 15 minutes. Fibers were then stained with Safron du Gâtinais solution for 15 minutes. Finally, tissues were dehydrated in an ascending alcohol series and coverslips were mounted onto slides with a drop of mounting medium.

Software-based morphometric analysis of Movat staining

The morphometric analysis of stainings was kindly performed by Dr. Annette Feuchtinger (Helmholtz Zentrum Muenchen, Neuherberg, Germany). Slides were analyzed using the Definiens Tissue Studio digital pathology image analysis software.

For evaluation of the stromal reaction, the stroma on Movat's-pentachrome-stained slides was manually selected as region of interest ("ROI"). Large non-stromal structures within the stroma, like ducts or vessels, were completely excluded manually ("non-ROI"). A threshold was set to determine when the program would count an area as yellow and when it would count an area as blue. The total blue area within the ROI, the total yellow area within the ROI, the total "neither blue nor yellow" area within the ROI, and the total "either blue or yellow, but not definitely distinguishable" area within the ROI ("candid", subsequently interpreted as "mixed areas" with both collagens and mucins) were calculated by the software. As a result of the computer-assisted analysis, we obtained absolute numbers for yellow and blue areas in each slide stained with Movat's stain. In order to take into account that each slide has a different total area, relative numbers, respectively percentages, for yellow and blue areas in each slide were calculated and used for further analysis. The percentages of

yellow areas in tissue sections from cases of chronic pancreatitis were compared to the percentages of yellow areas in tissue sections from cases of PDAC. Subsequently, percentages of blue areas in tissue sections from cases of chronic pancreatitis were compared to percentages of blue areas in tissue sections from cases of PDAC. Statistical significance was tested by performing the Mann-Whitney U test on the software GraphPad Prism 7.

In order to compare the stromal composition and IHC results, areas that were positive for either NT-3 or α-SMA/SPARC in IHC were manually defined as ROI within Movat-stained slides. The subsequent morphometric and statistical analyses were perfomed as described above.

4.2.5   Immunohistochemistry

Anti-NGF, anti-NGFR, anti-NT-3, anti-SPARC, anti-TrkC and anti-α-crystallin-B stainings were all established and performed using the Dako AutoStainer staining system.

Sections of formalin-fixed, paraffin-embedded tissues were mounted on microscope slides and dried at 37 °C in a dry incubator overnight. Slides were put into a 65 °C dry incubator the next day until paraffin was completely melted. They were then deparaffinized in xylol, rehydrated in a descending alcohol series and washed with 1X Dako wash buffer. Heat-induced or enzymatic epitope retrieval was then performed. For the former, slides were immersed in citrate buffer, boilt in a pressure cooker for 20 minutes and subsequently allowed to cool down in the buffer for 30 minutes (anti-NGF, anti-NGFR, anti-SPARC, anti-TrkC, anti-α-crystallin-B). The latter was conducted by incubating slides with pronase E diluted 1:20 with Dako wash buffer for 4 minutes at 37 °C (anti-NT-3). From this point on, all following steps were conducted at room temperature. Slides were rinsed in Dako wash buffer three times and loaded onto the Dako AutoStainer. Throughout the protocol, slides were rinsed with 1X Dako wash buffer between steps.

Endogenous peroxidase was blocked by adding 3 % H_2O_2 in methanol for 10 minutes. Afterwards, nonspecific antibody binding was blocked with 3 % normal goat serum for 30 minutes. Slides were subsequently incubated with the primary antibody at the appropriate dilution for 1 hour. Following this, slides were incubated with biotinylated secondary antibody goat anti-mouse (for SPARC staining), goat anti-rabbit (for NGFR staining) or Dako EnVision™ detection system anti-rabbit (for NGF, NT-3, TrkC and α-crystallin-B staining) for 30 minutes. When biotinylated secondary antibody was used, streptavidin horseradish peroxidase was subsequently added for 30 minutes. Next, Dako Bright DAB (3,3'-diaminobenzidine) was added for 5 minutes. Following this, slides were rinsed with distilled water, and Mayer's Hemalaun was added for 10 minutes for counterstaining. The slides were then rinsed with running tap water for another 10 minutes to achieve hemalaun bluing. Finally, slides were dehydrated in an ascending alcohol series and coverslips were applied using a robotic coverslipper.

Contrary to the aforementioned immunostainings, anti-α-SMA, anti-CD34, anti-CD56, anti-desmin, anti-synaptophysin and anti-tenascin-C stainings had already been established in routine diagnostics at the Institute of Pathology, Technische Universitaet Muenchen, Munich, Germany.

They were performed with the XT ultraView™ DAB v3 Detection Kit on the Ventana BenchMark XT automated IHC/ISH slide staining system. Ventana Liquid Coverslip (LCS) was applied throughout the protocol as appropriate in order to minimize the evaporation of aqueous reagents. Slides were rinsed between steps with Ventana Reaction Buffer (TRIS-based buffer at pH 7.6).

Sections of formalin-fixed, paraffin-embedded tissues were mounted on microscope slides, dried at 37 °C in a dry incubator overnight and loaded onto the Ventana BenchMark XT automated IHC/ISH staining system. Slides were deparaffinized at up to 76 °C heat with Ventana EZ Prep™ deparaffinization solution, followed by heat-induced epitope retrieval in Ventana Cell Conditioning 1 (EDTA buffer at pH 8.4) at up to 100 °C. Slides were incubated with Ventana ultraView™ Inhibitor (3 % H_2O_2) for 4 minutes to inactivate the endogenous peroxidase. Following this, slides were incubated with the appropriately diluted primary antibody at 37 °C for either 28 minutes (anti-α-SMA, anti-tenascin-C) or 32 minutes (anti-CD34, anti-CD56, anti-desmin, anti-synaptophysin). Subsequently, slides were incubated with Ventana ultraView™ Horseradish Peroxidase Universal Multimer (a cocktail of HRP-labeled anti-rabbit, anti-mouse IgG and anti-mouse IgM) for 8 minutes. Next, slides were incubated with Ventana ultraView™ DAB Chromogen (3,3-diaminobenzidine tetrahydrochloride) and Ventana ultraView™ DAB H_2O_2 (0.04 % H_2O_2) for 8 minutes. A drop of Ventana ultraView™ Copper (5 g/L copper sulfate) was added and incubated for 4 minutes to intensify the staining reaction. Slides were then counter-stained with hemalaun for 8 minutes. Bluing was achieved by adding Ventana Bluing Reagent for 4 minutes. Finally, slides were rinsed and taken out of the machine for coverslips to be mounted using a robotic coverslipper.

All IHC staining results were evaluated under a light microscope regarding the localization of the staining with reference to structures like acini (*periacinar*), ducts (*periductal*), lobuli (*inter-/perilobular*) or tumor cell formations (*perilesional*) and the respective frequency (e.g. how frequently a staining was observed in a certain localization in a slide) as well as the intensity of the staining. Both were graduated in + (low frequency/weak intensity), ++ (moderate frequency/intensity) and +++ (high frequency/strong intensity). The overall staining pattern was also categorized as either focal or diffuse.

4.2.6 Immunofluorescence

Cells were seeded onto sterilized coverslips with a diameter of 11 mm that had been placed in the wells of a 24-well cell culture plate. Cells were allowed to grow in their standard culture medium for

at least 24 hours. After this time, culture medium was removed, cells were washed briefly with PBS and subsequently fixed with chilled methanol for 5 minutes at room temperature. Cells were then washed with TBS buffer (50 mM TRIS, 138 mM NaCl, 2.7 mM KCl, pH 7.6) three times for 5 minutes each, permeabilized with permeabilizing solution (TBS containing 0.25 % Triton X-100) for 5 minutes and again washed with TBS buffer three times for 5 minutes each. Afterwards, nonspecific antibody binding was blocked by incubating the cells with blocking solution (TBS containing 10 % goat serum and 0.1 % Triton X-100) for 30 minutes at room temperature. After washing three times with TBS for 5 minutes each, cells were incubated with the primary antibody appropriately diluted in blocking solution overnight at 4 °C in a humidified chamber. After washing three times with TBS for a total of 15 minutes again, slides were incubated with the Alexa Fluor conjugated secondary antibody diluted in blocking solution (goat anti-mouse or goat anti-rabbit, 1:200 each) for 60 minutes at room temperature. This step, as well as all following steps, was performed with the 24-well plate wrapped in aluminum foil to prevent photo-sensitive reagents from fading. Cells were then washed with TBS again three times for 5 minutes each, before being counterstained with Hoechst 33342 (0.5 µg/mL) for 5 minutes. After they were washed with TBS twice for 5 minutes each and with distilled water for 5 minutes, cells on coverslips were taken out of the wells and placed onto microscopic glass slides provided with a drop of anti-fade mounting medium.

Slides were examined under a fluorescence microscope (Carl Zeiss AG, Jena, GER) and images were obtained with the Zeiss AxioVision software.

Cells from the glioblastoma cell line U251 were used as positive control for the tested neural markers.

4.2.7 Cell culture

4.2.7.1 Maintenance of cell lines

Pancreatic stellate cells (PSCs) as well as hepatic stellate cells (HSCs) were maintained in culture medium containing 50 % Ham's F-12 nutrient medium and 50 % low-glucose D-MEM (1 g/L) supplemented with 20 % FBS (heat denaturated at 56 °C for 30 minutes), 1 % penicillin/streptomycin and 1 % amphotericin B at 37 °C and 5 % CO_2.

U251, which served as positive control, were maintained in high-glucose D-MEM (4.5 g/L) supplemented with 10 % FBS (heat-denaturated at 56 °C for 30 minutes) and 1 % penicillin/streptomycin at 37 °C and 5 % CO_2.

4.2.7.2 Counting of cells

Cells were counted using an improved Neubauer hemocytometer. Cell suspensions of 15 μL were mixed with trypane blue 1:1 to distinguish dead cells from living cells.

4.2.7.3 Splitting of cells

80 % confluent cells were washed with PBS and detached by trypsinization at 37 °C. The reaction was stopped by adding standard culture medium and cells were transferred to a new flask at the appropriate concentration.

4.2.7.4 Freezing of cells

Cells at 80 % confluence were washed with PBS and detached by trypsinization at 37 °C. They were then resuspended in complete medium and centrifuged at 1200 rpm for 3 minutes at room temperature. Cell pellets were resuspended in complete medium containing 20 % DMSO. 1 mL aliquots were transferred into cryovials, frozen slowly at -80 °C in a cryo freezing container for at least 48 hours and then moved into liquid nitrogen for long term storage.

4.2.7.5 Thawing of cells

Cryo-vials containing frozen cells were taken from liquid nitrogen and put directly into a 37 °C water bath. When thawed, they were moved into 15 mL falcon tubes and 5 mL pre-warmed medium was added. Cells were then centrifuged at 1200 rpm for 3 minutes at room temperature. Subsequently, the resulting pellets were resuspended in complete medium and transferred to a culture flask or dish.

4.2.7.6 Mycoplasma test

Nested PCR was used to rule out the possibility of mycoplasma contamination (Uemori et al., 1992). For this purpose, 1 mL of medium was taken from an 80 % confluent cell culture flask. The medium was diluted 1:10, incubated for 5 minutes at 95 °C and subsequently centrifuged briefly. The supernatant was used directly as template for the PCR.

For the first PCR, a 25 μL reaction was set as follows:

dH$_2$O	15 μL
10X buffer (15 mM Mg^{2+})	2.5 μL
dNTPs (10 mM each)	0.5 μL

Primer supermix 1	1.0 µL
Taq polymerase	1.0 µL
Supernatant	5.0 µL

The amplification parameters were set as follows:

94 °C	4 min initial denaturation

35 cycles with:

95 °C	30 sec denaturation
55 °C	2 min annealing
72 °C	1 min elongation
72 °C	7 min final elongation

For the second PCR, a 25 µL reaction was set as follows:

dH$_2$O	19 µL
10X buffer (15 mM Mg^{2+})	2.5 µL
dNTPs (10 mM each)	0.5 µL
Primer supermix 2	1.0 µL
Taq polymerase	1.0 µL
Supernatant	1.0 µL

The amplification parameters were set as follows:

94 °C	4 min initial denaturation

30 cycles with:

95 °C	30 sec denaturation
55 °C	2 min annealing
72 °C	1 min elongation
72 °C	7 min final elongation

The amplification product was visualized by gel electrophoresis on 1 % agarose gel in TBE containing 0.5 µg/mL ethidium bromide. Gel images were taken with a gel documentation system.

4.2.7.7   Senescence test

To rule out cellular senescence, cells were tested with a β-galactosidase senescence staining kit that was used according to the manufacturer's instructions.

4.2.7.8   Matrigel^{TM} coating

To coat one well of a 6-well cell culture plate, 200 µL of Matrigel^{TM} diluted 1:3 with serum-free medium were used. Matrigel^{TM} was then allowed to solidify overnight at 37 °C. Subsequently, approximately 25 000 PSCs per well were seeded and maintained in medium containing 5 % FBS for 5-7 days.

4.2.7.9   Oil Red O staining

Approximately 25 000 PSCs per well were seeded onto either Matrigel^{TM}-coated or un-coated wells of a 6-well cell culture plate. They were allowed to grow in medium containing 5 % FBS (Matrigel^{TM}-coated wells) or their standard culture medium (un-coated wells).

All following steps were conducted at room temperature. Cells were fixed with 4 % formalin for 10 minutes. After being washed two times with PBS for 1 minute each, they were covered with ready-to-use Oil Red O solution for 10 minutes. Subsequently, they were washed extensively with distilled water and examined under a light microscope.

4.2.8   Protein extraction

Culture medium was removed from cells grown in 6-well cell culture plates and cells were rinsed with chilled PBS. Afterwards, chilled lysis buffer (20 mM TRIS pH 7.0, 150 mM NaCl, 1 mM EDTA, 1 mM EGTA, 1 % NP-40, 0.5 % deoxycholic acid) supplemented with commercial protease and phosphatase inhibitor cocktails was added, cells were scraped off and collected in Eppendorf tubes. After 15 minutes of incubation on ice, samples were centrifuged at 15 000 rpm for 15 minutes at 4 °C. Pellets of cell debris were discarded while supernatants were collected. The protein concentration in the soluble fractions was determined using the BCA protein assay. Extracts were aliquoted and stored at -20 °C.

4.2.9 Protein quantification

To ensure equal loading in SDS-PAGE, protein concentrations of the extracts were determined. For this purpose, a BCA protein assay kit was used according to the manufacturer's instructions. Absorbance was determined at 550 nm with a microplate reader, a standard curve was created and protein concentrations in samples were extrapolated from the linear part of this curve.

4.2.10 Western blot

Using the data collected via protein quantification, an appropriate volume of each sample was taken in order to obtain 50 µg of protein from each. These volumes were then mixed with 5 µL 5X Laemmli sample buffer (62.5 mM TRIS, 8 % glycerol, 2 % SDS, 0.001 % bromphenol blue, 4 % β-mercaptoethanol) and heated for 5 minutes at 95 °C and 700 rpm. Afterwards, samples were chilled on ice and centrifuged briefly. Gel electrophoresis was conducted in running buffer (12.5 mM TRIS base, 9.6 mM glycine, 0.05 % SDS) using the Biorad mini-PROTEAN Electrophoresis 3 cell system at 25 mA. Proteins were then transferred with blotting buffer (48 mM TRIS base, 39 mM glycine, 20 % methanol, 0.025 % SDS, pH 8.3) to nitrocellulose membranes, applying 100 V for around 2.5-3 hours, depending on protein size. Successful transfer was verified with Ponceau S staining, which was afterwards removed by rinsing the membranes with TBS-T (20 mM TRIS, 136 mM NaCl, 0.1 % Tween-20, pH 6.8). Membranes were blocked either with 5 % BSA in TBS-T for 2 hours at 37 °C or with 5 % nonfat dry milk in TBS-T at room temperature for 1 hour to inhibit unspecific binding. The primary antibody was applied after appropriate dilution in TBS-T with 3 % BSA and the membrane was incubated overnight at 4 °C. After three washes with TBS-T in order to remove unbound primary antibody, horseradish-peroxidase-conjugated secondary antibody (diluted 1:2000 in TBS-T with 5 % nonfat dry milk) was added for 1 hour at room temperature. The membrane was then washed three times with TBS-T again before signals were visualized with a chemiluminescent substrate kit and developed using a photo-sensitive imaging film. All steps were performed with gentle agitation on a rotary shaker. Membrane stripping was performed using a stripping buffer (10 % methanol and 10 % acetic acid) for 30 minutes at room temperature.

4.2.11 Statistical analysis

Results are given as medians. Graphs (boxplots) were created using the software R.
Mann-Whitney U test was performed using the software GraphPad Prism 7 to determine significance. Statistical significance was defined as $p < 0.05$.

5   Results

5.1   Histology

5.1.1   Hematoxylin & Eosin stain

H&E slides were prepared to select the cases to be investigated in this study and to assess their morphology. Hereafter, cases were chosen as follows: Five cases consistent with the typical histology of chronic alcoholic pancreatitis, three cases consistent with the typical histology of AIP type 1, three cases consistent with the typical histology of AIP type 2, one case consistent with the typical histology of hereditary pancreatitis (figure 2) as well as ten cases of PDAC (figure 3). Fibrosis patterns and characteristic morphologies of different subtypes of chronic pancreatitis have been previously described (see 2.2.1).
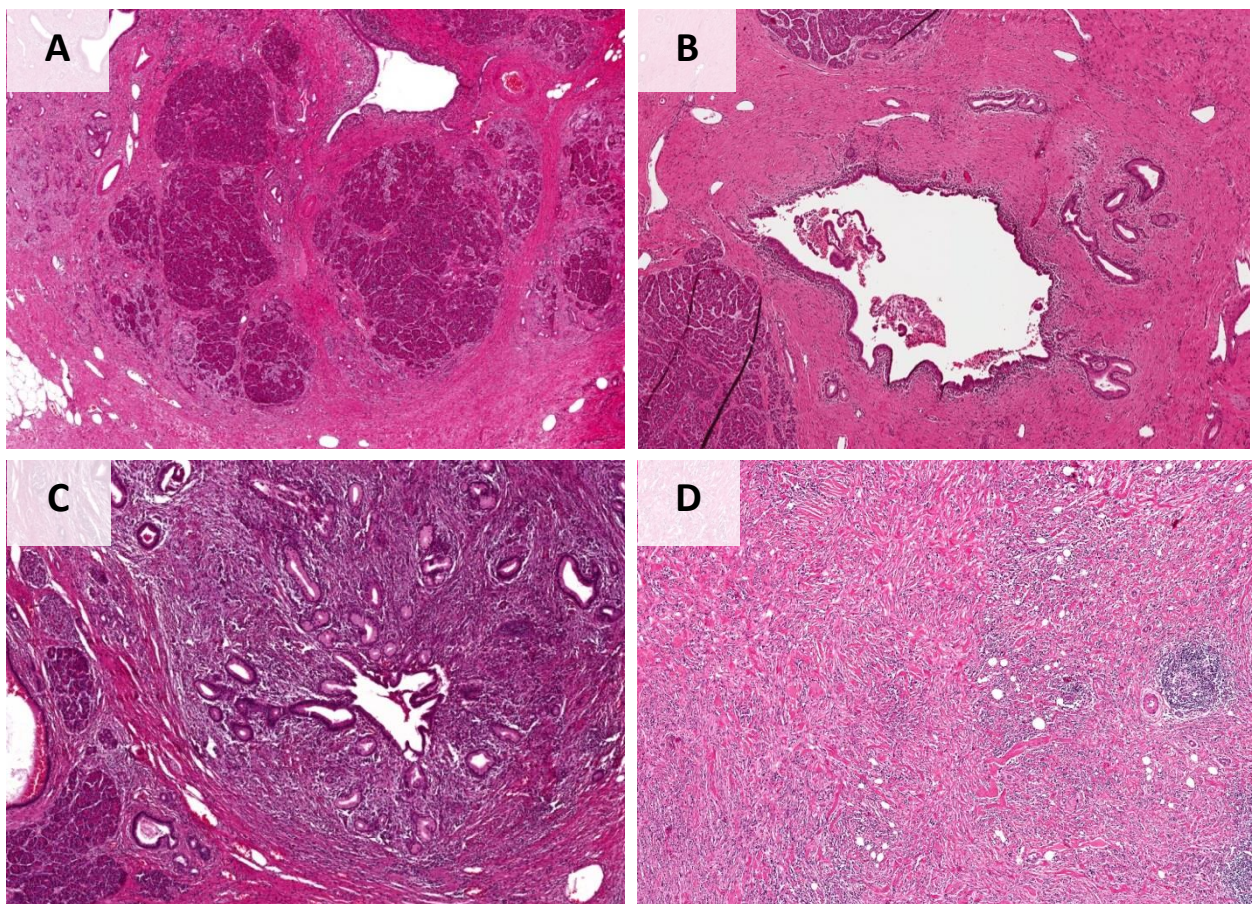
Figure 2. H&E staining of four exemplary CP cases. **A.** Chronic alcoholic pancreatitis with typical inter-/perilobular pattern of fibrosis. **B.** Hereditary pancreatitis with dilated duct and typical periductal pattern of fibrosis. **C.** AIP type 1 with abundant periductal lymphoplasmacellular infiltrate and narrowed duct. **D.** AIP type 2 with storiform fibrosis.

Cases of PDAC also display different patterns of fibrosis with a more densely vs. a more loosely packed stroma (figure 3).
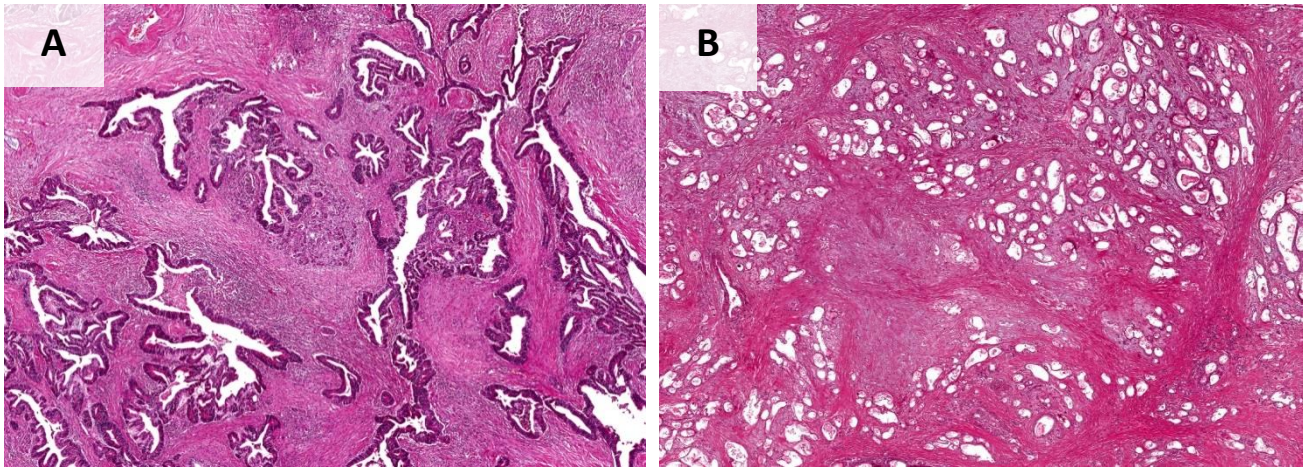

Figure 3. H&E staining of two exemplary PDAC cases. **A.** Dense stroma in PDAC. **B.** Loose stroma in PDAC.

5.1.2   Movat's pentachrome stain

To assess the composition of the stroma and distinguish areas of remodeling from areas of mature fibrosis, tissue sections of all cases included in this study were stained with Movat's pentachrome stain. Areas of mature fibrosis possess high amounts of collagen and therefore stain yellow. Areas of remodeling, which naturally comprise more mucins and ground substance than areas of mature fibrosis, stain blue or green.

Interestingly, cases of chronic pancreatitis showed significantly higher percentages of yellow-stained areas (median 42 %) compared to cases of PDAC (median 6 %) (p = 0.004, two-tailed, Mann-Whitney U = 18, n_1 = 12, n_2 = 10). In reverse, cases of PDAC showed significantly higher percentages of blue-stained areas (median 52 %) compared to cases of chronic pancreatitis (median 17 %) (p = 0.0002, two tailed, Mann-Whitney U = 8, n_1 = 12, n_2 = 10) (figure 4 & 5). Especially high yellow percentages were observed in cases of alcoholic pancreatis as well as in the case of hereditary pancreatitis, while cases of AIP showed lower percentages of yellow-stained areas.
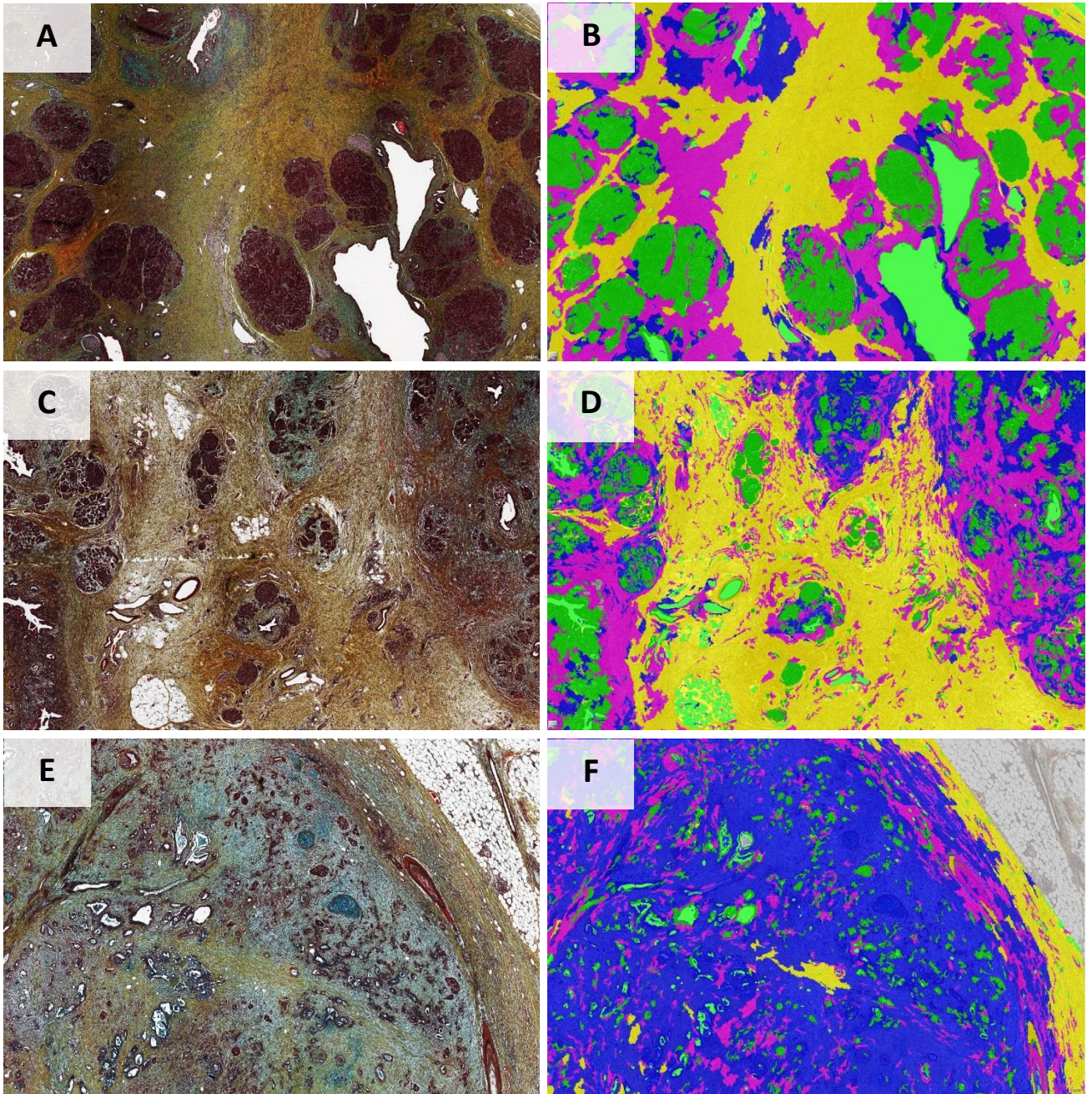
Figure 4. Tissue sections stained with Movat's pentachrome stain and how they were processed by the Definiens Tissue Studio software. Areas recognized as yellow or blue are displayed in the respective color. Pink areas represent "mixed" areas, which could not be assigned to yellow or blue. Green areas represent non-stromal areas such as ducts or acini. **A.** Alcoholic CP case stained with Movat's stain. **B.** Same case displayed in Definiens Tissue Studio. **C.** AIP case stained with Movat's stain. **D.** Same case displayed in Definiens Tissue Studio. **E.** PDAC case stained with Movat's stain. **F.** Same case displayed in Definiens Tissue Studio.
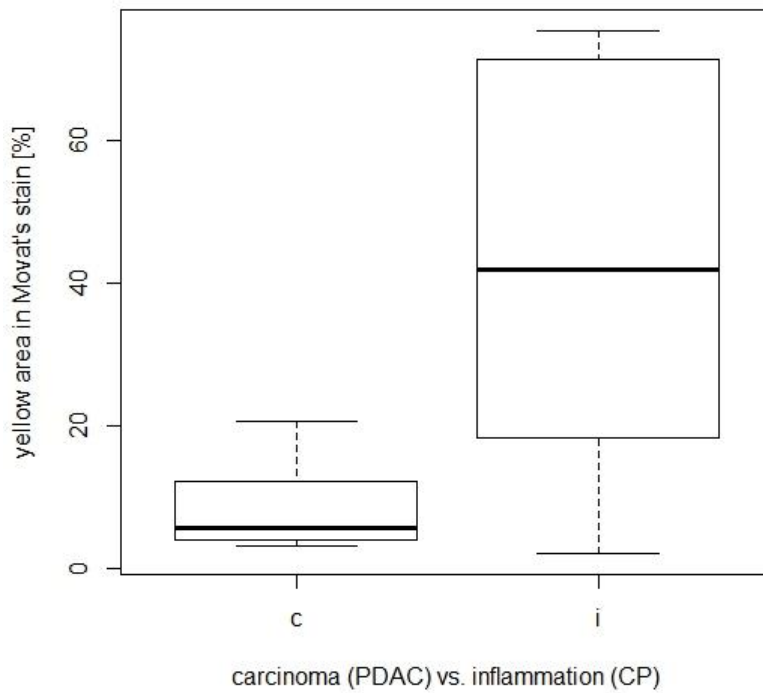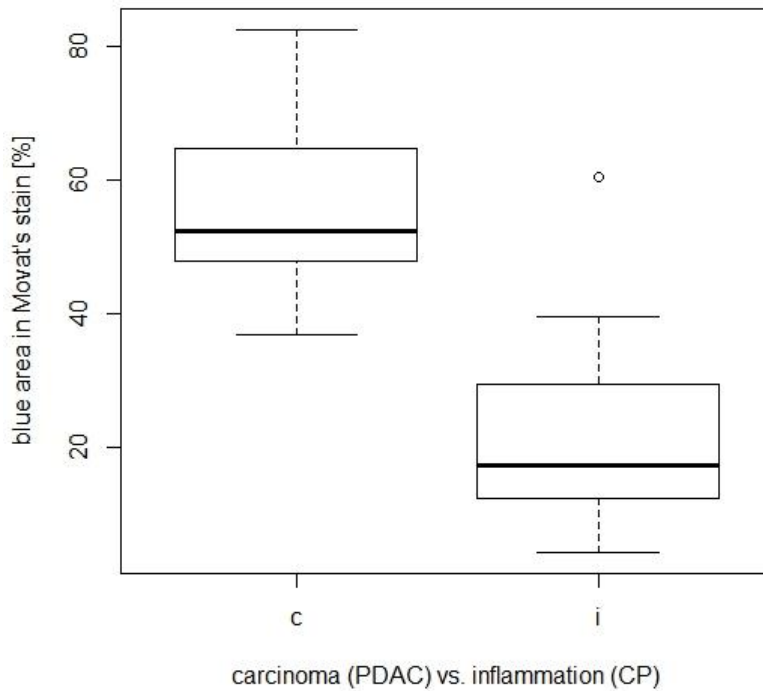
Figure 5. Boxplots comparing percentages of yellow and blue areas in cases of PDAC vs. cases of CP stained with Movat's pentachrome stain. **A.** Yellow areas are significantly larger in CP cases (median 41.965 %) than in PDAC cases (median 5.775 %) (p = 0.004). **B.** Conversely, blue areas are significantly larger in PDAC cases (median 52.41 %) than in CP cases (median 17.215 %) (p = 0.0002).

5.1.3   Immunohistochemistry

Tissue sections were examined by means of immunohistochemistry with antibodies raised against several proteins that have already been proposed as PSC markers. Moreover, using the previously elaborated similarities between PSCs and HSCs (see 2.4.2), tissue sections were tested for several HSC markers.

5.1.3.1   α-Crystallin B

Alpha-crystallins are structural proteins abundant in the vertebrate eye lens. They are members of the small heat-shock protein super family (sHSPs) and have chaperone-like abilities (Horwitz, 1992). Thus, they are thought to maintain the eye lens's transparency and refraction index by preventing denatured proteins from aggregating and precipitating (Christopher et al., 2014; Maulucci et al., 2011). While α-crystallin A is almost exclusively found in the lens, α-crystallin B is expressed widely in many tissues. For example, α-crystallin B shows a distinct expression in peripheral nerves and its overexpression seems to be associated with various neurological diseases (van Rijk & Bloemendal, 2000). It has also been proposed as a cancer biomarker, for example in breast cancer (Moyano et al., 2006).

Alpha-crystallin B is known to be expressed in HSCs (Cassiman et al., 2002; Cassiman et al., 2001b).

Own data demonstrate that alpha-crystallin B showed a **periacinar** staining of **low frequency** in 10 out of 12 CP cases (83.3 %) and in 7 out of 10 PDAC cases (70 %) (figure 6 A). Other localizations of α-crystallin-B-positive cells included **intralobular** and **inter-/perilobular** areas. Staining of single cells and/or a diffuse staining of fibrotic areas unrelated to lobuli or ducts were observed less frequently (figure 6 B). The staining had an overall **moderate intensity** in 12/22 cases (54.54 %), but showed a broad range from low over moderate to high intensity. The staining pattern was classified as **focal** in 16 out of 22 cases (72.72 %). Notably, α-crystallin-B-positive cells were mostly found in areas of well-preserved acini. A low-frequency medium-intensity periacinar staining could also be seen in normal pancreatic tissue. Taken together, this suggests that α-crystallin B might be a marker of quiescent PSCs. Tumor cells stained for α-crystallin B in 10 out of 10 PDAC cases (100 %), showing a high intensity and a diffuse staining pattern (figure 6 B).

Table 2. Evaluation of α-crystallin staining.

Case	Localization and frequency of staining in PSCs/fibrosis	Intensity of staining in PSCs/fibrosis	Pattern of staining	Comments
1 – AIP type 2	periacinar +	++	focal	-
2 – AIP type 2	periacinar + intralobular +	++	focal	-
3 – AIP type 1	periacinar + interlobular+	++	focal	weak staining of part of the ductal epithelium and acini
4 – AIP type 1	-	-	-	weak staining of part of the ductal epithelium and acini
5 – Hereditary CP	periacinar +	++	focal	weak staining of part of the ductal epithelium and acini
6 – Alcoholic CP	periacinar +	++	focal	weak staining of part of the ductal epithelium and acini
7 – Alcoholic CP	periacinar +	+	focal	weak staining of part of the ductal epithelium and acini
8 – Alcoholic CP	periacinar +	++	focal	weak staining of part of the ductal epithelium and acini
9 – Alcoholic CP	periacinar + intralobular +	++	focal	weak staining of part of the ductal epithelium
10 – Alcoholic CP	-	-	-	-
11 – PDAC	periacinar + single cells in fibrosis +	+	focal	staining of tumor cells
12 – PDAC	periacinar + single cells in fibrosis +	++	focal	staining of tumor cells
13 – PDAC	single cells in fibrosis +	++	focal	staining of tumor cells
14 – PDAC	periacinar + single cells in fibrosis +	+	focal	staining of tumor cells
15 – PDAC	periacinar +	++	focal	staining of tumor cells
16 – PDAC	periacinar + diffuse in fibrosis +++	++	diffuse	staining of tumor cells
17 – PDAC	-	-	-	staining of tumor cells
18 – PDAC	periacinar + diffuse in fibrosis ++	+	diffuse	staining of tumor cells

19 – PDAC	periacinar + inter-/perilobular + diffuse in fibrosis +	+++	focal	staining of tumor cells
20 – PDAC	-	-	-	staining of tumor cells
21 – AIP type 1	periacinar + intralobular + inter-/perilobular +	+++	focal	-
22 – AIP type 2	periacinar +	++	focal	-
Normal pancreatic tissue	periacinar +	++	focal	-
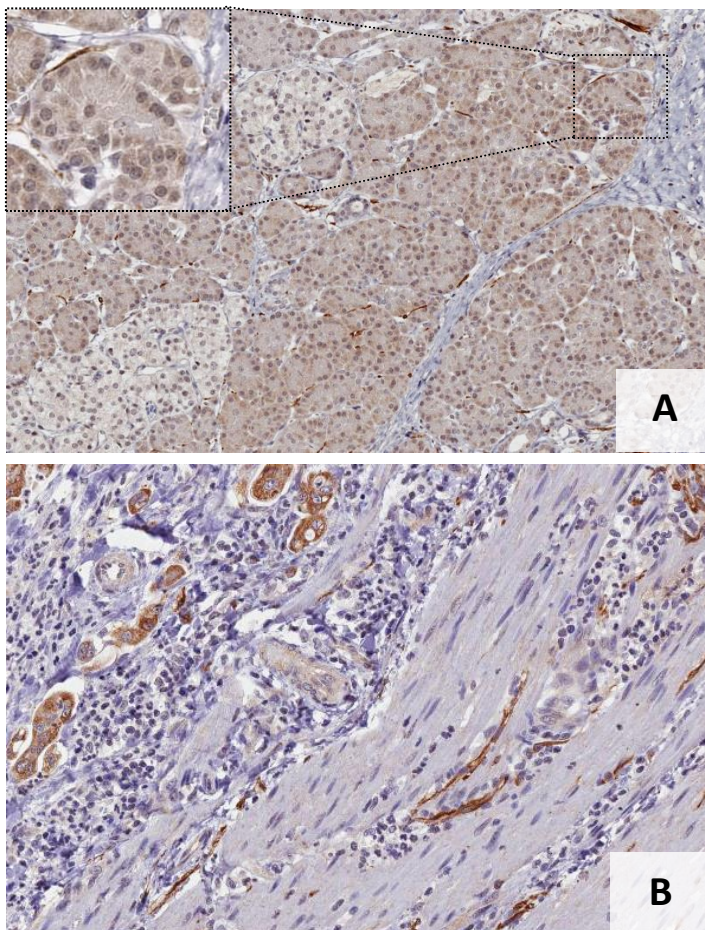
Figure 6. IHC for α-crystallin B. **A.** Periacinar and interlobular staining of single PSCs in a case of AIP type 1. **B.** Staining of single cells in the fibrosis areas as well as staining of tumor cells in a case of PDAC.

5.1.3.2 α-SMA

Actins comprise a family of microfilament-forming cytoskeletal proteins that play an important role in cell structure and motility (Mogilner & Oster, 1996; Pollard & Borisy, 2003). Alpha-smooth muscle actin (α-SMA) is the actin isoform found in smooth muscle, including vascular smooth muscle.

Alpha-SMA is well-established as a marker for activated HSCs (Ramadori et al., 1990; Rockey et al., 1992) as well as activated PSCs (Apte et al., 1998) or PSCs that undergo the transition from an inactivated to an activated phenotype, respectively (Krizhanovsky et al., 2008).

In our study, the localization of α-SMA staining was **inter-/perilobular** in 6 out of 12 CP cases (50 %) (figure 7 A). Other staining localizations that were less frequently observed in cases of CP include a **periductal** and **intralobular** staining as well as a **diffuse** staining of the fibrotic tissue (figure 7 B-D). In all cases of PDAC, a prominent **perilesional** staining for α-SMA could be seen (100 %) (figure 7 E & F). A perilesional staining of cells was also found in a lymph node metastasis included in one PDAC case (figure 7 G). The intensity of α-SMA **varied** strongly between individual cases. The predominant staining pattern of α-SMA was **diffuse**, as found in 19 out of 22 cases (83.36 %). Differently than in cases of CP or PDAC, α-SMA showed a periductal and intralobular staining in normal pancreatic tissue.

Table 3. Evaluation of α-SMA staining.

Case	Localization and frequency of staining in PSCs/fibrosis	Intensity of staining in PSCs/fibrosis	Pattern of staining	Comments
1 – AIP type 2	periductal ++ intralobular ++ inter-/perilobular ++	++	diffuse	-
2 – AIP type 2	inter-/perilobular ++	++	diffuse	-
3 – AIP type 1	inter-/perilobular +	++	diffuse	-
4 – AIP type 1	periductal ++ diffuse in fibrosis +++	++	diffuse	-
5 – Hereditary CP	diffuse in fibrosis ++	+	diffuse	-
6 – Alcoholic CP	periductal +	+++	focal	-
7 – Alcoholic CP	diffuse in fibrosis +	+	diffuse	-
8 – Alcoholic CP	inter-/perilobular ++	+++	diffuse	-
9 – Alcoholic CP	intralobular + inter-/perilobular +	++	diffuse	-
10 – Alcoholic CP	periductal +	+	diffuse	-
11 – PDAC	perilesional ++	++	diffuse	perilesional staining in lymph node metastasis
12 – PDAC	perilesional ++ inter-/perilobular ++	++	diffuse	-
13 – PDAC	perilesional +++	++	focal	-
14 – PDAC	perilesional +	+	diffuse	-
15 – PDAC	perilesional +	++	focal	-
16 – PDAC	perilesional +++	+++	diffuse	-
17 – PDAC	perilesional ++	++	diffuse	-
18 – PDAC	perilesional +++ inter-/perilobular +	+++	diffuse	-
19 – PDAC	perilesional +	++	diffuse	-
20 – PDAC	perilesional ++	+	diffuse	-
21 – AIP type 1	diffuse in fibrosis +++	+++	diffuse	-
22 – AIP type 2	inter-/perilobular +++	+++	diffuse	-
Normal pancreatic tissue	periductal ++ intralobular +	++	diffuse	-
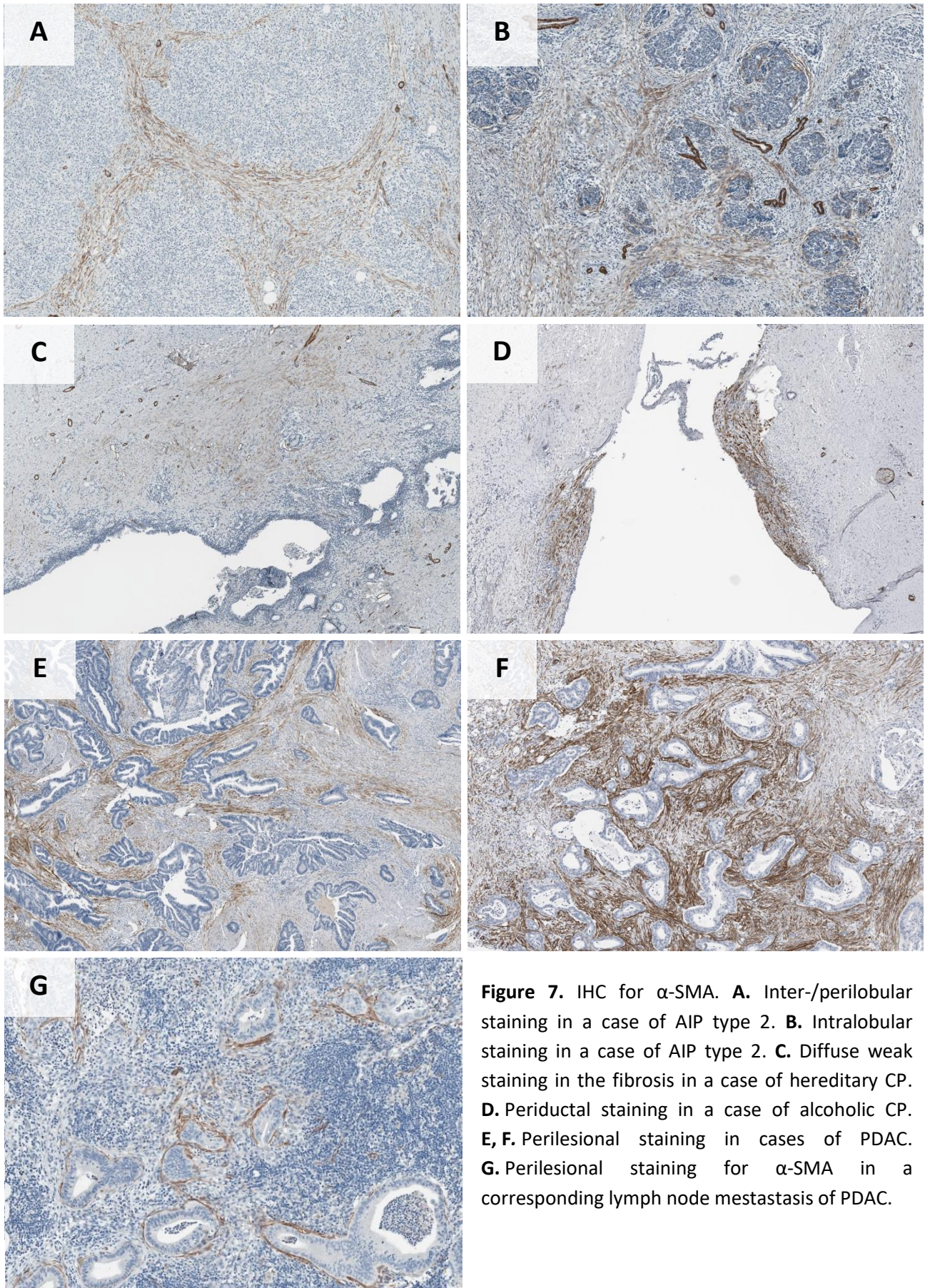
Figure 7. IHC for α-SMA. **A.** Inter-/perilobular staining in a case of AIP type 2. **B.** Intralobular staining in a case of AIP type 2. **C.** Diffuse weak staining in the fibrosis in a case of hereditary CP. **D.** Periductal staining in a case of alcoholic CP. **E, F.** Perilesional staining in cases of PDAC. **G.** Perilesional staining for α-SMA in a corresponding lymph node mestastasis of PDAC.

5.1.3.3 CD34

CD34 is a cell surface protein that was first identified in hematopoietic stem and progenitor cells (Civin et al., 1984). However, it has been established that CD34 can also be found in various other cell types, such as vascular endothelial cells (Fina et al., 1990; Sidney et al., 2014). This is why blood vessels, especially capillaries, stain positive for CD34. With its exact function still being unknown, CD34 is thought to play an important role in cell adhesion (Healy et al., 1995) and migration (Nielsen & McNagny, 2009).

CD34 has been proposed as a PSC marker (Habisch et al., 2010). In the following description, only the staining of stromal cells other than endothelia is considered.

IHC staining with an antibody raised against CD34 resulted in a **periacinar** staining in 10 out of 12 CP cases (83.3 %), an **inter-/perilobular** staining as well as an **intralobular** staining in 9 out of 12 CP cases (75 %) and a **periductal** staining in 7 out of 12 CP cases (58.3 %) (figure 8 A & B). A staining distributed **diffusely in the fibrosis** was less frequently observed in cases of CP (figure 8 C). In cases of PDAC, a **perilesional** staining could be observed in 7 out of 10 cases (70 %) (figure 8 D), while cells staining positive for CD34 were distributed diffusely in the whole fibrosis in the remaining cases. The staining intensity for CD34 was classified as **strong** in 9 out of 12 CP cases (75 %), while the staining intensity in PDAC cases was mostly **moderate** (8 out of 10 cases; 80 %). The overall staining pattern was **diffuse** in 22 out of 22 cases (100 %).

Table 4. Evaluation of CD34 staining.

Case	Localization and frequency of staining in PSCs/fibrosis	Intensity of staining in PSCs/fibrosis	Pattern of staining	Comments
1 – AIP type 2	peripheral periductal +++ periacinar +++ intralobular +++ inter-/perilobular +++	+++	diffuse	-
2 – AIP type 2	periacinar ++ intralobular ++ inter-/perilobular ++	++	diffuse	-
3 – AIP type 1	peripheral periductal +++ periacinar +++ intralobular +++ inter-/perilobular +++	+++	diffuse	-
4 – AIP type 1	periductal +++ periacinar +++	+++	diffuse	stained/non-stained areas contrary to α-SMA staining
5 – Hereditary CP	diffuse in fibrosis +++	+++	diffuse	no staining around the big ducts
6 – Alcoholic CP	diffuse in fibrosis +++	+++	diffuse	no staining around the big ducts
7 – Alcoholic CP	peripheral periductal +++ periacinar +++ intralobular +++ inter-/perilobular +++	+++	diffuse	-
8 – Alcoholic CP	periductal ++ periacinar ++ intralobular ++ inter-/perilobular ++	+++	diffuse	-
9 – Alcoholic CP	periductal ++ periacinar ++ intralobular ++ inter-/perilobular ++	+++	diffuse	-
10 – Alcoholic CP	periductal ++ periacinar ++ intralobular ++ inter-/perilobular ++	++	diffuse	-

11 – PDAC	diffuse in fibrosis ++	+++	diffuse	stained/non-stained areas contrary to α-SMA staining
12 – PDAC	perilesional ++	++	diffuse	stained/non-stained areas contrary to α-SMA staining
13 – PDAC	perilesional ++	++	diffuse	-
14 – PDAC	perilesional ++	++	diffuse	-
15 – PDAC	diffuse in fibrosis ++	++	diffuse	-
16 – PDAC	perilesional ++	++	diffuse	-
17 – PDAC	perilesional ++	++	diffuse	stained/non-stained areas contrary to α-SMA staining
18 – PDAC	perilesional ++	+	diffuse	stained/non-stained areas contrary to α-SMA staining
19 – PDAC	diffuse in fibrosis ++	++	diffuse	-
20 – PDAC	perilesional ++	++	diffuse	stained/non-stained areas contrary to α-SMA staining
21 – AIP type 1	periacinar + intralobular + inter-/perilobular +	++	diffuse	stained/non-stained areas contrary to α-SMA staining
22 – AIP type 2	periacinar + intralobular + inter-/perilobular +	+++	diffuse	stained/non-stained areas contrary to α-SMA staining
Normal pancreatic tissue	periductal ++ periacinar +++ intralobular +++ inter-/perilobular +++	+++	diffuse	-
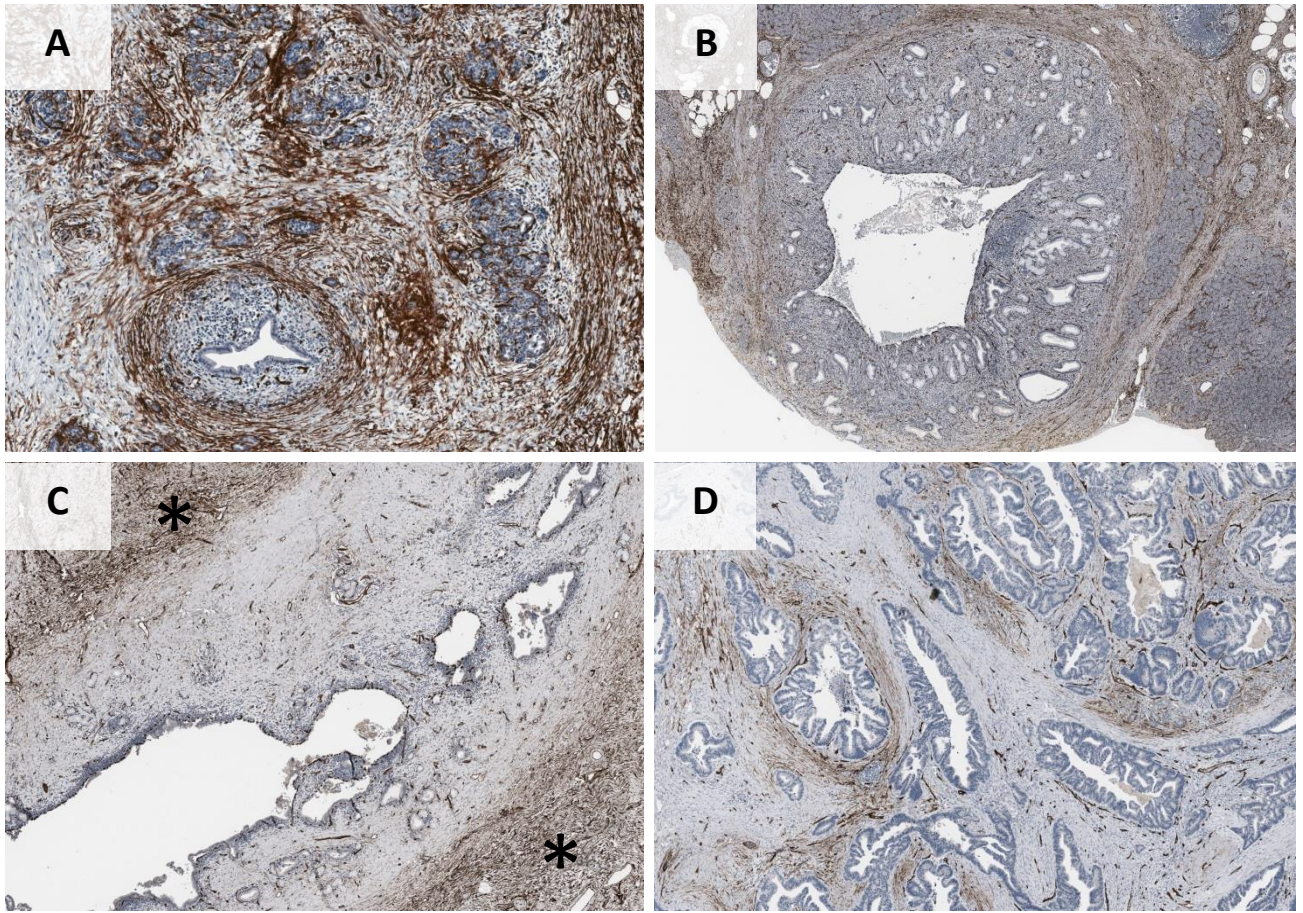
Figure 8. IHC for CD34. **A.** Periacinar, inter-/perilobular and intralobular and peripheral periductal staining in a case of AIP type 2. **B.** Peripheral periductal staining in a case of AIP type 1. **C.** Staining diffusely distributed in the fibrosis in a case of hereditary CP (stars), whereas in the immediately periductal tissue only endothelial staining is observed. **D.** Perilesional staining in a case of PDAC.

5.1.3.4 CD56 (NCAM)

The cell surface protein CD56, also known as NCAM (neural cell adhesion molecule), belongs to the immunoglobulin superfamily and is widely expressed in nerve tissue (Rutishauser et al., 1978; Thiery et al., 1977). It has also been found in various other tissues. It is, for example, expressed in neuroendocrine cells, like β-cells of the pancreas (Kiss et al., 1994). Its functions include cell-cell adhesion (Rutishauser et al., 1982) and cell-ECM adhesion (Cavallaro et al., 2001) as well as signaling properties (Ditlevsen et al., 2008; Panicker et al., 2003). The molecule is thought to play an important role in neural development and plasticity (Fields & Itoh, 1996; Kiss & Muller, 2001; Ronn et al., 1998). In some malignancies, like pancreatic cancer, a down-regulation or loss of CD56 seems to be associated with poor prognosis (Tezel et al., 2001), while in other tumors, such as neuroblastoma, increased CD56 expression indicates cancer progression (Gluer et al., 1998).

CD56 is also expressed in HSCs (Cassiman et al., 2002).

In our study, CD56 showed a **periacinar** staining in 10 out of 12 CP cases (83.3 %) (figure 9 A), while other staining localizations like an intralobular, periductal or diffuse staining unrelated to structures were rarely seen. In cases of PDAC, the staining localization observed in most cases was also a **periacinar** staining in remnant acini (in 6 out of 10 cases; 60 %). Other localizations (diffuse or perilesional) were only rarely observed (figure 9 B). The staining intensity, however, was **strong** in most cases. If any staining could be observed, the pattern was always **diffuse**. A periacinar staining was also seen in normal pancreatic tissue. Similar to the mostly periacinar staining for α-crystallin B, this could indicate that CD56 is a marker for quiescent PSCs rather than for activated PSCs.

Table 5. Evaluation of CD56 staining.

Case	Localization and frequency of staining in PSCs/fibrosis	Intensity of staining in PSCs/fibrosis	Pattern of staining	Comments
1 – AIP type 2	periacinar + intralobular +	+++	diffuse	membranous staining of islets and duct epithelium
2 – AIP type 2	periacinar +	+++	diffuse	membranous staining of islets and duct epithelium
3 – AIP type 1	periacinar + intralobular +	+++	diffuse	membranous staining of islets and duct epithelium
4 – AIP type 1	-	-	-	no acini remaining; membranous staining of islets and duct epithelium
5 – Hereditary CP	periacinar ++ diffuse in fibrosis +	+++	diffuse	membranous staining of islets and duct epithelium
6 – Alcoholic CP	periductal + periacinar +	+++	diffuse	membranous staining of islets and duct epithelium
7 – Alcoholic CP	periacinar + intralobular +	+++	diffuse	membranous staining of islets and duct epithelium
8 – Alcoholic CP	periacinar ++ diffuse in fibrosis +	+++	diffuse	membranous staining of islets and duct epithelium
9 – Alcoholic CP	-	-	-	-
10 – Alcoholic CP	periacinar +	++	diffuse	membranous staining of islets and duct epithelium

11 – PDAC	periacinar +	+++	diffuse	-
12 – PDAC	periacinar +	+++	diffuse	-
13 – PDAC	periacinar + single cells + perilesional +	+++	diffuse	staining of tumor cells
14 – PDAC	periacinar+	+++	diffuse	-
15 – PDAC	-	-	-	-
16 – PDAC	single cells in fibrosis +	++	diffuse	-
17 – PDAC	-	-	-	staining of tumor cells
18 – PDAC	periacinar +	+++	diffuse	-
19 – PDAC	periacinar + single cells in fibrosis +			-
20 – PDAC	-	-	-	staining of tumor cells
21 – AIP type 1	periacinar +	+++	diffuse	membranous staining of islets and duct epithelium
22 – AIP type 2	periacinar +	+++	diffuse	membranous staining of islets and duct epithelium
Normal pancreatic tissue	periacinar +	+++	diffuse	membranous staining of islets and duct epithelium

Figure 9. IHC for CD56. **A.** Case of AIP type 1: Periacinar staining of single cells is observed in healthy parenchyma, whereas only few positive cells are found in the interlobular fibrous septa. **B.** Case of PDAC: Perilesional staining of single cells is observed, but only very rarely.

5.1.3.5 Desmin

Desmin is the main intermediate filament protein found in the skeletal, cardiac and smooth muscles of vertebrates (Lazarides & Hubbard, 1976; Li et al., 1997). It maintains the structure of the contractile apparatus of muscle cells by linking the myofibrils, composed of actin and myosin, to one another and to the membrane of the muscle cell (sarcolemma) (Li et al., 1997).

Desmin is an established marker for HSCs (Cassiman et al., 2002; Yokoi et al., 1984) and PSCs (Apte et al., 1998; Bachem et al., 1998).

In our study, desmin staining was found in **varying locations**, but generally very rarely both in cases of CP (4 out of 12 cases; 33.3 %) and in cases of PDAC (1 out of 10 cases; 10 %). The staining intensity was mostly **moderate**. If any desmin staining was observed, the staining pattern was **focal** (figure 10).

Table 6. Evaluation of desmin staining.

Case	Localization and frequency of staining in PSCs/fibrosis	Intensity of staining in PSCs/fibrosis	Pattern of staining	Comments
1 – AIP type 2	-	-	-	-
2 – AIP type 2	-	-	-	-
3 – AIP type 1	-	-	-	-
4 – AIP type 1	focal in fibrosis +	++	focal	-
5 – Hereditary CP	-	-	-	-
6 – Alcoholic CP	periductal +	++	focal	-
7 – Alcoholic CP	-	-	-	-
8 – Alcoholic CP	inter-/perilobular +	++	focal	-
9 – Alcoholic CP	-	-	-	-
10 – Alcoholic CP	-	-	-	-
11 – PDAC	-	-	-	-
12 – PDAC	-	-	-	-
13 – PDAC	perilesional +	++	focal	-
14 – PDAC	-	-	-	-
15 – PDAC	-	-	-	-
16 – PDAC	-	-	-	-
17 – PDAC	-	-	-	-
18 – PDAC	-	-	-	-
19 – PDAC	-	-	-	-
20 – PDAC	-	-	-	-

21 – AIP type 1	focal in fibrosis +	+++	focal	
22 – AIP type 2	-	-	-	-
Normal pancreatic tissue	-	-	-	-
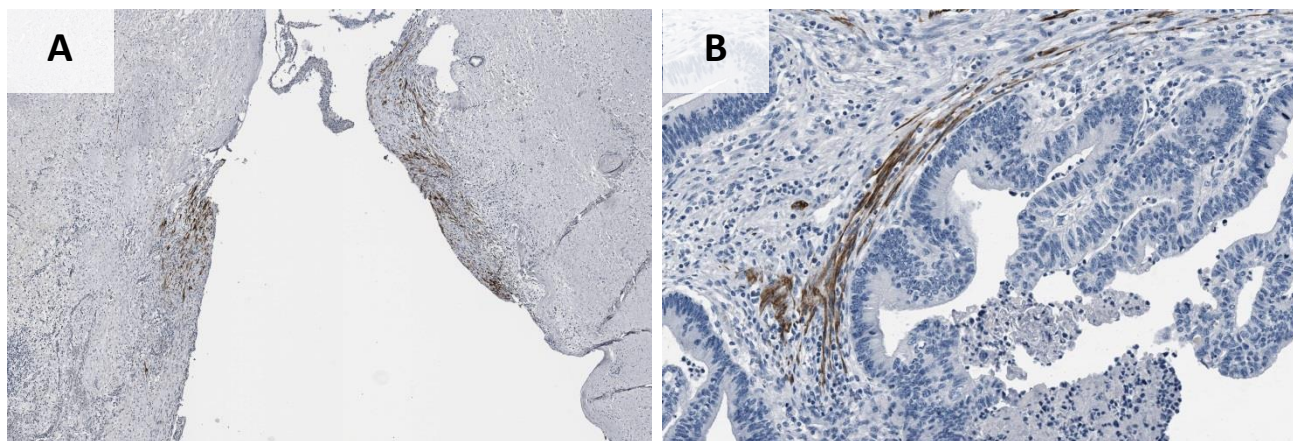
Figure 10. IHC for desmin. **A.** Focal periductal staining in a case of alcoholic CP. **B.** Focal perilesional staining in a case of PDAC.

5.1.3.6 NGF

The small secreted protein NGF (nerve growth factor) is the first-discovered member of the neurotrophin family and promotes the survival, growth and differentiation of neurons (Cohen et al., 1954; Levi-Montalcini & Hamburger, 1951). NGF exerts its cellular effects by binding to the tyrosin kinase receptor TrkA and to the low-affinity pan-neurotrophin receptor NGFR (nerve growth factor receptor) (Huang & Reichardt, 2003). In addition to its pivotal role in nerve formation and maintenance, NGF is also expressed in non-neural tissues. An enhanced expression of NGF is known in both chronic pancreatitis and pancreatic cancer and has been linked to neural morphological changes, pain and perineural invasion, respectively (Friess et al., 1999; Zhu et al., 1999).

NGF is expressed in HSCs (Cassiman et al., 2001a; Cassiman et al., 2002) and in PCCs (Zhu et al., 2001). In our study, NGF staining had a **periductal** localization in 5 out of 12 CP cases (41.6 %) (figure 11 A) and was distributed **diffusely in the fibrosis** in 3 out of 12 CP cases (25 %). In PDAC cases, a **perilesional** staining was observed in 5 out of 10 cases (50 %) (figure 11 B). The staining intensity for NGF was **weak** in all cases, the staining pattern always **diffuse**. In normal pancreatic tissue, NGF showed an inter-/perilobular localization. In addition, tumor cells also stained positive for NGF in 10 out of 10 (100 %) PDAC cases (figure 11 B).

Table 7. Evaluation of NGF staining.

Case	Localization and frequency of staining in PSCs/fibrosis	Intensity of staining in PSCs/fibrosis	Pattern of staining	Comments
1 – AIP type 2	interlobular +	+	diffuse	staining of acini, islets and duct epithelium
2 – AIP type 2	-	-	-	staining of acini, islets and duct epithelium
3 – AIP type 1	periductal + diffuse in fibrosis +	+	diffuse	staining of acini, islets and duct epithelium
4 – AIP type 1	-	-	-	-
5 – Hereditary CP	periductal +	+	diffuse	staining of acini, islets and duct epithelium
6 – Alcoholic CP	periductal +	+	diffuse	staining of acini, islets and duct epithelium
7 – Alcoholic CP	-	-	-	staining of acini, islets and duct epithelium
8 – Alcoholic CP	-	-	-	staining of acini, islets and duct epithelium
9 – Alcoholic CP	periductal +	+	diffuse	staining of acini, islets and duct epithelium
10 – Alcoholic CP	periductal +	+	diffuse	staining of acini, islets and duct epithelium
11 – PDAC	perilesional ++	+	diffuse	staining of tumor cells
12 – PDAC	-	-	-	staining of tumor cells
13 – PDAC	perilesional ++	+	diffuse	staining of tumor cells
14 – PDAC	-	-	-	staining of tumor cells
15 – PDAC	-	-	-	staining of tumor cells
16 – PDAC	perilesional +	+	diffuse	staining of tumor cells
17 – PDAC	-	-	-	staining of tumor cells
18 – PDAC	perilesional +	+	diffuse	staining of tumor cells
19 – PDAC	perilesional +	+	diffuse	staining of tumor cells
20 – PDAC	-	-	-	staining of tumor cells
21 – AIP type 1	diffuse in fibrosis +	+	diffuse	staining of acini, islets and duct epithelium
22 – AIP type 2	diffuse in fibrosis +	+	diffuse	staining of acini, islets and duct epithelium
Normal pancreatic tissue	inter-/perilobular +	+	diffuse	staining of acini, islets and duct epithelium

Figure 11. IHC for NGF. **A.** Weak periductal staining in a case of AIP type 1. **B.** Weak perilesional staining and staining of tumor cells in a case of PDAC.

5.1.3.7 NGFR

NGFR (nerve growth factor receptor), also known as LNGFR (low-affinity nerve growth factor receptor) or p75^{NTR}, belongs to the TNF (tumor necrosis factor) cytokine receptor superfamily and is able to bind all neurotrophins, including NGF and NT-3, with equal affinity (Chao, 1994). While NGFR can have positive effects on cell survival and differentiation in the presence of the NGF receptor TrkA, it can also have pro-apoptotic effects when expressed in the absence of TrkA (Rabizadeh & Bredesen, 1994). The level of NGFR expression in PDAC has been suggested to be correlated with level of perineural invasion (Wang et al., 2009).

NGFR is known to be expressed in HSCs and PSCs (Cassiman et al., 2001a; Cassiman et al., 2002; Trim et al., 2000) as well as in PCCs (Zhu et al., 1999).

NGFR staining showed **variable** locations in cases of CP, including a periductal (figure 12 A), intralobular, inter-/perilobular as well as a diffusely distributed staining in the fibrosis. However, a **perilesional** staining for NGFR could be seen in 7 out of 10 PDAC cases (70 %) (figure 12 B). The staining intensity for NGFR was **weak** in all cases and the staining pattern was classified as **diffuse** in all cases where a staining could be observed. Tumor cells stained positive for NGFR in 9 out of 10 PDAC cases (90 %) (figure 12 B).

Table 8. Evaluation of NGFR staining.

Case	Localization and frequency of staining in PSCs/fibrosis	Intensity of staining in PSCs/fibrosis	Pattern of staining	Comments
1 – AIP type 2	-	-	-	-
2 – AIP type 2	intralobular + inter-/perilobular +	+	diffuse	staining of acini and duct epithelium cells; prominent staining of islets
3 – AIP type 1	periductal +	+	diffuse	staining of acini and duct epithelium cells; prominent staining of islets
4 – AIP type 1	diffuse in fibrosis +	+	diffuse	staining of acini and duct epithelium cells; prominent staining of islets
5 – Hereditary CP	-	-	-	-
6 – Alcoholic CP	periductal +	+	diffuse	staining of acini and duct epithelium cells; prominent staining of islets
7 – Alcoholic CP	-	-	-	staining of acini and duct epithelium cells; prominent staining of islets
8 – Alcoholic CP	-	-	-	staining of acini and duct epithelium cells; prominent staining of islets
9 – Alcoholic CP	-	-	-	staining of acini and duct epithelium cells; prominent staining of islets
10 – Alcoholic CP	periductal +	+	diffuse	staining of acini and duct epithelium cells; prominent staining of islets
11 – PDAC	perilesional +	+	diffuse	staining of tumor cells
12 – PDAC	-	-	-	staining of tumor cells
13 – PDAC	-	-	-	staining of tumor cells
14 – PDAC	-	-	-	-
15 – PDAC	perilesional +	+	diffuse	staining of tumor cells

16 – PDAC	perilesional +	+	diffuse	staining of tumor cells
17 – PDAC	perilesional +	+	diffuse	staining of tumor cells
18 – PDAC	perilesional +	+	diffuse	staining of tumor cells
19 – PDAC	perilesional +	+	diffuse	staining of tumor cells
20 – PDAC	perilesional +	+	diffuse	staining of tumor cells
21 – AIP type 1	diffuse in fibrosis +	+	diffuse	staining of acini and duct epithelium cells; prominent staining of islets
22 – AIP type 2	-	-	-	-
Normal pancreatic tissue	-	-	-	staining of acini and duct epithelium cells; prominent staining of islets
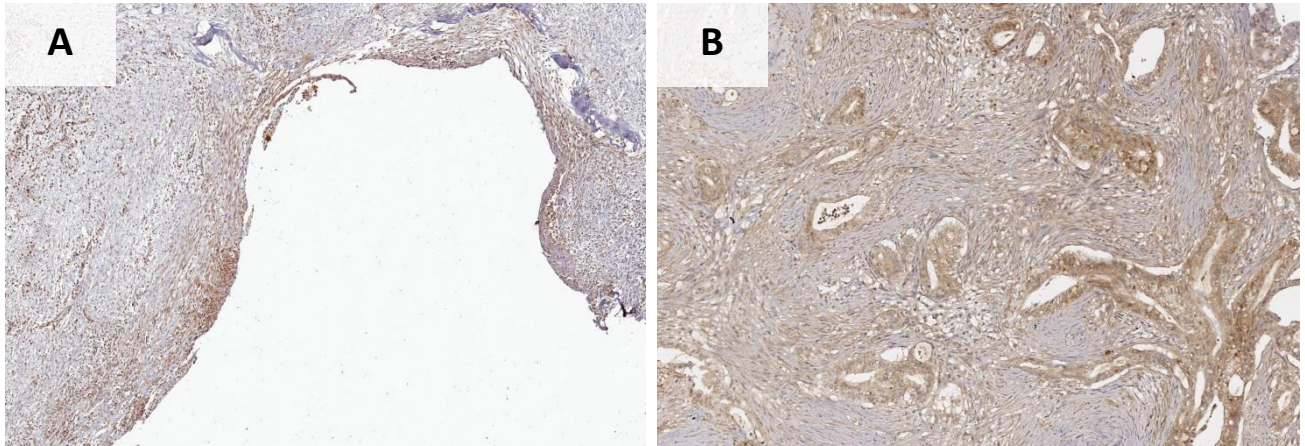
Figure 12. IHC for NGFR. **A.** Weak periductal staining in a case of alcoholic CP. **B.** Weak perilesional staining and staining of tumor cells in a case of PDAC.

5.1.3.8 NT-3

Like the previously mentioned NGF, the protein NT-3 (neurotrophin-3) belongs to the family of neurotrophins and therefore exerts similar functions as NGF in regards to the promotion of neural tissues. While it binds to its main receptor TrkC with the highest affinity, it is also able to bind to TrkB and NGFR (Barbacid, 1994).

NT-3 expression has been found in HSCs (Cassiman et al., 2001a; Cassiman et al., 2002).

In this study, NT-3 expression was observed in the fibrotic areas, both diffuse and in single stromal cells. A staining of the collagen-rich fibrosis was observed in 11 out of 12 CP cases (91.6 %), but only in 2 out of 10 PDAC cases (20 %). The most common staining localization observed in CP cases was **periductal**, as seen in 5 out of 12 CP cases (41.6 %) (figure 13 A), while other localications that were rarely seen in CP cases include an intralobular as well as an inter-/perilobular staining. NT-3 showed a **perilesional** staining localization in 10 out of 10 PDAC cases (100 %) (figure 13 C & D). The staining intensity varied, but was **moderate** or **strong** in most cases. Interestingly, most CP cases showed a **diffuse** staining pattern **with a focal accentuation** (10 out of 12; 83.3 %) (figure 13 B), while all PDAC cases showed a very prominent **focal** staining (10 out of 10; 100 %) (figure 13 C & D). NT-3 staining in normal pancreatic tissue was periductal.

A partial staining of tumor cells with a weak staining intensity could be observed for NT-3 in 9 out of 10 PDAC cases (90 %).

Table 9. Evaluation of NT-3 staining.

Case	Localization and frequency of staining in PSCs/fibrosis	Intensity of staining in PSCs/fibrosis	Pattern of staining	Comments
1 – AIP type 2	*collagen-rich fibrosis ++*	++	diffuse, focally accentuated	staining of islets and individual duct epithelium cells
2 – AIP type 2	*collagen-rich fibrosis +*	++	diffuse, focally accentuated	staining of islets and individual duct epithelium cells
3 – AIP type 1	peripheral periductal ++ periductal ++ *collagen-rich fibrosis +*	cells +++ *fibrosis ++*	diffuse, focally accentuated	staining of islets and individual duct epithelium cells
4 – AIP type 1	*collagen-rich fibrosis +*	++	diffuse, focally accentuated	staining of islets and individual duct epithelium cells
5 – Hereditary CP	*collagen-rich fibrosis ++*	+	diffuse, focally accentuated	staining of islets and individual duct epithelium cells
6 – Alcoholic CP	periductal + *collagen-rich fibrosis ++*	cells +++ *fibrosis ++*	diffuse, focally accentuated	staining of islets and individual duct epithelium cells
7 – Alcoholic CP	intralobular + inter-/perilobular ++ *collagen-rich fibrosis ++*	cells +++ *fibrosis ++*	diffuse, focally accentuated	staining of islets and individual duct epithelium cells
8 – Alcoholic CP	periductal + intralobular + *collagen-rich fibrosis ++*	cells +++ *fibrosis ++*	diffuse, focally accentuated	staining of islets and individual duct epithelium cells
9 – Alcoholic CP	periductal + *collagen-rich fibrosis ++*	cells +++ *fibrosis ++*	focal	staining of islets and individual duct epithelium cells
10 – Alcoholic CP	periductal + *collagen-rich fibrosis ++*	cells +++ *fibrosis ++*	diffuse, focally accentuated	staining of islets and individual duct epithelium cells
11 – PDAC	perilesional ++ *collagen-rich fibrosis ++*	++	focal	partial staining of tumor cells
12 – PDAC	perilesional +	+	focal	partial staining of tumor cells
13 – PDAC	perilesional ++	+++	focal	partial staining of tumor cells
14 – PDAC	perilesional ++	++	focal	partial staining of tumor cells
15 – PDAC	perilesional ++ *collagen-rich fibrosis ++*	cells +++ *fibrosis ++*	focal	partial staining of tumor cells

16 – PDAC	perilesional +++	+++	focal	partial staining of tumor cells
17 – PDAC	perilesional ++	++	focal	-
18 – PDAC	perilesional ++	++	focal	partial staining of tumor cells
19 – PDAC	peripheral perilesional +++	++	focal	partial staining of tumor cells
20 – PDAC	perilesional +++	+++	focal	partial staining of tumor cells
21 – AIP type 1	*collagen-rich fibrosis ++*	+++	diffuse, focally accentuated	-
22 – AIP type 2	-	-	-	partial staining of tumor cells
Normal pancreatic tissue	periductal ++	+++	-	staining of islets and individual duct epithelium cells
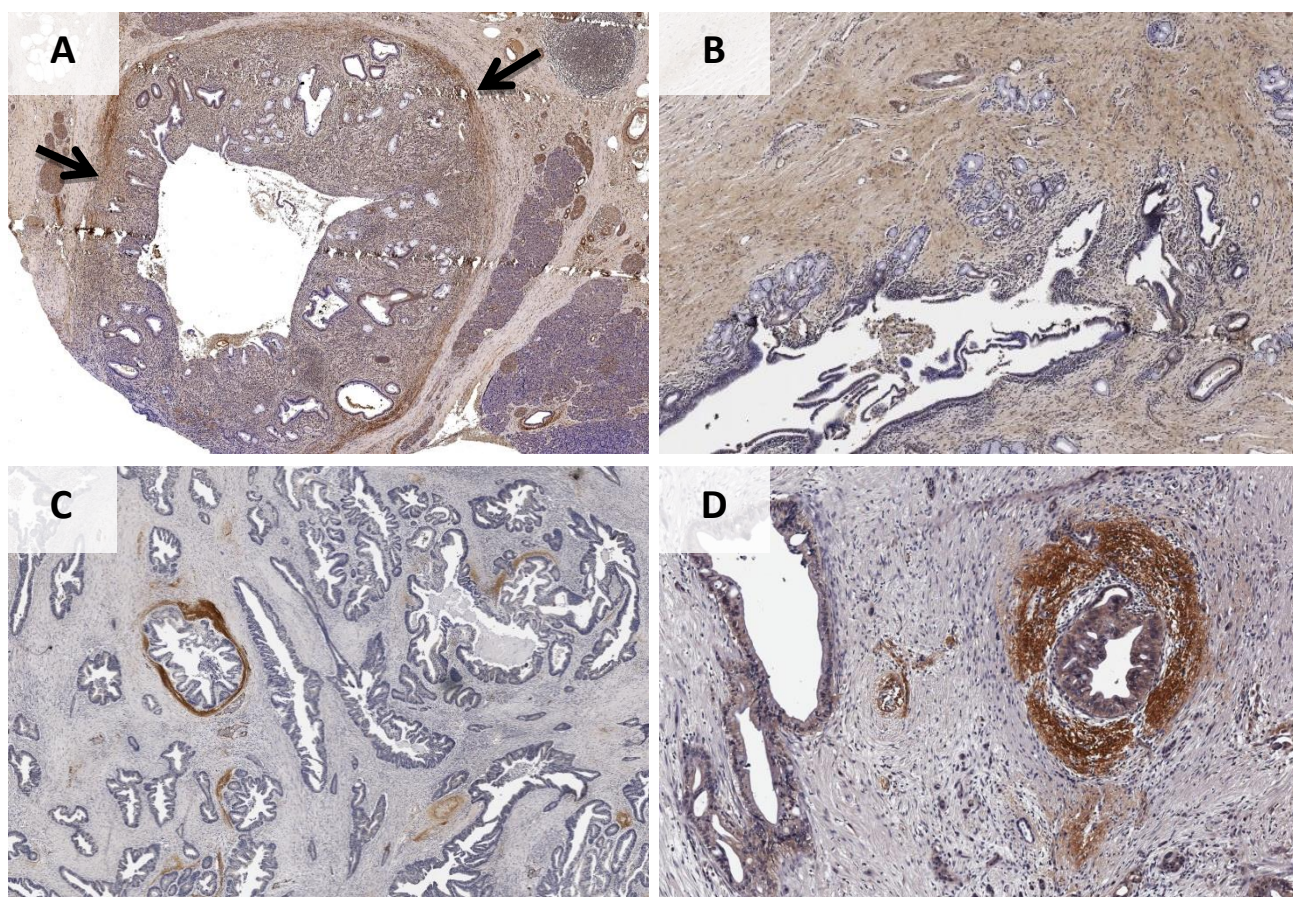
Figure 13. IHC for NT-3. **A.** Peripheral periductal staining (arrows) in a case of AIP type 1. **B.** Diffuse, weak staining of the collagen-rich fibrosis with focal accentuation in hereditary CP. **C, D.** Strong and focal perilesional staining for NT-3 was typically observed in PDAC.

5.1.3.9 SPARC

The extracellular glycoprotein SPARC (secreted protein acidic and rich in cysteine), also known as osteonectin or BM-40, is primarily expressed in tissues that undergo high protein turnover, for example as a result of recurring tissue injury (Bradshaw & Sage, 2001). SPARC is able to bind several ECM proteins, such as collagens I-V, to increase the expression of matrix metalloproteinases and to inhibit cell adhesion and it is therefore suggested that it plays an important role in cell-ECM interaction (Bradshaw & Sage, 2001). Correspondingly, SPARC is overexpressed in chronic pancreatitis as well as in PDAC and its metastases, and therefore thought to promote the invasiveness of PDAC (Guweidhi et al., 2005).

SPARC is expressed in PSCs and, to a lesser extent, in PCCs (Guweidhi et al., 2005).

While staining localizations for SPARC **varied** a lot in cases of CP (periacinar, intralobular, inter-/perilobular, as well as diffuse staining in the fibrosis unrelated to morphological structures) (figure 14 A), SPARC showed a **perilesional** staining in most cases of PDAC (9 out of 10; 90 %) (figure 14 B-D). In most PDAC cases, additional staining locations, like the above mentioned, could be observed. As seen for α-SMA, cells within the same PDAC lymph node metastasis also stained positive for SPARC (figure 14 E). Staining intensity for SPARC was **strong** in most cases (16 out of 22; 72.2 %). If any staining was observed, the staining pattern was **diffuse**. In normal pancreatic tissue, SPARC staining displayed an inter-/perilobular localization. Notably, SPARC-positive areas in cases of PDAC often showed an overlap with α-SMA-positive areas.

Table 10. Evaluation of SPARC staining.

Case	Localization and frequency of staining in PSCs/fibrosis	Intensity of staining in PSCs/fibrosis	Pattern of staining	Comments
1 – AIP type 2	periacinar ++ intralobular ++ inter-/perilobular ++	+++	diffuse	-
2 – AIP type 2	periacinar + inter-/perilobular ++	+++	diffuse	-
3 – AIP type 1	-	-	-	-
4 – AIP type 1	diffuse in fibrosis +	++	diffuse	-
5 – Hereditary CP	-	-	diffuse	-
6 – Alcoholic CP	periductal ++	+++	diffuse	-
7 – Alcoholic CP	diffuse in fibrosis ++	+++	diffuse	-
8 – Alcoholic CP	-	-	-	-

9 – Alcoholic CP	-	-	-	-
10 – Alcoholic CP	periductal ++ diffuse in fibrosis ++	+++	diffuse	-
11 – PDAC	perilesional ++	+++	diffuse	perilesional staining in lymph node metastasis
12 – PDAC	perilesional ++ inter-/perilobular +	+++	diffuse	-
13 – PDAC	perilesional ++ focally in fibrosis +++	+++	diffuse	-
14 – PDAC	perilesional ++ periacinar + inter-/perilobular ++	+++	diffuse	-
15 – PDAC	perilesional + periacinar + inter-/perilobular +	++	diffuse	-
16 – PDAC	perilesional ++ focally in fibrosis ++	+++	diffuse	-
17 – PDAC	perilesional +++ focally in fibrosis ++	+++	diffuse	-
18 – PDAC	perilesional +++	+++	diffuse	-
19 – PDAC	diffuse in fibrosis ++	+++	diffuse	-
20 – PDAC	perilesional ++ diffuse in fibrosis +	+++	diffuse	-
21 – AIP type 1	diffuse in fibrosis +++	+++	diffuse	-
22 – AIP type 2	diffuse in fibrosis ++	+++	diffuse	-
Normal pancreatic tissue	inter-/perilobular +	+++	diffuse	-
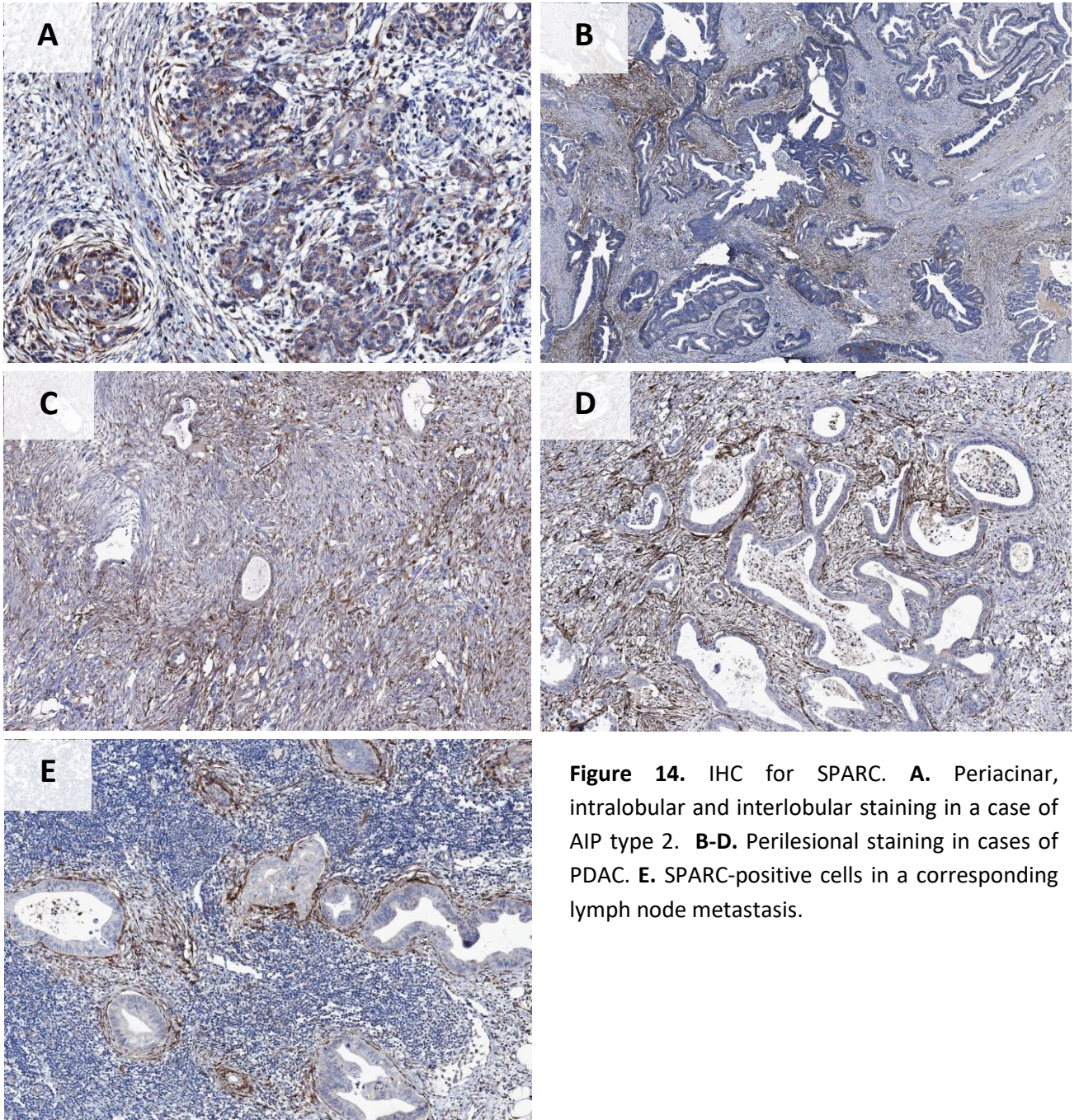
Figure 14. IHC for SPARC. **A.** Periacinar, intralobular and interlobular staining in a case of AIP type 2. **B-D.** Perilesional staining in cases of PDAC. **E.** SPARC-positive cells in a corresponding lymph node metastasis.

5.1.3.10 Synaptophysin

Synaptophysin, also known as major synaptic vesicle protein p38, is found in neural and neuroendocrine tissues and seems to act as a regulator of synaptic vesicle exo- and endocytosis (Edelmann et al., 1995; Kwon & Chapman, 2011), although its exact function and mechanism of action remains still unknown. As synaptophysin is expressed in neuroendocrine tissues, pancreatic islets stain positive for this protein.

Synaptophysin has been described as a marker for HSCs (Cassiman et al., 2002; Cassiman et al., 1999). In this study, we found a mainly **periacinar** staining (figure 15). Interestingly, the periacinar staining was seen in 10 out of 12 CP cases (83.3 %), but only in 2 out of 10 PDAC cases (20 %). The periacinar staining was generally found more frequently around acini in remnant relatively unaltered pancreatic tissue. A staining of scattered cells in the fibrosis unrelated to acini or any other structures could be seen in 2 out of 12 CP cases (16.6 %). If any staining was observed, the intensity was **weak** and the overall staining pattern was **diffuse** in all cases. Normal pancreatic tissue also showed a periacinar staining. The staining localization of synaptophysin seems similar to the one observed for α-crystallin B, so synaptophysin could be another marker for quiescent PSCs. In 7 out of 10 PDAC cases (70 %), isolated tumor cells stained positive for synaptophysin.

Table 11. Evaluation of synaptophysin staining.

Case	Localization and frequency of staining in PSCs/fibrosis	Intensity of staining in PSCs/fibrosis	Pattern of staining	Comments
1 – AIP type 2	-	-	-	-
2 – AIP type 2	periacinar +	+	diffuse	staining of islets
3 – AIP type 1	periacinar +	+	diffuse	staining of islets
4 – AIP type 1	-	-	-	staining of islets
5 – Hereditary CP	periacinar +	+	diffuse	staining of islets
6 – Alcoholic CP	periacinar + scatteredly in fibrosis +	+	diffuse	staining of islets
7 – Alcoholic CP	periacinar +	+	diffuse	staining of islets
8 – Alcoholic CP	periacinar ++ scatteredly in fibrosis +	+	diffuse	staining of islets
9 – Alcoholic CP	periacinar +	+	diffuse	staining of islets
10 – Alcoholic CP	periacinar +	+	diffuse	staining of islets
11 – PDAC	periacinar +	+	diffuse	staining of individual tumor cells
12 – PDAC	-	-	-	staining of islets

13 – PDAC	-	-	-	staining of individual tumor cells
14 – PDAC	-	-	-	staining of individual tumor cells
15 – PDAC	-	-	-	-
16 – PDAC	-	-	-	staining of individual tumor cells
17 – PDAC	-	-	-	staining of individual tumor cells
18 – PDAC	-	-	-	-
19 – PDAC	periacinar +	+	diffuse	staining of individual tumor cells
20 – PDAC	-	-	-	staining of individual tumor cells
21 – AIP type 1	periacinar +	+	diffuse	staining of islets
22 – AIP type 2	periacinar +	+	diffuse	staining of islets
Normal pancreatic tissue	periacinar +	+	diffuse	staining of islets
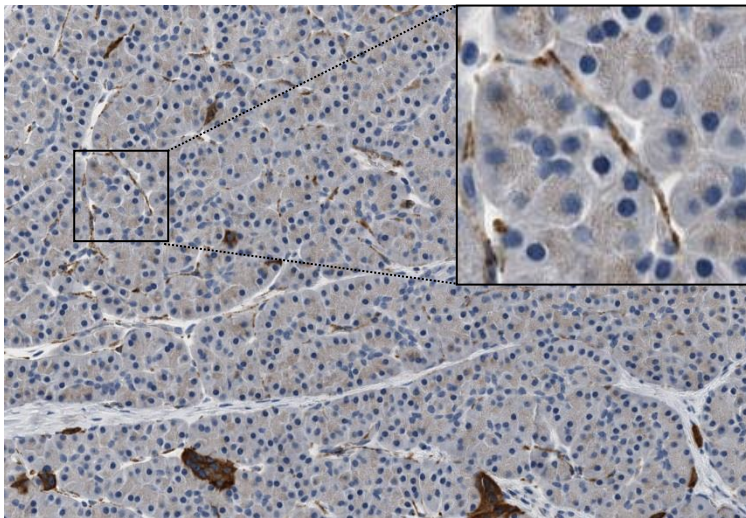
Figure 15. IHC for synaptophysin. Periacinar single cell staining in normal acinar parenchyma in a case of hereditary CP. Langerhans islets served as internal positive control.

5.1.3.11 Tenascin C

Tenascin C is an ECM protein that is expressed in the context of tissue remodeling, as for example during chronic inflammation and cancerogenesis (Jones & Jones, 2000). The protein is therefore expressed in chronic pancreatitis and shows an increasing expression in the development and progression of pancreatic cancer, with PSCs being the known source of tenascin C (Esposito et al., 2006). Studies have shown that tenascin C promotes PCC growth, motility and migration (Paron et al., 2011).

In our study, tenascin C staining was mostly located **periductal**, as seen in 7 out of 12 CP cases (58.3 %), but a periacinar and an intralobular staining as well as a diffuse staining unrelated to morphologic structures, although sometimes focally accentuated, were also found (figure 16 A). In cases of PDAC, a **perilesional** staining could be seen in all cases (10 out of 10; 100 %) (figure 16 B), while a periacinar, an inter-/perilobular and a diffuse staining of the fibrotic tissue were less frequently observed. As seen for α-SMA and SPARC, tenascin C staining could also be found in stromal cells located around tumor cells within a PDAC lymph node metastasis (figure 16 C). The intensity of tenascin C staining was heterogeneous in some cases, i.e. both areas with strong staining intensity and areas with moderate staining intensity could be found within a single case (in 13 of 22 cases; 59 %). However, the predominant overall staining intensity was **strong** (14 out of 22 cases; 63.6 %), followed by moderate (6 out of 22 cases; 27.2 %). The general staining pattern for tenascin C was mostly **focal** (13 out of 22 cases; 59 %). In normal pancreatic tissue, tenascin C staining was periductal and of weak staining intensity.

Table 12. Evaluation of tenascin C staining.

Case	Localization and frequency of staining in PSCs/fibrosis	Intensity of staining in PSCs/fibrosis	Pattern of staining	Comments
1 – AIP type 2	periductal +++ periacinar + intralobular ++	heterogeneous +++	focal	-
2 – AIP type 2	periductal ++ periacinar +++ intralobular +++	heterogeneous +++	diffuse	-
3 – AIP type 1	periductal +++	heterogeneous ++	focal	-
4 – AIP type 1	diffuse in fibrosis +++	homogeneous +++	diffuse	-
5 – Hereditary CP	-	-	-	-
6 – Alcoholic CP	periductal +++	homogeneous +++	focal	-
7 – Alcoholic CP	diffuse in fibrosis ++	heterogeneous ++	focal	-
8 – Alcoholic CP	periductal ++	heterogeneous ++	focal	-
9 – Alcoholic CP	periductal +	homogeneous ++	focal	-
10 – Alcoholic CP	periductal +	homogeneous +	focal	-
11 – PDAC	perilesional ++	heterogeneous ++	diffuse, focally accentuated	perilesional staining in lymph node metastasis
12 – PDAC	perilesional +++ periacinar ++ inter-/perilobular ++	heterogeneous ++	focal	-
13 – PDAC	perilesional +++	heterogeneous +++	diffuse, focally accentuated	-
14 – PDAC	perilesional +++ periacinar + inter-/perilobular ++	heterogeneous +++	diffuse	-
15 – PDAC	perilesional ++ inter-/perilobular +	homogeneous +++	focal	-
16 – PDAC	perilesional ++ focal/patchy in fibrosis +++	homogeneous +++	focal	-
17 – PDAC	perilesional +++ focal/patchy in fibrosis +++	heterogeneous +++	diffuse, focally accentuated	-
18 – PDAC	perilesional +++	heterogeneous +++	diffuse	-

	focal/patchy in fibrosis +++	74		
19 – PDAC	perilesional + periacinar + focal in fibrosis ++	heterogeneous +++	focal	-
20 – PDAC	perilesional +++ focal/patchy in fibrosis +++	heterogeneous +++	diffuse	-
21 – AIP type 1	focally accentuated in well-marked fibrosis +++	homogeneous +++	focal	-
22 – AIP type 2	focally accentuated in well-marked fibrosis +++	homogeneous +++	focal	-
Normal pancreatic tissue	periductal +	homogeneous +	focal	-
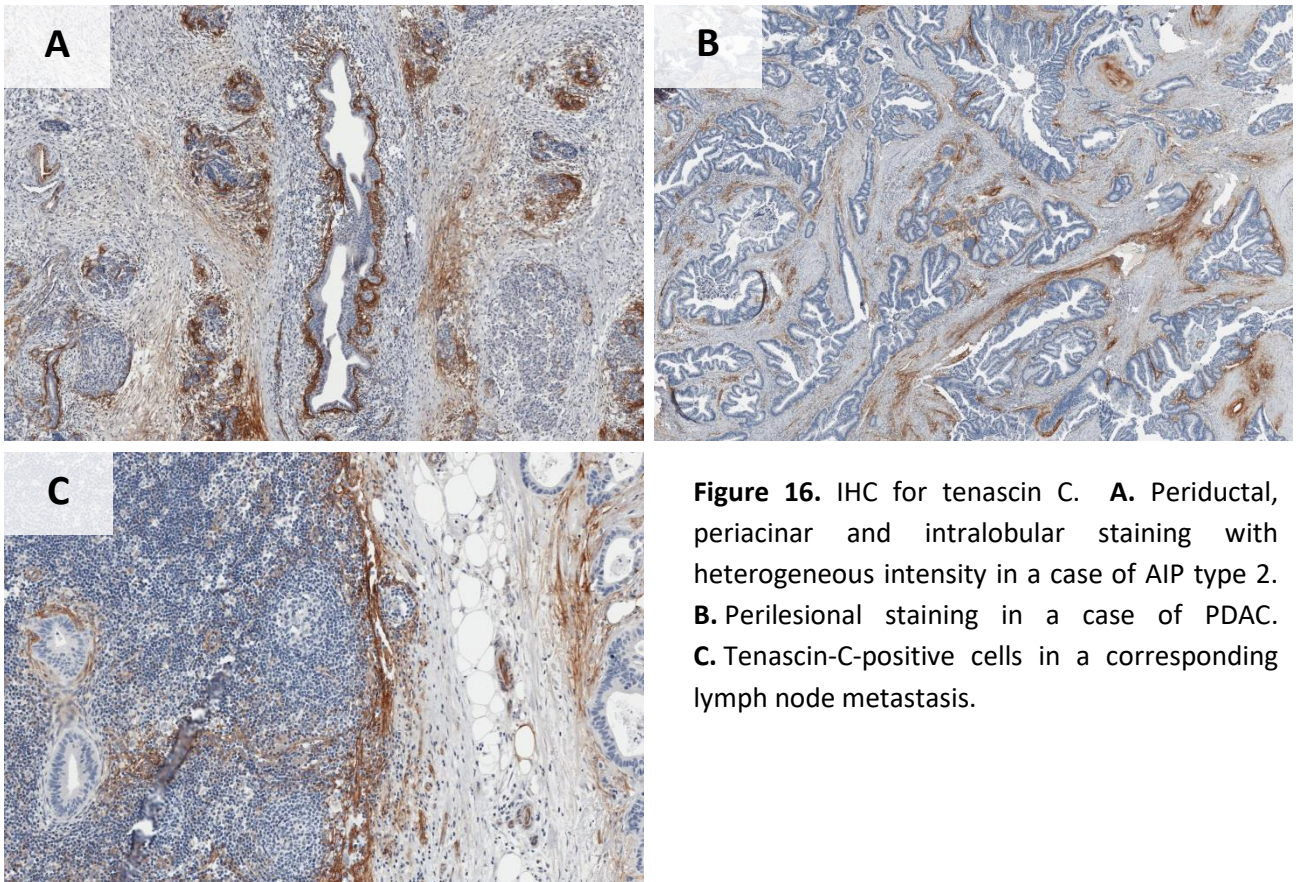
Figure 16. IHC for tenascin C. **A.** Periductal, periacinar and intralobular staining with heterogeneous intensity in a case of AIP type 2. **B.** Perilesional staining in a case of PDAC. **C.** Tenascin-C-positive cells in a corresponding lymph node metastasis.

5.1.3.12 TrkC

The tyrosine kinase TrkC is the high affinity specific receptor for NT-3 (Lamballe et al., 1991). Notably, TrkC expression seems to be correlated with cancer invasion, and especially perineural invasion, in PDAC (Sakamoto et al., 2001).

TrkC expression has been found in HSCs (Cassiman et al., 2001a; Cassiman et al., 2002).

Cells in the fibrosis stained positive for TrkC in 8 out of 12 cases of CP (66.6 %). Staining localizations in CP cases **varied** and included a periductal (figure 17 A) and inter-/perilobular staining as well as a staining of cells located diffusely in the fibrosis. In cases of PDAC, a **perilesional** staining was found in 5 out of 10 cases (50 %) (figure 17 B), while a staining unrelated to tumor cells was found in 2 out of 10 cases (20 %). If any staining was observed, it had a **weak** staining intensity and a **diffuse** staining pattern. In normal pancreatic tissue, no TrkC-positive cells could be found. In cases of PDAC, tumor cells showed an at least partial positivity for TrkC (figure 17 B).

Table 13. Evaluation of TrkC staining.

Case	Localization and frequency of staining in PSCs/fibrosis	Intensity of staining in PSCs/fibrosis	Pattern of staining	Comments
1 – AIP type 2	-	-	-	staining of acini, islets and duct epithelium
2 – AIP type 2	inter-/perilobular +	+	diffuse	staining of acini, islets and duct epithelium
3 – AIP type 1	periductal +	+	diffuse	staining of acini, islets and duct epithelium
4 – AIP type 1	diffuse in fibrosis +	+	diffuse, focally accentuated	staining of acini, islets and duct epithelium
5 – Hereditary CP	diffuse in fibrosis +	+	diffuse	staining of acini, islets and duct epithelium
6 – Alcoholic CP	periductal +	+	diffuse	staining of acini, islets and duct epithelium
7 – Alcoholic CP	-	-	-	staining of acini, islets and duct epithelium
8 – Alcoholic CP	-	-	-	staining of acini, islets and duct epithelium
9 – Alcoholic CP	periductal + inter-/perilobular +	+	diffuse	staining of acini, islets and duct epithelium
10 – Alcoholic CP	diffuse in fibrosis +	+	diffuse	staining of acini, islets and duct epithelium
11 – PDAC	-	-	-	partial staining of tumor cells

12 – PDAC	perilesional +	+	diffuse	partial staining of tumor cells
13 – PDAC	perilesional +	+	diffuse	partial staining of tumor cells
14 – PDAC	-	-	-	partial staining of tumor cells
15 – PDAC	-	-	-	partial staining of tumor cells
16 – PDAC	diffuse in fibrosis +	+	diffuse	partial staining of tumor cells
17 – PDAC	-	-	-	partial staining of tumor cells
18 – PDAC	perilesional + diffuse in fibrosis +	+	diffuse	partial staining of tumor cells
19 – PDAC	perilesional +	+	diffuse	partial staining of tumor cells
20 – PDAC	perilesional +	+	diffuse	partial staining of tumor cells
21 – AIP type 1	diffuse in fibrosis +	+	diffuse	staining of acini, islets and duct epithelium
22 – AIP type 2	-	-	-	staining of acini, islets and duct epithelium
Normal pancreatic tissue	-	-	-	-
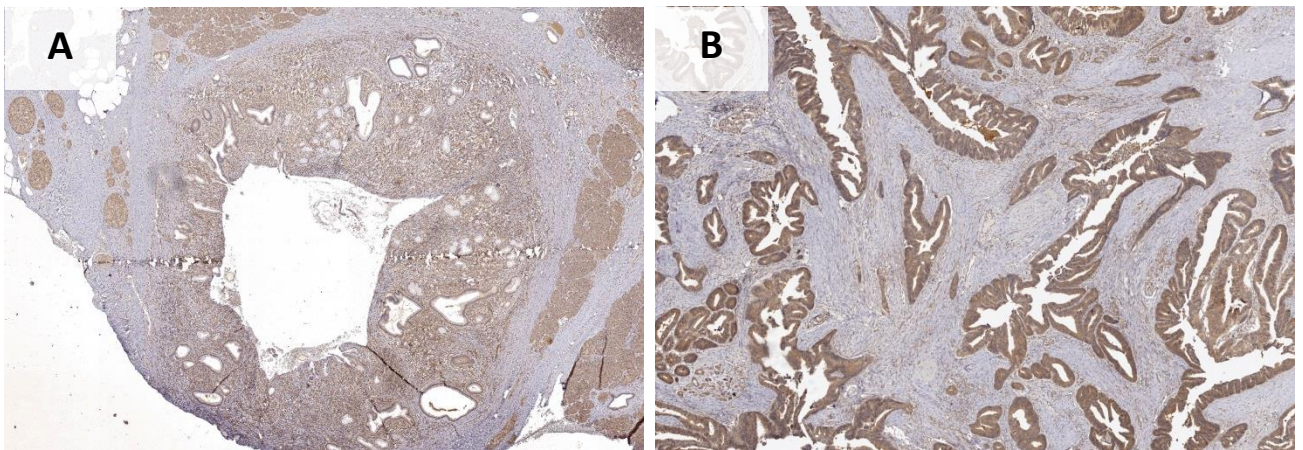
Figure 17. IHC for TrkC. **A.** Weak periductal staining in a case of AIP type 1. **B.** Weak perilesional staining and staining of tumor cells in a case of PDAC.

5.1.3.13 Correlation between Movat's pentachrome staining and IHC

Upon comparison of IHC results with the results of the Movat's pentachrome staining, it was observed that α-SMA-positive areas (which often overlapped with SPARC-positive areas) often co-localized with yellow Movat staining, suggesting that α-SMA-positive areas represent areas of collagen-rich mature fibrosis. On the other hand, NT-3-positive areas often correlated with blue areas in Movat's pentachrome staining, suggesting that NT-3-positive areas are areas of mucin-rich active fibrosis. Morphometric analysis of histochemistry and immunohistochemistry on consecutive sections confirmed that α-SMA-positive areas showed significantly higher percentages of yellow-stained areas in Movat's stain (median 27 %) compared to NT-3-positive areas (median 1 %) ($p = 0.012$, two-tailed, Mann-Whitney $U = 101$, $n_1 = 21$, $n_2 = 18$), whereas NT-3-positive areas showed significantly higher percentages of blue-stained areas in Movat's stain (median 41 %) compared to α-SMA-positive areas (median 24 %) ($p = 0.008$, two-tailed, Mann-Whitney $U = 96.5$, $n_1 = 21$, $n_2 = 18$) (figures 18-20).
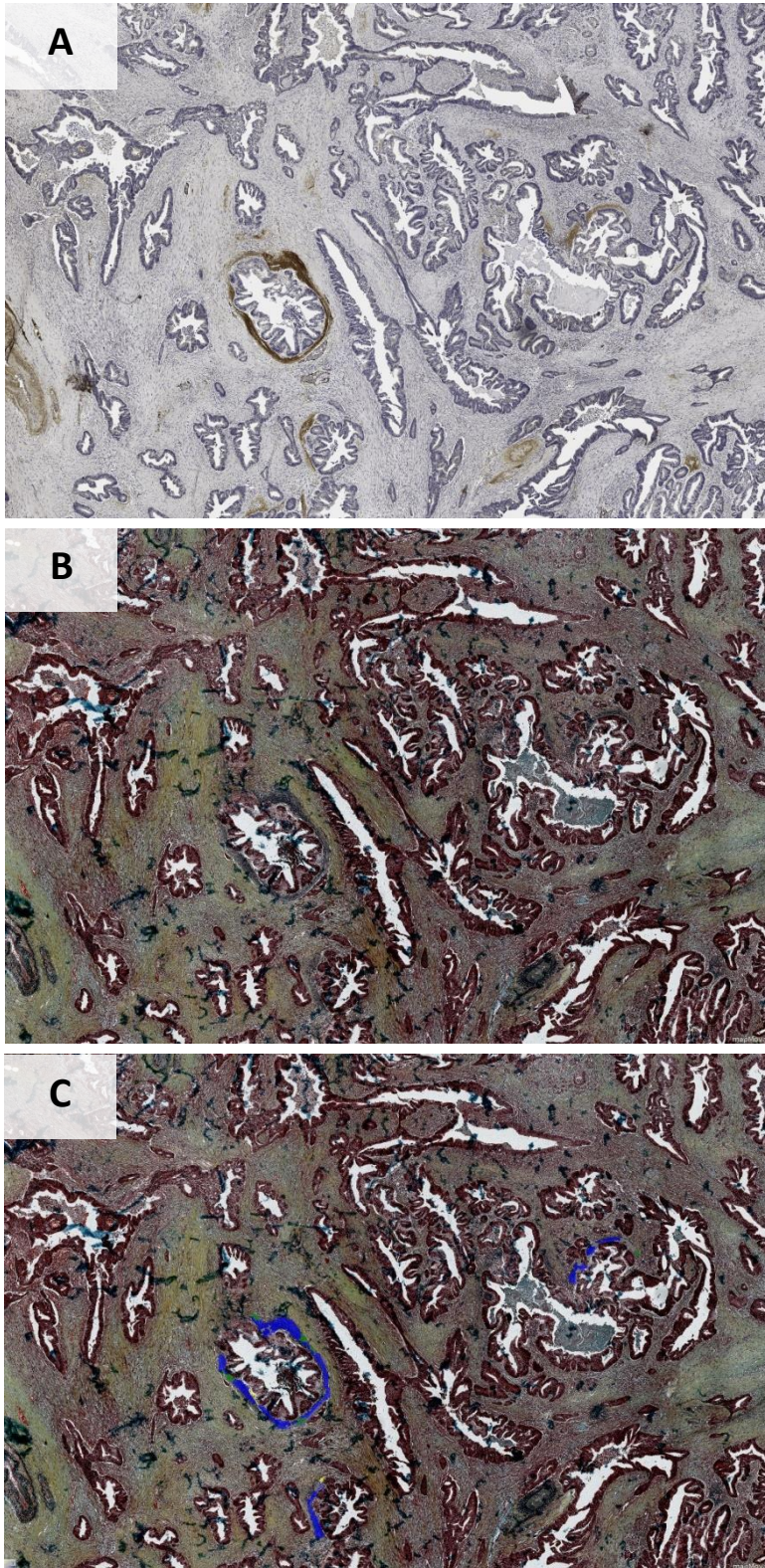
Figure 18. Exemplary case of PDAC. **A.** IHC for NT-3 shows focal perilesional positivity. **B.** Movat's staining shows blue staining (indicating mucin-rich active stroma) in NT-3-positive areas. **C.** Analysis with Definiens Tissue Studio software confirms NT-3-positive areas as blue in Movat's stain.
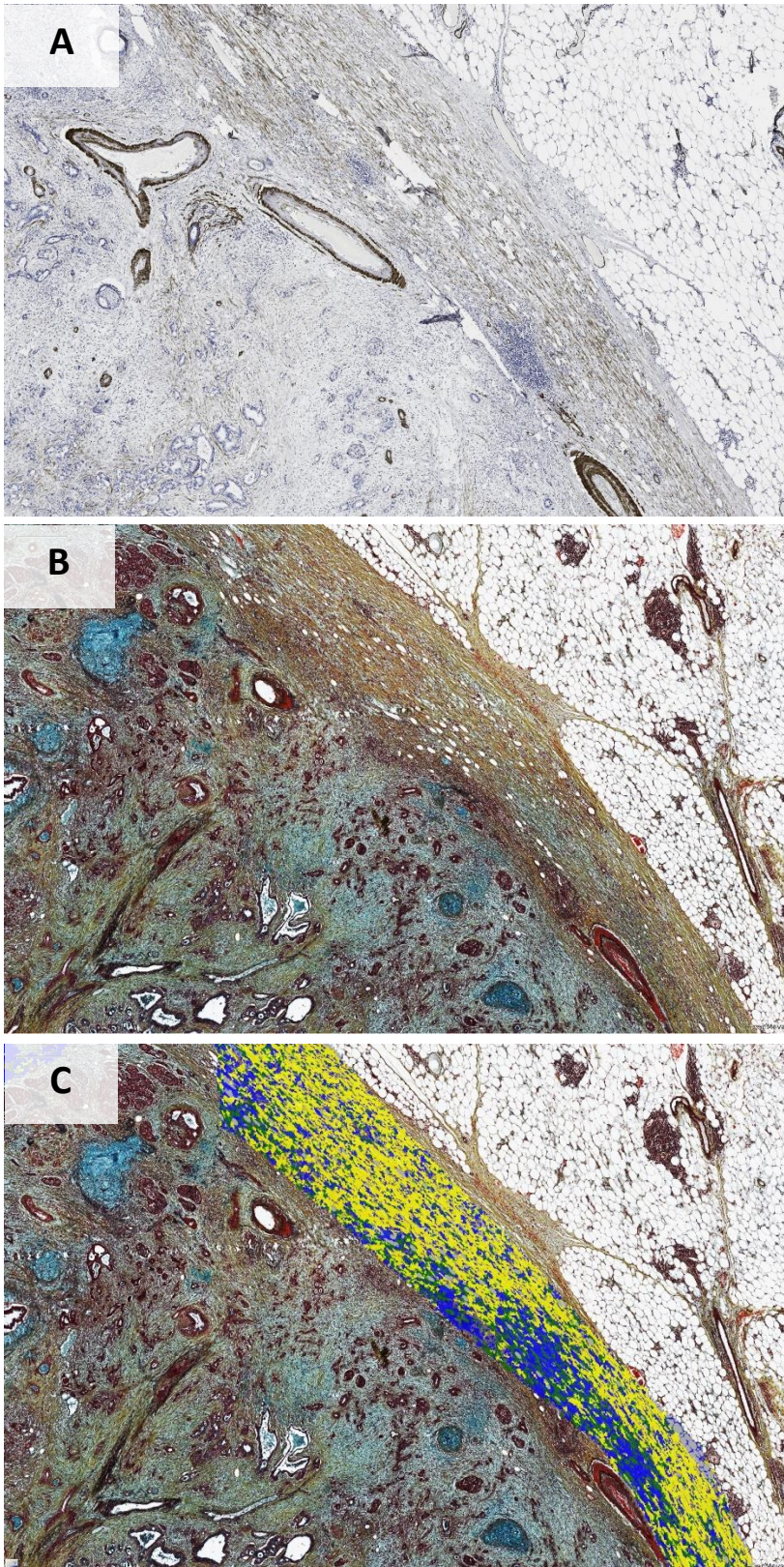
Figure 19. Different exemplary case of PDAC. **A.** IHC for α-SMA shows positivity in the peripheral region of the tumor. **B.** Movat's staining shows mostly yellow staining (collagen-rich stroma) as well as some blue staining (mucin-rich stroma) in α-SMA-positive areas. **C.** Analysis with Definiens Tissue Studio software confirms α-SMA-positive areas as mostly yellow with some blue parts. Areas depicted green in the software-assisted analysis could not be assigned to either blue or yellow with certainty („candid").
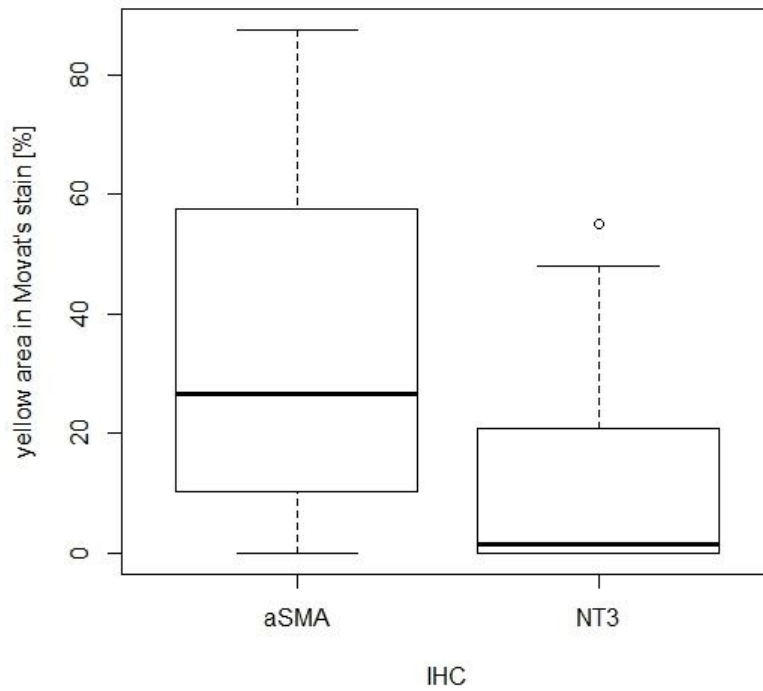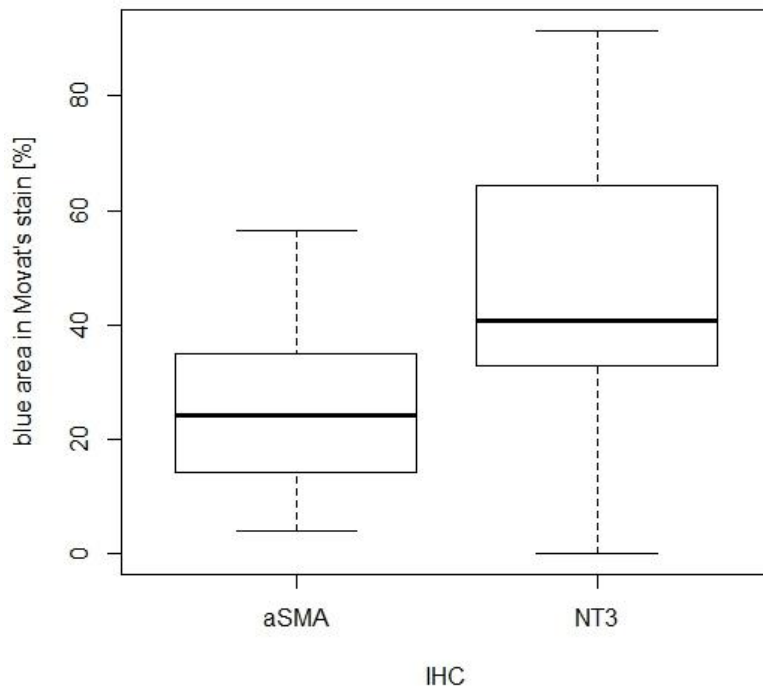
Figure 20. Boxplots comparing areas stained yellow, respectively blue, in Movat's pentachrome stain within α-SMA-positive vs. NT-3-positive areas. **A.** Yellow areas are significantly larger in areas that stained positive for α-SMA in IHC (median 26.58 %) than in areas that stained positive for NT-3 in IHC (median 1.40 %) (p = 0.012). **B.** Blue areas are significantly larger in areas that stained positive for NT-3 in IHC (median 40.745 %) than in areas that stained positive for α-SMA in IHC (median 24.23 %) (p = 0.008).

5.2 Cells in culture

5.2.1 Immunofluorescence

An immunofluorescence staining for α-crystallin B, NGF, NT-3 and TrkC was performed with HSCs to confirm them as HSC markers. In order to prove that the tested cells are indeed activated myofibroblasts, we also performed a double-staining for α-SMA and each respective marker. HSCs tested positive for all tested markers, as expected (figure 21).

PSCs freshly isolated from three patients suffering from chronic pancreatitis as well as from two patients with PDAC were then tested for α-crystallin B, NGF, NGFR, NT-3 and TrkC by means of immunofluorescence. As for HSCs, a double-staining with α-SMA and each respective marker was also performed with PSCs.

PSCs from patients with chronic pancreatitis as well as PSCs from patients with PDAC tested positive for α-SMA and all tested markers, confirming their expression in PSCs and underlining their similarities with HSCs, which also express all these markers (figures 22-25).

PSCs isolated from patients with PDAC (figures 24 & 25) generally showed a stronger positivity for α-SMA than PSCs isolated from chronic pancreatitis patients (figures 22 & 23), suggesting a higher level of activation in PSCs of PDAC.

In all double immunofluorescence stainings for both HSCs and PSCs, single-positive cells were found among double-positive cells (figures 21-25).
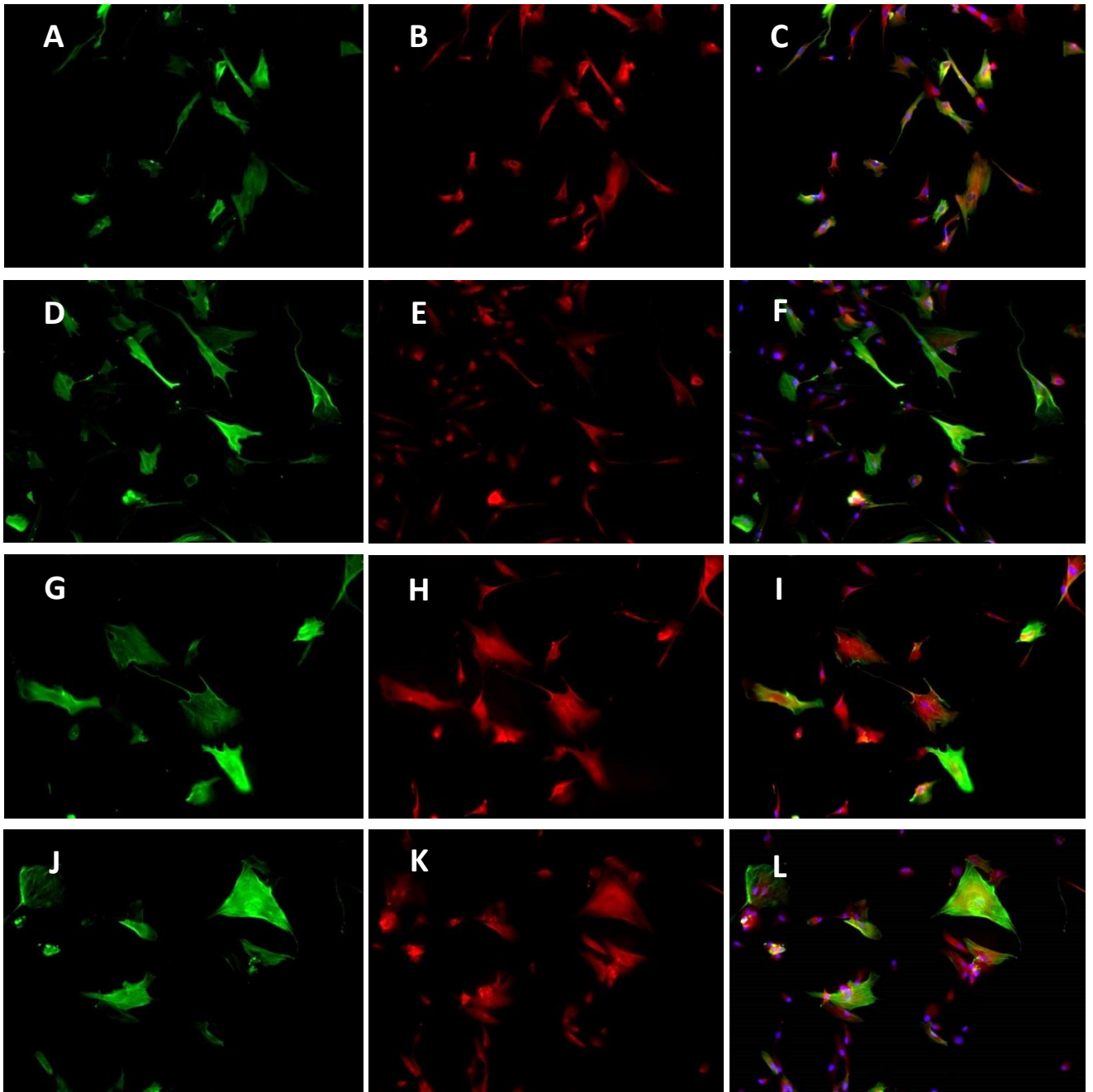
Figure 21. Double immunofluorescence staining of HSCs (M1248) for α-SMA, α-crystallin B, NGF, NT-3 and TrkC. A, D, G and J. HSCs show cytoplasmic positivity for α-SMA (green). **B.** HSCs show strong cytoplasmic positivity for α-crystallin B (red). **C.** Merged picture of A, B and counterstaining of nuclei with Hoechst33342 (blue) shows co-localization of α-SMA and α-crystallin B staining. **E.** HSCs show cytoplasmic positivity for NGF (red). **F.** Merged picture of D, E and counterstaining of nuclei with Hoechst33342 (blue) shows co-localization of α-SMA and NGF staining. **H.** HSCs show strong cytoplasmic positivity for NT-3 (red). **I.** Merged picture of G, H and counterstaining of nuclei with Hoechst33342 (blue) shows co-localization of α-SMA and NT-3 staining. **K.** HSCs show strong cytoplasmic positivity for TrkC (red). **L.** Merged picture of J, K and counterstaining of nuclei with Hoechst33342 (blue) shows co-localization of α-SMA and TrkC staining.
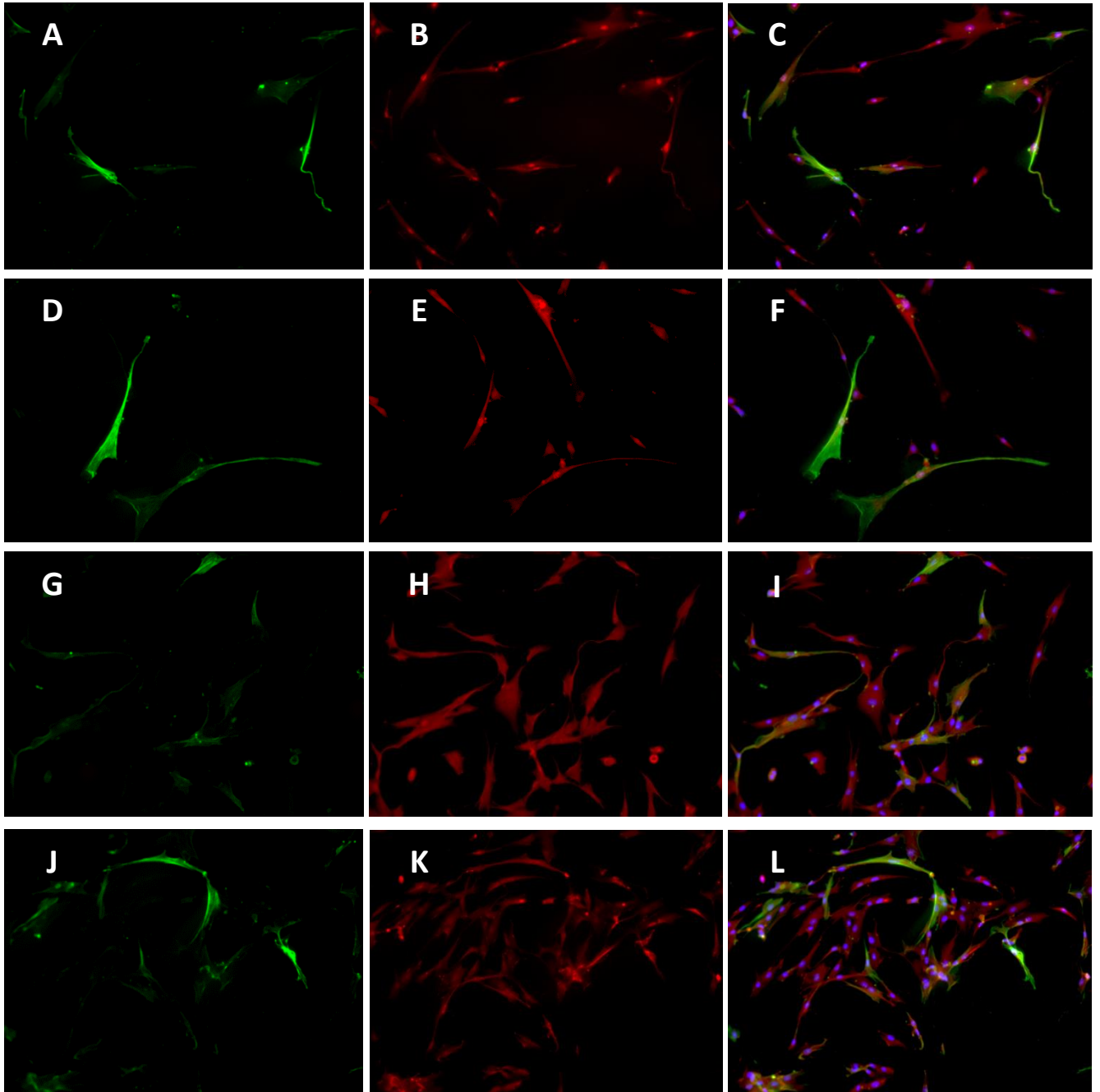
Figure 22. Double immunofluorescence staining of PSCs from a patient with chronic pancreatitis (M1223) for α-SMA and α-crystallin, NGFR, NT-3 and TrkC. A, D, G and J. PSCs show cytoplasmic positivity for α-SMA (green). **B.** PSCs show strong cytoplasmic and nuclear positivity for α-crystallin B (red). **C.** Merged picture of A, B and counterstaining of nuclei with Hoechst33342 (blue) shows co-localization of α-SMA and α-crystallin B staining. **E.** PSCs show cytoplasmic and nuclear positivity for NGFR (red). **F.** Merged picture of D, E and counterstaining of nuclei with Hoechst33342 (blue) shows co-localization of α-SMA and NGFR staining. **H.** PSCs show strong cytoplasmic positivity for NT-3 (red). **I.** Merged picture of G, H and counterstaining of nuclei with Hoechst33342 (blue) shows co-localization of α-SMA and NT-3 staining. **K.** PSCs show strong cytoplasmic positivity for TrkC (red). **L.** Merged picture of J, K and counterstaining of nuclei with Hoechst33342 (blue) shows co-localization of α-SMA and TrkC staining.
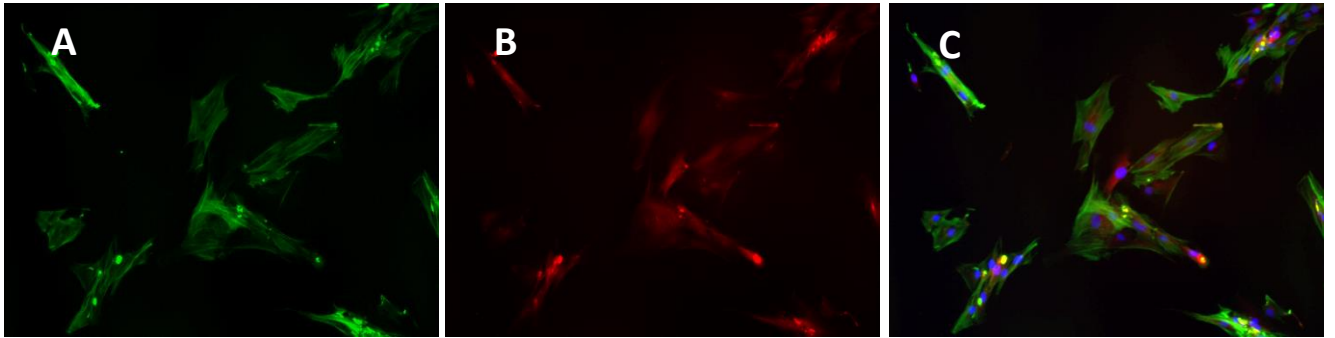
Figure 23. Double immunofluorescence staining of PSCs from a patient with chronic pancreatitis (M151) for α-SMA and NGF. A. PSCs show cytoplasmic positivity for α-SMA (green). **B.** PSCs show weak cytoplasmic positivity for NGF (red). **C.** Merged picture of A, B and counterstaining of nuclei with Hoechst33342 (blue) shows co-localization of α-SMA and NGF staining.
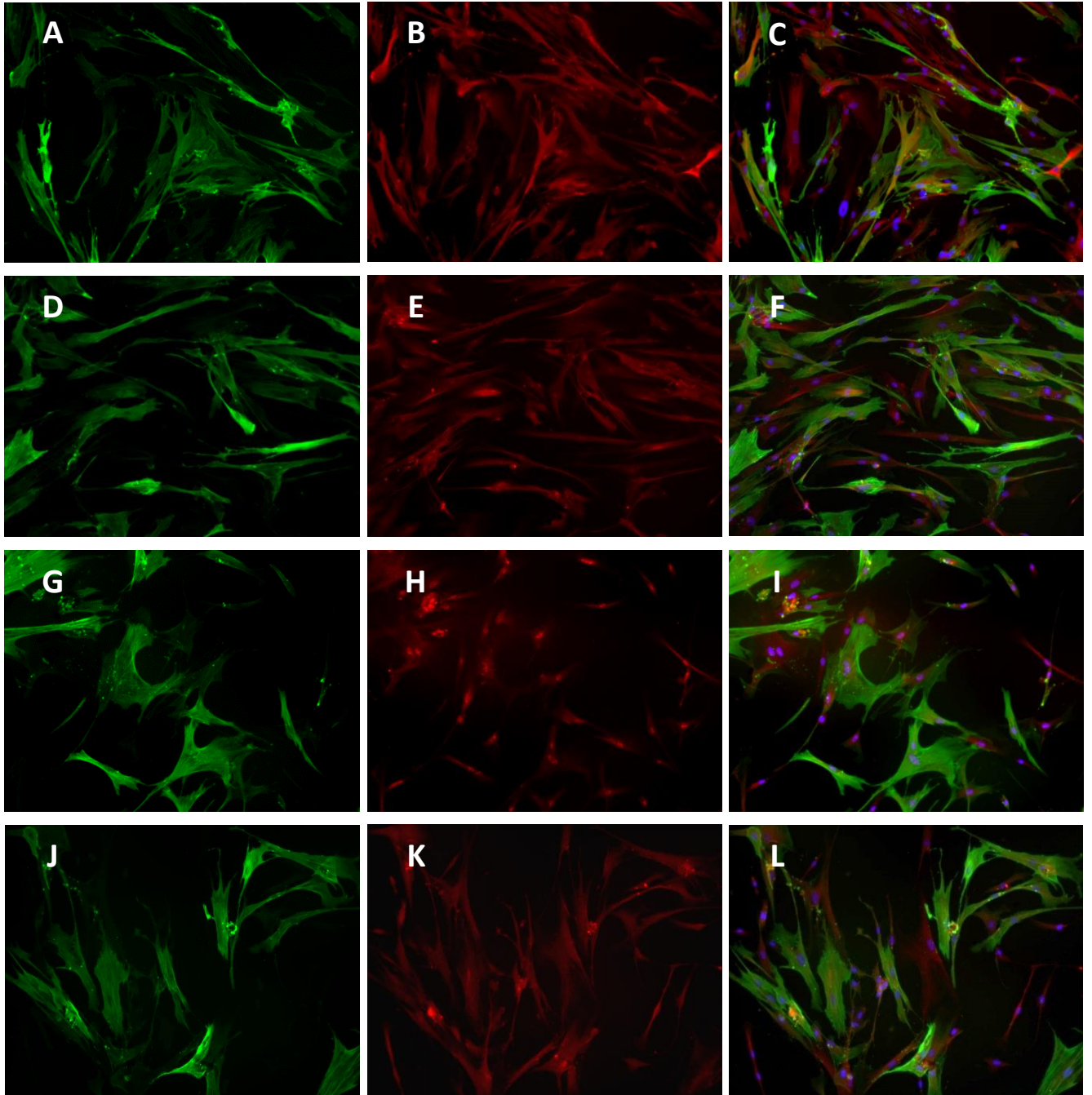
Figure 24. Double immunofluorescence staining of PSCs from a patient with PDAC (M1198) for α-SMA and α-crystallin, NGF, NGFR and TrkC. A, D, G and J. PSCs show cytoplasmic positivity for α-SMA (green). **B.** PSCs show strong cytoplasmic positivity for α-crystallin B (red). **C.** Merged picture of A, B and counterstaining of nuclei with Hoechst33342 (blue) shows co-localization of α-SMA and α-crystallin B staining. **E.** PSCs show weak cytoplasmic positivity for NGF (red). **F.** Merged picture of D, E and counterstaining of nuclei with Hoechst33342 (blue) shows co-localization of α-SMA and NGF staining. **H.** PSCs show weak cytoplasmic as well as nuclear positivity for NGFR (red). **I.** Merged picture of G, H and counterstaining of nuclei with Hoechst33342 (blue) shows co-localization of α-SMA and NGFR staining. **K.** PSCs show strong cytoplasmic positivity for TrkC (red). **L.** Merged picture of J, K and counterstaining of nuclei with Hoechst33342 (blue) shows co-localization of α-SMA and TrkC staining.
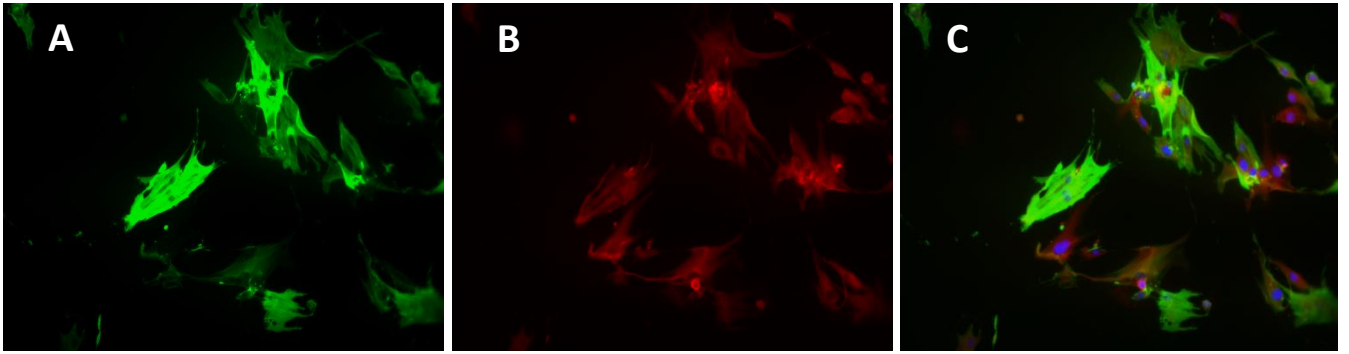
Figure 25. Double immunofluorescence staining of PSCs from a patient with PDAC (M1245) for α-SMA and NT-3. A. PSCs show cytoplasmic positivity for α-SMA (green). **B.** PSCs show strong cytoplasmic positivity for NT-3 (red). **C.** Merged picture of A, B and counterstaining of cells with Hoechst33342 (blue) shows co-localization of α-SMA and NT-3 staining.

5.2.2 Inactivation of PSCs

Primary human PSCs acquire an activated status when cultured on plastic. A quiescent status can be achieved by culturing the cells on Matrigel™-coated cell culture plates for 5-7 days (Jesnowski et al., 2005). We used this method in order to test whether the tested markers are also expressed in deactivated PSCs.

5.2.2.1 Morphological changes of PSCs cultured on Matrigel™
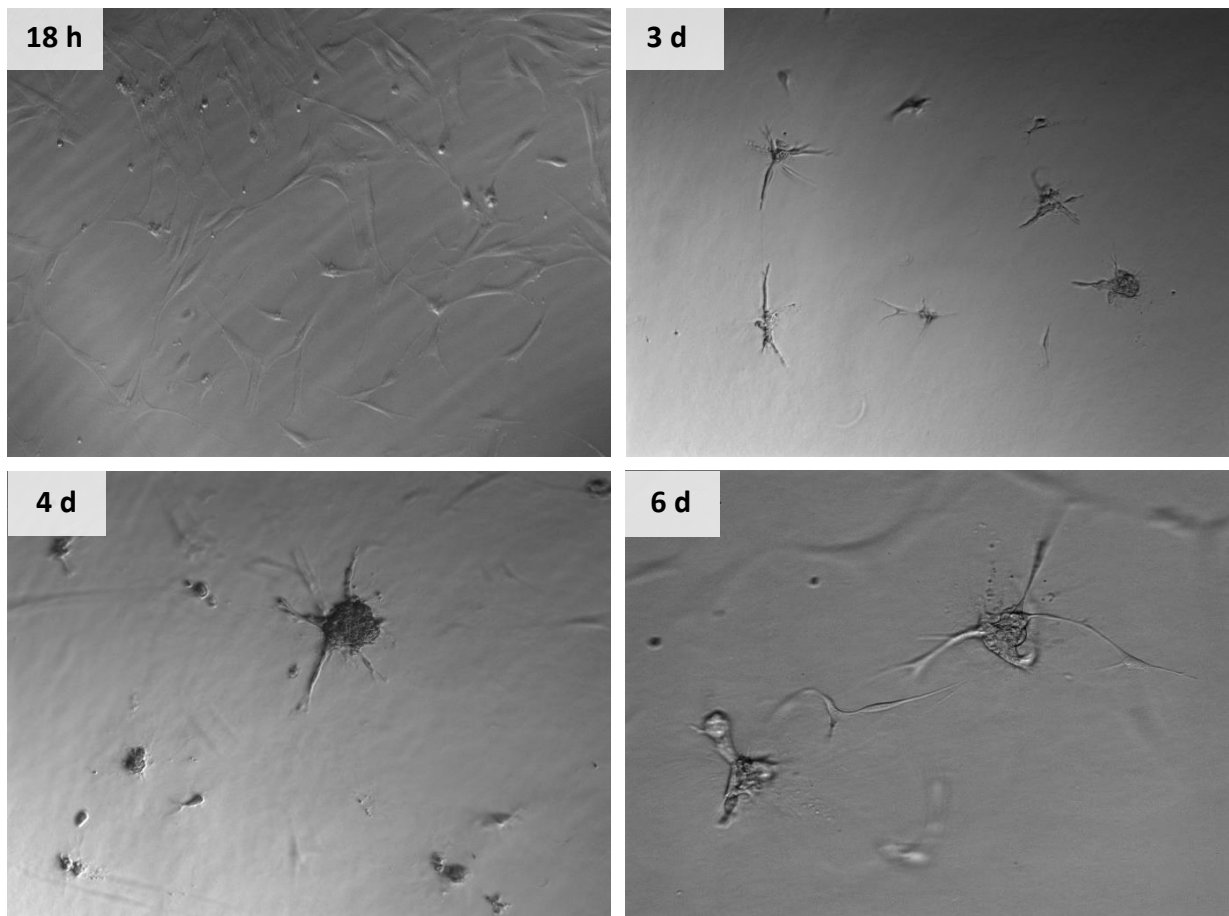
Figure 26. PSCs seeded on a layer of Matrigel™ after 18 hrs, 3 days, 4 days and 6 days.

PSCs were cultured on Matrigel™ for approximately 6 days. They gradually lost their flat "spread-out" appearance and formed three-dimensional cell clusters, some with large cytoplasmic projections (figure 26).

5.2.2.2 Western blot, Oil Red O staining and senescence staining of PSCs on Matrigel™

To verify that cells on Matrigel™ were indeed deactivated, we performed Western blot analyses as well as an Oil Red O staining. As α-SMA is an established marker of PSC activation, Western blot was used to determine whether PSCs cultured on Matrigel™ express less α-SMA than PSCs cultured on plastic, where they automatically become activated (see 2.4.1). In addition to this approach on protein level, an Oil Red O staining was performed on PSCs cultured on Matrigel™ in order to visualize the characteristic lipid droplets that PSCs regain after deactivation (see 2.4.1).
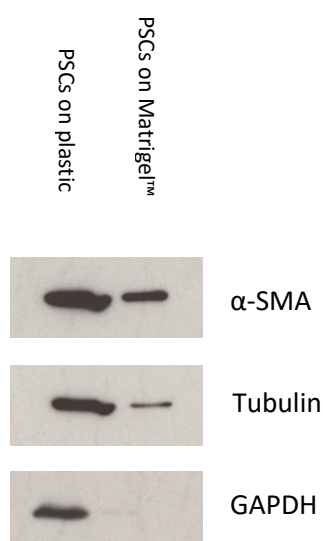
Figure 27. Western blot of protein extracts from PSCs cultured on plastic and PSCs cultured on Matrigel™. Expression of α-SMA, Tubulin and GAPDH is decreased in Matrigel™-cultured PSCs.
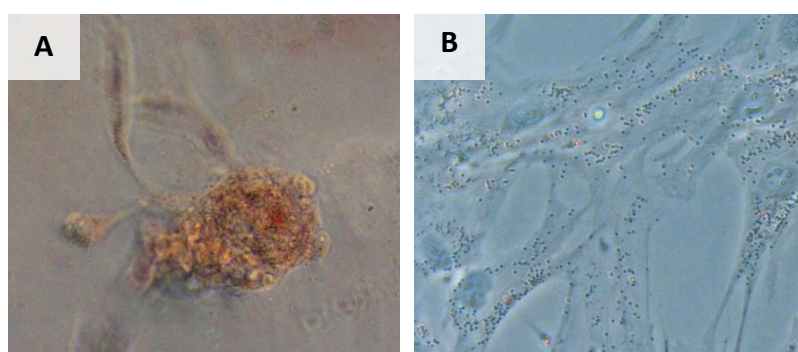
Figure 28. Results of Oil Red O staining. **A.** Oil Red O staining of PSCs seeded on Matrigel™. Cell clusters formed by PSCs cultured on Matrigel™ display a distinct orange staining, indicating the presence of lipid droplets. **B.** Oil Red O staining of PSCs seeded on plastic as negative control. PSCs show no morphological change and considerably less orange staining (lipid droplets).

A decreased expression of the activation marker α-SMA in Western blot strongly indicated deactivation of the cells (figure 27). The also observed decrease in expression of the structural protein tubulin might be explained by the morphological changes of the cells during inactivation, as they lose their typical myofibroblast-like cell structure. It is not entirely clear why cells showed a decreased expression of the housekeeping protein GAPDH, as this protein is not involved in structural changes. However, a reduced metabolic activity might be a possible explanation. While no housekeeping gene with equal expression in PSCs with and without Matrigel™ was found to be used as a control, equal loading in SDS-PAGE was ensured by measuring the protein concentration using a BCA protein assay, as described in the

Material & Methods section. Oil Red O staining displayed the presence of abundant lipid droplets in PSCs cultured on Matrigel™, suggesting successful deactivation (figure 28).

To rule out the possibility that the morphological changes in PSCs cultured on Matrigel™ are a result of cellular senescence, a β-galactosidase-based senescence staining kit was used to stain Matrigel™-cultured cells according to the manufacturer's instructions. PSCs cultured on Matrigel™ did not show β-galactosidase activity at any point, proving that their morphological changes as well as changes in lipid droplet storage are not a result of cellular senescence (figure 29).
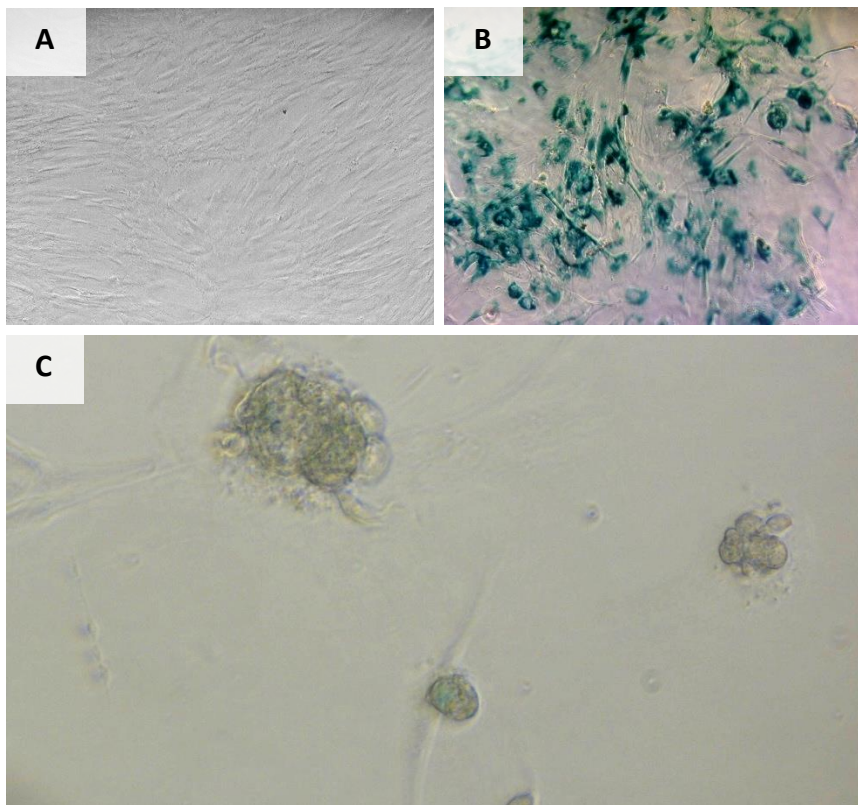
Figure 29. Results of senescence staining. **A.** Senescence staining of freshly thawed PSCs seeded on plastic. **B.** Senescence staining of PSCs cultured for 8 passages. **C.** Senescence staining of freshly thawed PSCs seeded on a layer of Matrigel™.
PSCs that had been in culture for 8 passages showed the characteristic blue staining indicating β-galactosidase activity and therefore cellular senescence (B), while neither freshly thawed PSCs (A) nor morphologically altered PSCs on Matrigel™ (C) showed any positivity in the senescence staining.

5.2.2.3 Immunofluorescence of PSCs on Matrigel™

To determine whether there are any differences between activated and deactivated PSCs regarding the expression of the tested markers, we also performed an immunofluorescence double staining for α-SMA and each respective marker on PSCs that were seeded and cultured on Matrigel™.

While immunofluorescence staining did not deliver satisfying results for cells that had formed clusters and were drastically morphologically altered, immunofluorescence was successfully performed on PSCs cultured on Matrigel™ that had not undergone such drastic changes in morphology.

While Matrigel™-cultured PSCs still stained positive for all tested markers, the number of cells staining positive for α-SMA was visibly reduced, suggesting a decreased activation level (figure 30).
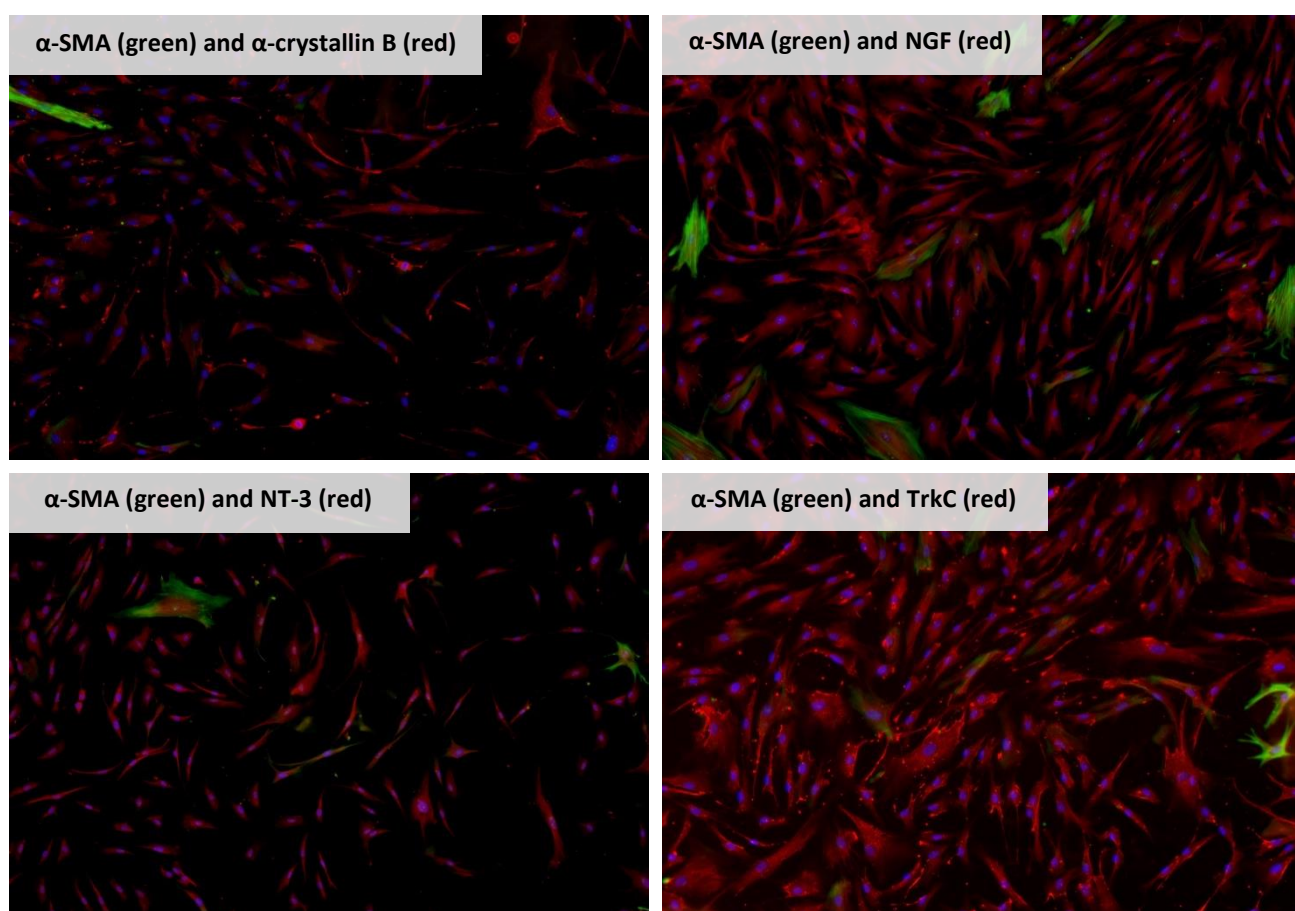
Figure 30. Double immunofluorescence staining of PSCs (M1223) cultured on Matrigel™ for 4 days. PSCs show cytoplasmic positivity for all tested markers. Few PSCs show cytoplasmic positivity for α-SMA.

6 Discussion

An excessive stromal reaction is a histopathological hallmark of both chronic pancreatitis and PDAC. After being considered as merely a side effect of chronic inflammation and carcinogenesis for decades, this stromal reaction has become an area of interest in pancreas research, especially regarding PDAC. While there are findings suggesting that the stroma can have a protective effect in PDAC (Ozdemir et al., 2014; Rhim et al., 2014), a lot of data point to the stroma as a crucial supporter of PDAC growth and therapy resistance: Aside from physically creating a barrier that encloses the tumor, leaving it hypoxic and hard to reach for chemotherapeutic agents (Harris, 2002; Oberstein & Olive, 2013), ECM proteins of the stroma seem to have growth- and survival-supporting effects on PCCs (Edderkaoui et al., 2005; Erkan et al., 2007; Vaquero et al., 2003; Vaquero et al., 2004). The established main source of the stromal reaction in the pancreas are specialized pancreatic stromal cells called pancreatic stellate cells (PSCs) (Apte et al., 2004; Apte & Wilson, 2003; Esposito et al., 2006).

The aim of this study was therefore the exact morphological and immunophenotypical characterization of the stromal cells in inflammatory diseases of the pancreas and in PDAC, in order to identify markers (or sets of markers) labelling subtypes of stromal cells involved in different disease processes. A similar approach has previously been used for the characterization of hepatic stromal cells (Cassiman et al., 2002), which are known to share similarities with their pancreatic counterparts. A further aim of the study was therefore to use these sets of markers to compare PSCs with HSCs and ascertain similarities and differences between the two cell types.

6.1 Characterization of the stromal reaction in chronic pancreatitis and PDAC

Cases of various subtypes of chronic pancreatitis (alcoholic chronic pancreatitis, AIP type 1, AIP type 2 and hereditary pancreatitis) and cases of PDAC were selected to be investigated in this study. While an abundant stroma is a typical characteristic of all the aforementioned diseases, morphological differences between the respective stromal reactions can already be observed in H&E-stained sections: First, each subtype of chronic pancreatitis shows a distinctive fibrosis pattern (predominantly inter-/perilobular in alcoholic CP, predominantly periductal and interlobular in AIP and predominantly periductal in hereditary pancreatitis) (Klöppel et al., 2004). Second, the stroma in PDAC can be categorized in subgroups, for example in dense, moderate and loose stroma. Data exist, which suggest that highly-dense PDAC stroma with mature collagen fibres correlates with a better outcome compared to a loose myxoid PDAC stroma (Erkan et al., 2008; Wang et al., 2015).

In the presented project, the stromal composition was further characterized by staining sections of all cases with Movat's pentachrome stain, which dyes collagens yellow and mucin and ground substance

blue and has previously been used to assess PDAC desmoplasia (Whatcott et al., 2015). Although a certain degree of heterogeneity among chronic pancreatitis cases and PDAC cases was observed, altogether the PDAC stroma was significantly more mucin-rich, while the stroma in cases of chronic pancreatitis was significantly more collagen-rich. This suggests that the stroma in PDAC is undergoing dynamic remodeling, while the stroma in chronic pancreatitis is more mature. This could be due to the fact that the stroma in PDAC interacts frequently with PCCs and therefore harbors a large number of activated PSCs. These results are in line with the above-mentioned findings that, in PDAC, stroma with a lower collagen density and a more myxoid composition correlates with a higher aggressiveness of the tumor (Erkan et al., 2008; Wang et al., 2015). Pointing into a similar direction, data from another study demonstrate that PDAC contains increased amounts of mucins compared to normal pancreas (4-fold increase in total glycosaminoglycans). Moreover, the composition of glycosaminoglycans changes, showing a 12-fold increase in hyaluronan and 22-fold increase in chondroitin sulfate, while the main glycosaminoglycan of normal pancreas, heparan sulfate, becomes a minor glycosaminoglycan in PDAC. And lastly, the condroitin sulfate in PDAC is also altered in its disaccharide composition (Theocharis et al., 2000). The mucin component hyaluronan is thought to promote malignancy and chemoresistance in cancer cells (Toole & Slomiany, 2008). Hyaluronan depletion using PEGylated human recombinant hyaluronidase (PEGPH20) has been demonstrated to achieve permanent stroma remodeling and therefore a prolonged survival in mice with PDAC (Provenzano et al., 2012). Recently, PEGPH20 has also been tested in a phase Ib study, delivering promising results especially for patients with PDAC high in hyaluronan (Hingorani et al., 2016). All these findings strongly suggest that especially the mucinous components of the stroma play a role in the aggressiveness of PDAC.

PSCs are established as the main source of the stromal reaction in both chronic pancreatitis and PDAC (Apte et al., 2004; Apte & Wilson, 2003; Esposito et al., 2006). After evaluating chronic pancreatitis stroma and PDAC stroma via H&E and Movat's stain, our next step was consequently the characterization of these effector cells. As PSCs share many morphological and functional similarities with the better-characterized HSCs of the liver (see 2.4.2), we chose to test the stroma of chronic pancreatitis cases and PDAC cases not only for previously suggested PSC markers (α-SMA, CD34, desmin, NGFR, SPARC and tenascin C), but also for established HSC markers (α-crystallin B, CD56, NGF, NT-3, synaptophysin and TrkC) by means of immunohistochemistry.

The IHC staining of chronic pancreatitis cases with the different markers, which were tested in this study, did not show any correlation between localizations and the above mentioned typical fibrosis patterns that are distinctive for individual subtypes of chronic pancreatitis (Klöppel et al., 2004). Staining patterns for tested markers were heterogeneous within and between different subtypes of chronic pancreatitis.

In IHC of PDAC cases, most tested markers showed a perilesional staining (i.e. staining around the tumor glands), highlighting the location of PSCs in close proximity to PCCs. This observation corresponds well with data demonstrating that PSCs interact bidirectionally with PCCs (Bachem et al., 2005; Esposito et al., 2006; Vonlaufen et al., 2008).

While a predominantly diffuse perilesional staining was found for α-SMA, CD34, CD56, NGF, NGFR, SPARC and TrkC, a predominantly focal perilesional staining was obtained for desmin and NT-3. In tenascin-C-stained PDAC cases, a roughly equal amount of diffuse and focal perilesional staining was found. Interestingly, when comparing the different markers to each other, definite and consistent overlaps of the perilesional staining patterns in PDAC cases could only be observed between α-SMA and SPARC. Altogether, cases of PDAC showed a similar degree of heterogeneity as cases of chronic pancreatitis. This heterogeneity might reflect a varying marker expression in PSCs with different levels of activation or differentiation, or even the coexistence of multiple unique PSC (or pancreatic myofibroblast) subpopulations. The idea that cancer-associated fibroblast populations are heterogeneous and variant has already been studied and substantiated in mouse models (Sugimoto et al., 2006). Correspondingly, Cassiman and colleagues were able to distinguish HSCs and different subtypes of hepatic myofibroblasts in the liver (Cassiman et al., 2002). Accordingly, an only focal perilesional staining in PDAC cases – as observed for desmin and NT-3 – might indicate that these markers are not expressed in all PSCs, but only in certain specialized subpopulations.

On comparing the Movat's-stained PDAC and CP cases with the IHC stainings of the respective cases, it was observed – as already mentioned above – that areas stained positive for α-SMA often overlapped with SPARC-positive areas and both correlated with collagen-rich stromal areas. On the other hand, areas stained positive for NT-3 correlated with mucin-rich stromal areas. This suggests that PSCs in different activation or differentiation levels or different subpopulations of PSCs or pancreatic myfibroblasts (α-SMA- and SPARC-positive PSCs or pancreatic myofibroblasts vs. NT-3-positive PSCs or pancreatic myofibroblasts) are located in differently composed stromal areas (collagen-rich mature stroma vs. mucin-rich immature stroma).

All this underscores the advantage of using a panel of multiple PSC markers for IHC, as opposed to using only one marker at a time. One marker might merely be expressed by a fraction of the stromal cells actually present, meaning that a number of stromal cells might be undetected when using one marker only. The heterogeneity of staining patterns between different PSC markers, as well as between and within subtypes of chronic pancreatitis and between cases of PDAC, also strongly suggests that the stroma is in a state of constant transition and plays an active role in chronic pancreatitis and PDAC.

Lastly, markers were also tested on freshly isolated HSCs and PSCs by means of immunofluorescence. Both HSCs and PSCs were positive for all tested markers. However, double stainings revealed the existence of single-positive as well as double-positive cells. This corroborates the suggested hypothesis that either PSCs in different states of activation and differentiation are present or that unique PSC or myofibroblast subpopulations are existent. In order to assess the expression of markers of deactivated PSCs, we cultured PSCs on Matrigel™, which has been demonstrated to induce deactivation of PSCs (Jesnowski et al., 2005). As a result, all tested markers were similarly expressed in Matrigel™-deactivated PSCs, indicating them as PSC markers independent from the activation status of the cells. This is in contrast to the IHC staining results showing that markers like α-crystallin B and synaptophysin show no perilesional staining in PDAC and are generally mostly expressed in stromal cells located around well-preserved pancreas tissue. Here the data indicate that these are markers for quiescent PSCs rather than for active PSCs. However, there is also the possibility that only a partial inactivation was achieved by culturing PSCs on Matrigel™. Further methods of stroma remodeling towards a mature stroma content, for example using Vitamin D receptor (VDR) ligands (Sherman et al., 2014), and their influence on the expression of PSC markers should be investigated in the future.

6.2   Similarities between PSCs and HSCs

Due to their relatively late discovery, isolation and cultivation (Apte et al., 1998; Bachem et al., 1998; Watari & Hotta, 1982) as well as the fact that research on cancer-supporting stromal cells had been sidelined by the focus on cancer cells themselves, PSCs lack the in-depth characterization of their hepatic counterparts. However, the important role of PSCs in chronic pancreatitis as well as PDAC (Apte et al., 2004; Apte & Wilson, 2003; Esposito et al., 2006) makes a detailed characterization of these cells an important goal for pancreas researchers. A number of striking similarities between PSCs and their hepatic counterparts, HSCs, have already been demonstrated: Morphologically, both cell types share an angular-shaped fat-storing phenotype in their quiescent state, and can transform into an activated myofibroblast-like phenotype, which is characterized by the expression of α-SMA and the loss of lipid droplets (Apte et al., 1998; Friedman, 1993). In their activated form, HSCs and PSCs synthesize large amounts of ECM proteins, e.g. collagens I and III (Apte et al., 2004; Friedman, 1993). Accordingly, both cell types are key effectors in physiological ECM turnover as well as pathological fibrosis of the liver or pancreas, respectively (Gressner & Bachem, 1995). Other functions of HSCs, for example a role in immunoregulation, have been demonstrated (Maher, 2001), but it has yet to be elucidated whether PSCs might play a similar role as well. HSCs and PSCs moreover share many similarities on a genomic level, but there are also some differences: Using transcriptome analysis including 21,329 genes, Buchholz and colleagues were able to find 88 genes that are expressed

differently between HSCs and skin fibroblasts and 73 genes that are expressed differently between PSCs and skin fibroblast, while they found only 29 genes that are expressed differently between HSCs and PSCs. The genes that are differently expressed between HSCs and PSCs include genes associated with ECM production and turnover, cell adhesion, cell communication and also transcription factors (Buchholz et al., 2005).

The presented study did not only investigate established and proposed PSC markers, but also known HSC markers like α-crystallin B, CD56, NGF, NT-3, synaptophysin and TrkC (Cassiman et al., 2002). As a result, all HSC markers were found to be expressed in PSCs as well. This implies that the tested HSC markers can be used as PSC markers and further highlights the similarities between HSCs and PSCs.

A common origin of HSCs and PSCs is one possible explanation for the many shared characteristics between the two cell types. A neuroectodermal origin of these cells would be in line with the expression of the above mentioned neural proteins (α-crystallin B, CD56, NGF, NT-3, synaptophysin and TrkC) found in this study – however, a neuroectodermal origin has already been refuted in the case of HSCs by cell lineage tracking techniques (Cassiman et al., 2006; Mederacke et al., 2013). Lineage tracing for PSCs was not performed so far. While another common origin for HSCs and PSCs is still thinkable, multipotent precursor cells that can differentiate into PSCs have been found in the adult mouse pancreas (Seaberg et al., 2004). This suggests that PSCs could possibly derive from a local precursor specific to the pancreas and not share a common origin with HSCs after all. The close similarities of the two cell types in morphology and function might then be explained as a result of similar microenvironments (Buchholz et al., 2005).

The consistent expression of neural markers by PSCs could also be of relevance concerning another important feature of both chronic pancreatitis and PDAC, namely neural alterations. In this respect there are findings that point to PSCs as possible "mediators" between PCCs and neural cells. For example, it has been demonstrated that PSC are able to secrete the neurotransmitter acetylcholine, thus attracting PCCs to spread along nerves (Phillips et al., 2010). Interestingly, neural alterations, for example increased neural density and hypertrophy, are found in chronic pancreatitis and PDAC, but not in other pancreatic disorders (Ceyhan et al., 2009). In chronic pancreatitis, the neural changes mainly manifest themselves as pancreatic neuritis, resulting in severe neuropathic pain (Ceyhan et al., 2009). Neuropathic pain also occurs in PDAC; moreover, perineural invasion is found in nearly all PDAC cases and plays a pivotal role in the poor prognosis of PDAC in general, as it is an important reason for tumor progression and local recurrence (Demir et al., 2010). Notably, a high correlation between the extent of desmoplasia in PDAC and the severity of perineural invasion has been found (Ceyhan et al., 2009). It has yet to be elucidated if there is not only a correlation, but also causation, and if so, how exactly the stroma facilitates perineural invasion in PCCs.

Discussion

In conclusion, we were able to improve the characterization of stromal cells of the pancreas by confirming six known PSC markers (α-SMA, CD34, desmin, NGFR, SPARC and tenascin C) and identifying six new PSC markers (α-crystallin B, CD56, NGF, NT-3, synaptophysin and TrkC). The markers show variant expression patterns in the stroma of chronic pancreatitis and most show a perilesional expression in the stroma of PDAC, which can be explained in the context of tumor-stroma interaction. The expression patterns of these markers in chronic pancreatitis as well as in PDAC cases are strikingly heterogeneous and seem to correlate with the ECM composition of the stroma (mucinous vs. collagen-rich). These in vivo findings, together with the existence of double- and single-stained cells in vitro, are consistent with the presence of PSCs in different states of activation or differentiation or even multiple subpopulations of PSCs and/or pancreatic myofibroblasts. Further studies are needed to investigate whether the expression of the tested markers is truly independent of the activation level of PSCs, possibly with the help of more reliable methods of PSC deactivation than cultivation on Matrigel™. In addition, the potential existence of PSC subpopulations or pancreatic myofibroblast subpopulations should be investigated further in the future, as pancreatic myofibroblasts might be another potential source of fibrosis in the pancreas, in addition to PSCs.

We were also able to underline the close similarities of PSCs with HSCs in this study by demonstrating that six markers that were already established for HSCs are also expressed in PSCs. However, it is still unclear whether the reason for these similarities is a common origin or whether the similarities are the result of a similar microenvironment, and whether PSCs might use neural markers to communicate with neural cells, e.g. in the context of perineural invasion in PDAC. In the future, additional studies using cell lineage tracing techniques similar to the ones used on HSCs, could determine the origin of PSCs and further advance the much-needed functional characterization of PSCs.

7 Abstract

Background/aims: An abundant stromal reaction is one of the hallmarks of pancreatic ductal adenocarcinoma (PDAC) and chronic pancreatitis. The cells mainly responsible for the stromal reaction are activated pancreatic stellate cells (PSCs). Despite their crucial role in two major pancreatic diseases, PSCs are not well characterized regarding their origin, function and immunophenotype. However, it is known that PSCs share numerous characteristics with hepatic stellate cells (HSCs), which have been described and established as key effectors in liver fibrosis long before their pancreatic counterparts. The aim of this study was a detailed immunophenotypical analysis of PSCs in PDAC and cases of chronic pancreatitis of various etiologies as well as the comparison of PSCs with HSCs in order to ascertain similarities and differences between the two cell types.

Methods: Resection specimens of PDAC (n=10) and chronic pancreatitis (n=12) were studied by means of histochemistry and immunohistochemistry. The composition of the stroma was characterized using Movat's pentachrome stain. Cases were then tested for a panel consisting of PSC markers (α-SMA, CD34, desmin, NGFR, SPARC and tenascin C) as well as established HSC markers (α-crystallin B, CD56, NGF, NT-3, synaptophysin and TrkC). PSCs freshly isolated from PDAC and chronic pancreatitis tissue samples were evaluated by immunofluorescence in an activated state and after being deactivated by cultivation on Matrigel™.

Results: While the stroma of chronic pancreatitis cases was characterized by a mature fibrosis, PDAC stroma displayed significantly more active remodeling. PSCs expressed all tested markers in analogy to HSCs. In cases of PDAC, a perilesional staining could be observed for most tested markers. Cases of chronic pancreatitis showed a more varying expression of the tested markers. Staining patterns were heterogeneous in cases of PDAC and in cases of chronic pancreatitis. The overlapping stainings for α-SMA and SPARC correlated with a collagen-rich fibrosis, while NT-3 staining was associated with intense remodeling of the stroma.

Conclusion: The close similarities between PSCs and HSCs were confirmed. Heterogeneous expression patterns of the tested markers might reflect different levels of activation or differentiation of PSCs or even the presence of multiple subpopulations of PSCs or pancreatic myofibroblasts. Along with the heterogeneity of the stromal composition highlighted by Movat's stain, this strongly suggests an active role of the stroma in PDAC and chronic pancreatitis.

8 Zusammenfassung

Hintergrund/Zielsetzung: Eine ausgeprägte Stromareaktion ist eines der Hauptmerkmale des duktalen Pankreaskarzinoms (*pancreatic ductal adenocarcinoma*, PDAC) und der chronischen Pankreatitis (CP). Aktivierte Stellatumzellen des Pankreas (*pancreatic stellate cells*, PSCs) sind hauptsächlich für diese Stromareaktion verantwortlich. Trotz ihrer zentralen Rolle in zwei bedeutenden Erkrankungen des Pankreas sind PSCs nicht ausreichend bezüglich ihres Ursprungs, ihrer Funktion und ihres Immunphänotyps charakterisiert. Es ist allerdings bekannt, dass PSCs viele Merkmale mit den Stellatumszellen der Leber (*hepatic stellate cells*, HSCs) teilen, welche als Haupteffektoren der Leberfibrose bereits ausführlich beschrieben worden sind. Das Ziel dieser Arbeit war eine detaillierte Analyse des Immunphänotyps der PSCs im PDAC und in der chronischen Pankreatitis sowie ein Vergleich der PSCs mit den HSCs.

Methoden: Gewebeproben aus PDACs (n=10) und chronischen Pankreatitiden (n=12) wurden histochemisch und immunhistochemisch analysiert. Die Zusammensetzung des Stromas der Proben wurde anhand der Movat-Pentachromfärbung untersucht. Die Proben wurden in der Immunhistochemie auf die Expression von etablierten PSC-Markern (α-SMA, CD34, Desmin, NGFR, SPARC und Tenascin C) sowie HSC-Markern (α-Crystallin B, CD56, NGF, NT-3, Synaptophysin und TrkC) getestet. PSCs, die aus frisch entnommenen Gewebeproben von Patienten mit PDAC oder chronischer Pankreatitis isoliert wurden, wurden mittels Immunfluoreszenz sowohl in ihrer aktivierten Form als auch nach Deaktivierung durch Kultivierung auf Matrigel™ untersucht.

Ergebnisse: Während sich das Stroma in chronischen Pankreatitiden durch eine reife Fibrose auszeichnete, zeigte das PDAC-Stroma signifikant mehr aktives Remodeling. PSCs exprimierten alle getesteten Marker in Analogie zu HSCs. In PDAC-Fällen zeigten die meisten untersuchten Marker periläsionale Expressionsmuster. In CP-Fällen variierten die Expressionsmuster stärker. Sowohl in PDAC-Fällen als auch in CP-Fällen waren die Expressionsmuster heterogen. Generell korrelierten die α-SMA- und die SPARC-Färbung mit einer kollagenreichen reifen Fibrose, während die NT-3-Färbung mit intensivem Stromaumbau assoziiert war.

Schlussfolgerung: Die starke Ähnlichkeit von PSCs und HSCs konnte bestätigt werden. Die heterogenen Expressionsmuster der getesteten Marker können ein Hinweis auf das Vorliegen von PSCs in verschiedenen Aktivitäts- oder Differenzierungsleveln oder sogar auf verschiedene Subpopulationen von PSCs oder Myofibroblasten des Pankreas sein. In Zusammenschau mit der Heterogenität des Stromas, die sich in der Movatfärbung nachweisen ließ, spricht dies stark für eine aktive Rolle des Stromas im PDAC und in der chronischen Pankreatitis.

9 List of tables

10 List of figures

11 References

Amann, R. W., Heitz, P. U., & Klöppel, G. (1996). Course of alcoholic chronic pancreatitis: a prospective clinico-morphological long-term study. *Gastroenterology, 111*(1), 224-231.

Andriulli, A., Botteri, E., Almasio, P. L., Vantini, I., Uomo, G., Maisonneuve, P., & ad hoc Committee of the Italian Association for the Study of the Pancreas (2010). Smoking as a cofactor for causation of chronic pancreatitis: a meta-analysis. *Pancreas, 39*(8), 1205-1210. doi:10.1097/MPA.0b013e3181df27c0

Apte, M. V., Haber, P. S., Applegate, T. L., Norton, I. D., McCaughan, G. W., Korsten, M. A., Pirola, R. C., & Wilson, J. S. (1998). Periacinar stellate shaped cells in rat pancreas: identification, isolation, and culture. *Gut, 43*(1), 128-133.

Apte, M. V., Park, S., Phillips, P. A., Santucci, N., Goldstein, D., Kumar, R. K., Ramm, G. A., Buchler, M., Friess, H., McCarroll, J. A., Keogh, G., Merrett, N., Pirola, R., & Wilson, J. S. (2004). Desmoplastic reaction in pancreatic cancer: role of pancreatic stellate cells. *Pancreas, 29*(3), 179-187.

Apte, M. V., Phillips, P. A., Fahmy, R. G., Darby, S. J., Rodgers, S. C., McCaughan, G. W., Korsten, M. A., Pirola, R. C., Naidoo, D., & Wilson, J. S. (2000). Does alcohol directly stimulate pancreatic fibrogenesis? Studies with rat pancreatic stellate cells. *Gastroenterology, 118*(4), 780-794.

Apte, M. V., & Wilson, J. S. (2003). Stellate cell activation in alcoholic pancreatitis. *Pancreas, 27*(4), 316-320.

Armstrong, T., Packham, G., Murphy, L. B., Bateman, A. C., Conti, J. A., Fine, D. R., Johnson, C. D., Benyon, R. C., & Iredale, J. P. (2004). Type I collagen promotes the malignant phenotype of pancreatic ductal adenocarcinoma. *Clinical Cancer Research, 10*(21), 7427-7437. doi:10.1158/1078-0432.CCR-03-0825

Asahina, K., Tsai, S. Y., Li, P., Ishii, M., Maxson, R. E., Jr., Sucov, H. M., & Tsukamoto, H. (2009). Mesenchymal origin of hepatic stellate cells, submesothelial cells, and perivascular mesenchymal cells during mouse liver development. *Hepatology, 49*(3), 998-1011. doi:10.1002/hep.22721

Bachem, M. G., Schneider, E., Gross, H., Weidenbach, H., Schmid, R. M., Menke, A., Siech, M., Beger, H., Grünert, A., & Adler, G. (1998). Identification, culture, and characterization of pancreatic stellate cells in rats and humans. *Gastroenterology, 115*(2), 421-432.

Bachem, M. G., Schünemann, M., Ramadani, M., Siech, M., Beger, H., Buck, A., Zhou, S., Schmid-Kotsas, A., & Adler, G. (2005). Pancreatic carcinoma cells induce fibrosis by stimulating proliferation and matrix synthesis of stellate cells. *Gastroenterology, 128*(4), 907-921.

Balkwill, F., & Mantovani, A. (2001). Inflammation and cancer: back to Virchow? *Lancet, 357*(9255), 539-545. doi:10.1016/S0140-6736(00)04046-0

Banks, P. A., Conwell, D. L., & Toskes, P. P. (2010). The management of acute and chronic pancreatitis. *Gastroenterology & Hepatology, 6*(2 Suppl 5), 1-16.

Barbacid, M. (1994). The Trk family of neurotrophin receptors. *Journal of Neurobiology, 25*(11), 1386-1403. doi:10.1002/neu.480251107

Bartsch, D. K., Gress, T. M., & Langer, P. (2012). Familial pancreatic cancer--current knowledge. *Nature Reviews Gastroenterology & Hepatology, 9*(8), 445-453. doi:10.1038/nrgastro.2012.111

Beger, H. G., Rau, B., Gansauge, F., Poch, B., & Link, K.-H. (2003). Treatment of pancreatic cancer: challenge of the facts. *World Journal of Surgery, 27*(10), 1075-1084. doi:10.1007/s00268-003-7165-7

Berchtold, S., Grunwald, B., Kruger, A., Reithmeier, A., Hahl, T., Cheng, T., Feuchtinger, A., Born, D., Erkan, M., Kleeff, J., & Esposito, I. (2015). Collagen type V promotes the malignant phenotype of pancreatic ductal adenocarcinoma. *Cancer Letters, 356*(2 Pt B), 721-732. doi:10.1016/j.canlet.2014.10.020

Bhaw-Luximon, A., & Jhurry, D. (2015). New avenues for improving pancreatic ductal adenocarcinoma (PDAC) treatment: selective stroma depletion combined with nano drug delivery. *Cancer Letters, 369*(2), 266-273. doi:10.1016/j.canlet.2015.09.007

References

Binkley, C. E., Zhang, L., Greenson, J. K., Giordano, T. J., Kuick, R., Misek, D., Hanash, S., Logsdon, C. D., & Simeone, D. M. (2004). The molecular basis of pancreatic fibrosis: common stromal gene expression in chronic pancreatitis and pancreatic adenocarcinoma. *Pancreas, 29*(4), 254-263.

Bordalo, O., Bapista, A., Dreiling, D., & Noronha, M. (1984). Early pathomorphological pancreatic changes in chronic alcoholism. In Gyr, K. E., Singer, M. V., & Sarles, H. (Eds.), *Pancreatitis—Concepts and Classification*. Amsterdam: Elsevier.

Bosetti, C., Lucenteforte, E., Silverman, D. T., Petersen, G., Bracci, P. M., Ji, B. T., Negri, E., Li, D., Risch, H. A., Olson, S. H., Gallinger, S., Miller, A. B., Bueno-de-Mesquita, H. B., Talamini, R., Polesel, J., Ghadirian, P., Baghurst, P. A., Zatonski, W., Fontham, E., Bamlet, W. R., Holly, E. A., Bertuccio, P., Gao, Y. T., Hassan, M., Yu, H., Kurtz, R. C., Cotterchio, M., Su, J., Maisonneuve, P., Duell, E. J., Boffetta, P., & La Vecchia, C. (2012). Cigarette smoking and pancreatic cancer: an analysis from the International Pancreatic Cancer Case-Control Consortium (Panc4). *Annals of Oncology, 23*(7), 1880-1888. doi:10.1093/annonc/mdr541

Bradshaw, A. D., & Sage, E. H. (2001). SPARC, a matricellular protein that functions in cellular differentiation and tissue response to injury. *Journal of Clinical Investigation, 107*(9), 1049-1054. doi:10.1172/jci12939

Braganza, J. M. (1983). Pancreatic disease: a casualty of hepatic "detoxification"? *Lancet, 2*(8357), 1000-1003.

Braganza, J. M., Lee, S. H., McCloy, R. F., & McMahon, M. J. (2011). Chronic pancreatitis. *Lancet, 377*(9772), 1184-1197. doi:10.1016/S0140-6736(10)61852-1

Broughton, G., Janis, J. E., & Attinger, C. E. (2006). Wound healing: an overview. *Plastic and Reconstructive Surgery, 117*(7 Suppl), 1e-S-32e-S. doi:10.1097/01.prs.0000222562.60260.f9

Buchholz, M., Kestler, H. A., Holzmann, K., Ellenrieder, V., Schneiderhan, W., Siech, M., Adler, G., Bachem, M. G., & Gress, T. M. (2005). Transcriptome analysis of human hepatic and pancreatic stellate cells: organ-specific variations of a common transcriptional phenotype. *Journal of Molecular Medicine, 83*(10), 795-805. doi:10.1007/s00109-005-0680-2

Burris, H. A., Moore, M. J., Andersen, J., Green, M. R., Rothenberg, M. L., Modiano, M. R., Cripps, M. C., Portenoy, R. K., Storniolo, A. M., Tarassoff, P., Nelson, R., Dorr, F. A., Stephens, C. D., & Hoff, D. D. V. (1997). Improvements in survival and clinical benefit with gemcitabine as first-line therapy for patients with advanced pancreas cancer: a randomized trial. *Journal of Clinical Oncology, 15*(6), 2403-2413. doi:10.1200/JCO.1997.15.6.2403

Cascinu, S., Falconi, M., Valentini, V., Jelic, S., & ESMO Guidelines Working Group (2010). Pancreatic cancer: ESMO Clinical Practice Guidelines for diagnosis, treatment and follow-up. *Annals of Oncology, 21 Suppl 5*, v55-58. doi:10.1093/annonc/mdq165

Cassiman, D., Barlow, A., Vander Borght, S., Libbrecht, L., & Pachnis, V. (2006). Hepatic stellate cells do not derive from the neural crest. *Journal of Hepatology, 44*(6), 1098-1104. doi:10.1016/j.jhep.2005.09.023

Cassiman, D., Denef, C., Desmet, V. J., & Roskams, T. (2001a). Human and rat hepatic stellate cells express neurotrophins and neurotrophin receptors. *Hepatology, 33*(1), 148-158. doi:10.1053/jhep.2001.20793

Cassiman, D., Libbrecht, L., Desmet, V., Denef, C., & Roskams, T. (2002). Hepatic stellate cell/myofibroblast subpopulations in fibrotic human and rat livers. *Journal of Hepatology, 36*(2), 200-209.

Cassiman, D., Roskams, T., van Pelt, J., Libbrecht, L., Aertsen, P., Crabbe, T., Vankelecom, H., & Denef, C. (2001b). Alpha B-crystallin expression in human and rat hepatic stellate cells. *Journal of Hepatology, 35*(2), 200-207.

Cassiman, D., van Pelt, J., De Vos, R., Van Lommel, F., Desmet, V., Yap, S. H., & Roskams, T. (1999). Synaptophysin: a novel marker for human and rat hepatic stellate cells. *American Journal of Pathology, 155*(6), 1831-1839. doi:10.1016/s0002-9440(10)65501-0

Cavallaro, U., Niedermeyer, J., Fuxa, M., & Christofori, G. (2001). N-CAM modulates tumour-cell adhesion to matrix by inducing FGF-receptor signalling. *Nature Cell Biology, 3*(7), 650-657. doi:10.1038/35083041

Ceyhan, G. O., Bergmann, F., Kadihasanoglu, M., Altintas, B., Demir, I. E., Hinz, U., Muller, M. W., Giese, T., Buchler, M. W., Giese, N. A., & Friess, H. (2009). Pancreatic neuropathy and neuropathic pain--a comprehensive pathomorphological study of 546 cases. *Gastroenterology, 136*(1), 177-186.e171. doi:10.1053/j.gastro.2008.09.029

Chao, M. V. (1994). The p75 neurotrophin receptor. *Journal of Neurobiology, 25*(11), 1373-1385. doi:10.1002/neu.480251106

Chari, S. T., Kloeppel, G., Zhang, L., Notohara, K., Lerch, M. M., Shimosegawa, T., & Autoimmune Pancreatitis International Cooperative Study Group (APICS) (2010). Histopathologic and clinical subtypes of autoimmune pancreatitis: the Honolulu consensus document. *Pancreas, 39*(5), 549-554. doi:10.1097/MPA.0b013e3181e4d9e5

Christopher, K. L., Pedler, M. G., Shieh, B., Ammar, D. A., Petrash, J. M., & Mueller, N. H. (2014). Alpha-crystallin-mediated protection of lens cells against heat and oxidative stress-induced cell death. *Biochimica et Biophysica Acta, 1843*(2), 309-315. doi:10.1016/j.bbamcr.2013.11.010

Civin, C. I., Strauss, L. C., Brovall, C., Fackler, M. J., Schwartz, J. F., & Shaper, J. H. (1984). Antigenic analysis of hematopoiesis. III. A hematopoietic progenitor cell surface antigen defined by a monoclonal antibody raised against KG-1a cells. *Journal of Immunology, 133*(1), 157-165.

Cohen, S., Levi-Montalcini, R., & Hamburger, V. (1954). A nerve growth-stimulating factor isolated from sarcom as 37 and 180. *Proceedings of the National Academy of Sciences of the United States of America, 40*(10), 1014-1018.

Conklin, M. W., & Keely, P. J. (2012). Why the stroma matters in breast cancer. *Cell Adhesion & Migration, 6*(3), 249-260. doi:10.4161/cam.20567

Conroy, T., Desseigne, F., Ychou, M., Bouché, O., Guimbaud, R., Bécouarn, Y., Adenis, A., Raoul, J.-L., Gourgou-Bourgade, S., de la Fouchardière, C., Bennouna, J., Bachet, J.-B., Khemissa-Akouz, F., Péré-Vergé, D., Delbaldo, C., Assenat, E., Chauffert, B., Michel, P., Montoto-Grillot, C., Ducreux, M., Groupe Tumeurs Digestives of Unicancer, & PRODIGE Intergroup (2011). FOLFIRINOX versus gemcitabine for metastatic pancreatic cancer. *New England Journal of Medicine, 364*(19), 1817-1825. doi:10.1056/NEJMoa1011923

Coté, G. A., Yadav, D., Slivka, A., Hawes, R. H., Anderson, M. A., Burton, F. R., Brand, R. E., Banks, P. A., Lewis, M. D., Disario, J. A., Gardner, T. B., Gelrud, A., Amann, S. T., Baillie, J., Money, M. E., O'Connell, M., Whitcomb, D. C., Sherman, S., & North American Pancreatitis Study Group (2011). Alcohol and smoking as risk factors in an epidemiology study of patients with chronic pancreatitis. *Clinical Gastroenterology and Hepatology, 9*(3), 266-273; quiz e27. doi:10.1016/j.cgh.2010.10.015

Coussens, L. M., & Werb, Z. (2002). Inflammation and cancer. *Nature, 420*(6917), 860-867. doi:10.1038/nature01322

Dakhova, O., Rowley, D., & Ittmann, M. (2014). Genes upregulated in prostate cancer reactive stroma promote prostate cancer progression in vivo. *Clinical Cancer Research, 20*(1), 100-109. doi:10.1158/1078-0432.CCR-13-1184

De Gonzalez, A. B., Sweetland, S., & Spencer, E. (2003). A meta-analysis of obesity and the risk of pancreatic cancer. *British Journal of Cancer, 89*(3), 519-523. doi:10.1038/sj.bjc.6601140

Demir, I. E., Ceyhan, G. O., Liebl, F., D'Haese, J. G., Maak, M., & Friess, H. (2010). Neural invasion in pancreatic cancer: the past, present and future. *Cancers, 2*(3), 1513-1527. doi:10.3390/cancers2031513

Ditlevsen, D. K., Povlsen, G. K., Berezin, V., & Bock, E. (2008). NCAM-induced intracellular signaling revisited. *Journal of Neuroscience Research, 86*(4), 727-743. doi:10.1002/jnr.21551

Edderkaoui, M., Hong, P., Vaquero, E. C., Lee, J. K., Fischer, L., Friess, H., Buchler, M. W., Lerch, M. M., Pandol, S. J., & Gukovskaya, A. S. (2005). Extracellular matrix stimulates reactive oxygen species production and increases pancreatic cancer cell survival through 5-lipoxygenase and NADPH oxidase. *American Journal of Physiology - Gastrointestinal and Liver Physiology, 289*(6), G1137-1147. doi:10.1152/ajpgi.00197.2005

References

Edelmann, L., Hanson, P. I., Chapman, E. R., & Jahn, R. (1995). Synaptobrevin binding to synaptophysin: a potential mechanism for controlling the exocytotic fusion machine. *EMBO Journal, 14*(2), 224-231.

Erkan, M., Adler, G., Apte, M. V., Bachem, M. G., Buchholz, M., Detlefsen, S., Esposito, I., Friess, H., Gress, T. M., Habisch, H.-J., Hwang, R. F., Jaster, R., Kleeff, J., Klöppel, G., Kordes, C., Logsdon, C. D., Masamune, A., Michalski, C. W., Oh, J., Phillips, P. A., Pinzani, M., Reiser-Erkan, C., Tsukamoto, H., & Wilson, J. (2012). StellaTUM: current consensus and discussion on pancreatic stellate cell research. *Gut, 61*(2), 172-178. doi:10.1136/gutjnl-2011-301220

Erkan, M., Kleeff, J., Gorbachevski, A., Reiser, C., Mitkus, T., Esposito, I., Giese, T., Büchler, M. W., Giese, N. A., & Friess, H. (2007). Periostin creates a tumor-supportive microenvironment in the pancreas by sustaining fibrogenic stellate cell activity. *Gastroenterology, 132*(4), 1447-1464. doi:10.1053/j.gastro.2007.01.031

Erkan, M., Michalski, C. W., Rieder, S., Reiser-Erkan, C., Abiatari, I., Kolb, A., Giese, N. A., Esposito, I., Friess, H., & Kleeff, J. (2008). The activated stroma index is a novel and independent prognostic marker in pancreatic ductal adenocarcinoma. *Clinical Gastroenterology and Hepatology, 6*(10), 1155-1161. doi:10.1016/j.cgh.2008.05.006

Erkan, M., Reiser-Erkan, C., Michalski, C. W., & Kleeff, J. (2010). Tumor microenvironment and progression of pancreatic cancer. *Experimental Oncology, 32*(3), 128-131.

Esposito, I., Born, D., Bergmann, F., Longerich, T., Welsch, T., Giese, N. A., Buchler, M. W., Kleeff, J., Friess, H., & Schirmacher, P. (2008). Autoimmune pancreatocholangitis, non-autoimmune pancreatitis and primary sclerosing cholangitis: a comparative morphological and immunological analysis. *PLOS ONE, 3*(7), e2539. doi:10.1371/journal.pone.0002539

Esposito, I., Penzel, R., Chaib-Harrireche, M., Barcena, U., Bergmann, F., Riedl, S., Kayed, H., Giese, N., Kleeff, J., Friess, H., & Schirmacher, P. (2006). Tenascin C and annexin II expression in the process of pancreatic carcinogenesis. *Journal of Pathology, 208*(5), 673-685. doi:10.1002/path.1935

Etemad, B., & Whitcomb, D. C. (2001). Chronic pancreatitis: diagnosis, classification, and new genetic developments. *Gastroenterology, 120*(3), 682-707.

Fields, R. D., & Itoh, K. (1996). Neural cell adhesion molecules in activity-dependent development and synaptic plasticity. *Trends in Neurosciences, 19*(11), 473-480. doi:10.1016/s0166-2236(96)30013-1

Fina, L., Molgaard, H. V., Robertson, D., Bradley, N. J., Monaghan, P., Delia, D., Sutherland, D. R., Baker, M. A., & Greaves, M. F. (1990). Expression of the CD34 gene in vascular endothelial cells. *Blood, 75*(12), 2417-2426.

Friedman, S. L. (1993). The cellular basis of hepatic fibrosis – mechanisms and treatment strategies. *New England Journal of Medicine, 328*(25), 1828-1835. doi:10.1056/NEJM199306243282508

Friess, H., Zhu, Z. W., di Mola, F. F., Kulli, C., Graber, H. U., Andren-Sandberg, A., Zimmermann, A., Korc, M., Reinshagen, M., & Buchler, M. W. (1999). Nerve growth factor and its high-affinity receptor in chronic pancreatitis. *Annals of Surgery, 230*(5), 615-624.

Gapstur, S. M., Jacobs, E. J., Deka, A., McCullough, M. L., Patel, A. V., & Thun, M. J. (2011). Association of alcohol intake with pancreatic cancer mortality in never smokers. *Archives of Internal Medicine, 171*(5), 444-451. doi:10.1001/archinternmed.2010.536

Gluer, S., Schelp, C., Madry, N., von Schweinitz, D., Eckhardt, M., & Gerardy-Schahn, R. (1998). Serum polysialylated neural cell adhesion molecule in childhood neuroblastoma. *British Journal of Cancer, 78*(1), 106-110.

Goldstein, D., El-Maraghi, R. H., Hammel, P., Heinemann, V., Kunzmann, V., Sastre, J., Scheithauer, W., Siena, S., Tabernero, J., Teixeira, L., Tortora, G., Van Laethem, J. L., Young, R., Penenberg, D. N., Lu, B., Romano, A., & Von Hoff, D. D. (2015). Nab-Paclitaxel plus gemcitabine for metastatic pancreatic cancer: long-term survival from a phase III trial. *Journal of the National Cancer Institute, 107*(2). doi:10.1093/jnci/dju413

Gressner, A. M., & Bachem, M. G. (1995). Molecular mechanisms of liver fibrogenesis--a homage to the role of activated fat-storing cells. *Digestion, 56*(5), 335-346. doi:10.1159/000201257

References

Guweidhi, A., Kleeff, J., Adwan, H., Giese, N. A., Wente, M. N., Giese, T., Buchler, M. W., Berger, M. R., & Friess, H. (2005). Osteonectin influences growth and invasion of pancreatic cancer cells. *Annals of Surgery, 242*(2), 224-234.

Haber, P. S., Keogh, G. W., Apte, M. V., Moran, C. S., Stewart, N. L., Crawford, D. H., Pirola, R. C., McCaughan, G. W., Ramm, G. A., & Wilson, J. S. (1999). Activation of pancreatic stellate cells in human and experimental pancreatic fibrosis. *American Journal of Pathology, 155*(4), 1087-1095. doi:10.1016/S0002-9440(10)65211-X

Habisch, H., Zhou, S., Siech, M., & Bachem, M. G. (2010). Interaction of stellate cells with pancreatic carcinoma cells. *Cancers, 2*(3), 1661-1682. doi:10.3390/cancers2031661

Halangk, W., Krüger, B., Ruthenbürger, M., Stürzebecher, J., Albrecht, E., Lippert, H., & Lerch, M. M. (2002). Trypsin activity is not involved in premature, intrapancreatic trypsinogen activation. *American Journal of Physiology - Gastrointestinal and Liver Physiology, 282*(2), G367-374. doi:10.1152/ajpgi.00315.2001

Harris, A. L. (2002). Hypoxia--a key regulatory factor in tumour growth. *Nature Reviews Cancer, 2*(1), 38-47. doi:10.1038/nrc704

Hart, P. A., Kamisawa, T., Brugge, W. R., Chung, J. B., Culver, E. L., Czakó, L., Frulloni, L., Go, V. L. W., Gress, T. M., Kim, M.-H., Kawa, S., Lee, K. T., Lerch, M. M., Liao, W.-C., Löhr, M., Okazaki, K., Ryu, J. K., Schleinitz, N., Shimizu, K., Shimosegawa, T., Soetikno, R., Webster, G., Yadav, D., Zen, Y., & Chari, S. T. (2013). Long-term outcomes of autoimmune pancreatitis: a multicentre, international analysis. *Gut, 62*(12), 1771-1776. doi:10.1136/gutjnl-2012-303617

Haubrich, W. S. (2004). Kupffer of Kupffer cells. *Gastroenterology, 127*(1), 16.

He, J., Sun, X., Qian, K. Q., Liu, X., Wang, Z., & Chen, Y. (2009). Protection of cerulein-induced pancreatic fibrosis by pancreas-specific expression of Smad7. *Biochimica et Biophysica Acta, 1792*(1), 56-60. doi:10.1016/j.bbadis.2008.10.010

Healy, L., May, G., Gale, K., Grosveld, F., Greaves, M., & Enver, T. (1995). The stem cell antigen CD34 functions as a regulator of hemopoietic cell adhesion. *Proceedings of the National Academy of Sciences of the United States of America, 92*(26), 12240-12244.

Herold, G. (2013). *Innere Medizin*. Köln.

Hingorani, S. R., Harris, W. P., Beck, J. T., Berdov, B. A., Wagner, S. A., Pshevlotsky, E. M., Tjulandin, S. A., Gladkov, O. A., Holcombe, R. F., Korn, R., Raghunand, N., Dychter, S., Jiang, P., Shepard, H. M., & Devoe, C. E. (2016). Phase Ib study of PEGylated recombinant human hyaluronidase and gemcitabine in patients with advanced pancreatic cancer. *Clinical Cancer Research, 22*(12), 2848-2854. doi:10.1158/1078-0432.ccr-15-2010

Horwitz, J. (1992). Alpha-crystallin can function as a molecular chaperone. *Proceedings of the National Academy of Sciences of the United States of America, 89*(21), 10449-10453.

Huang, E. J., & Reichardt, L. F. (2003). Trk receptors: roles in neuronal signal transduction. *Annual Review of Biochemistry, 72*, 609-642. doi:10.1146/annurev.biochem.72.121801.161629

Ito, T. (1951). Cytological studies on stellate cells of Kupffer and fat storing cells in the capillary wall of the human liver. *Acta Anatomica Nipponica, 26*, 42.

Jesnowski, R., Furst, D., Ringel, J., Chen, Y., Schrodel, A., Kleeff, J., Kolb, A., Schareck, W. D., & Lohr, M. (2005). Immortalization of pancreatic stellate cells as an in vitro model of pancreatic fibrosis: deactivation is induced by matrigel and N-acetylcysteine. *Laboratory Investigation, 85*(10), 1276-1291. doi:10.1038/labinvest.3700329

Jones, F. S., & Jones, P. L. (2000). The tenascin family of ECM glycoproteins: structure, function, and regulation during embryonic development and tissue remodeling. *Developmental Dynamics, 218*(2), 235-259. doi:10.1002/(sici)1097-0177(200006)218:2<235::aid-dvdy2>3.0.co;2-g

Kiss, J. Z., & Muller, D. (2001). Contribution of the neural cell adhesion molecule to neuronal and synaptic plasticity. *Reviews in the Neurosciences, 12*(4), 297-310.

Kiss, J. Z., Wang, C., Olive, S., Rougon, G., Lang, J., Baetens, D., Harry, D., & Pralong, W. F. (1994). Activity-dependent mobilization of the adhesion molecule polysialic NCAM to the cell surface of neurons and endocrine cells. *EMBO Journal, 13*(22), 5284-5292.

Klöppel, G. (2013). Type 2 Autoimmune Pancreatitis. *The Pancreapedia: Exocrine Pancreas Knowledge Base.* doi: 10.3998/panc.2013.22.

Klöppel, G., Detlefsen, S., & Feyerabend, B. (2004). Fibrosis of the pancreas: the initial tissue damage and the resulting pattern. *Virchows Archiv, 445*(1), 1-8. doi:10.1007/s00428-004-1021-5

Krizhanovsky, V., Yon, M., Dickins, R. A., Hearn, S., Simon, J., Miething, C., Yee, H., Zender, L., & Lowe, S. W. (2008). Senescence of activated stellate cells limits liver fibrosis. *Cell, 134*(4), 657-667. doi:10.1016/j.cell.2008.06.049

Kwon, S. E., & Chapman, E. R. (2011). Synaptophysin regulates the kinetics of synaptic vesicle endocytosis in central neurons. *Neuron, 70*(5), 847-854. doi:10.1016/j.neuron.2011.04.001

Lamballe, F., Klein, R., & Barbacid, M. (1991). TrkC, a new member of the trk family of tyrosine protein kinases, is a receptor for neurotrophin-3. *Cell, 66*(5), 967-979.

Lankisch, P. G., Lowenfels, A. B., & Maisonneuve, P. (2002). What is the risk of alcoholic pancreatitis in heavy drinkers? *Pancreas, 25*(4), 411-412.

LaRusch, J., & Whitcomb, D. C. (2011). Genetics of pancreatitis. *Current Opinion in Gastroenterology, 27*(5), 467-474. doi:10.1097/MOG.0b013e328349e2f8

Layer, P., Yamamoto, H., Kalthoff, L., Clain, J. E., Bakken, L. J., & DiMagno, E. P. (1994). The different courses of early- and late-onset idiopathic and alcoholic chronic pancreatitis. *Gastroenterology, 107*(5), 1481-1487.

Lazarides, E., & Hubbard, B. D. (1976). Immunological characterization of the subunit of the 100 A filaments from muscle cells. *Proceedings of the National Academy of Sciences of the United States of America, 73*(12), 4344-4348.

Levi-Montalcini, R., & Hamburger, V. (1951). Selective growth stimulating effects of mouse sarcoma on the sensory and sympathetic nervous system of the chick embryo. *Journal of Experimental Zoology, 116*(2), 321-361.

Li, Z., Mericskay, M., Agbulut, O., Butler-Browne, G., Carlsson, L., Thornell, L. E., Babinet, C., & Paulin, D. (1997). Desmin is essential for the tensile strength and integrity of myofibrils but not for myogenic commitment, differentiation, and fusion of skeletal muscle. *Journal of Cell Biology, 139*(1), 129-144.

Ling, S., Feng, T., Jia, K., Tian, Y., & Li, Y. (2014). Inflammation to cancer: The molecular biology in the pancreas (Review). *Oncology Letters, 7*(6), 1747-1754. doi:10.3892/ol.2014.2003

Maher, J. J. (2001). Interactions between hepatic stellate cells and the immune system. *Seminars in Liver Disease, 21*(3), 417-426. doi:10.1055/s-2001-17555

Maulucci, G., Papi, M., Arcovito, G., & De Spirito, M. (2011). The thermal structural transition of alpha-crystallin inhibits the heat induced self-aggregation. *PLOS ONE, 6*(5), e18906. doi:10.1371/journal.pone.0018906

Mederacke, I., Hsu, C. C., Troeger, J. S., Huebener, P., Mu, X., Dapito, D. H., Pradere, J. P., & Schwabe, R. F. (2013). Fate tracing reveals hepatic stellate cells as dominant contributors to liver fibrosis independent of its aetiology. *Nature Communication, 4*, 2823. doi:10.1038/ncomms3823

Mews, P., Phillips, P., Fahmy, R., Korsten, M., Pirola, R., Wilson, J., & Apte, M. (2002). Pancreatic stellate cells respond to inflammatory cytokines: potential role in chronic pancreatitis. *Gut, 50*(4), 535-541.

Midha, S., Khajuria, R., Shastri, S., Kabra, M., & Garg, P. K. (2010). Idiopathic chronic pancreatitis in India: phenotypic characterisation and strong genetic susceptibility due to SPINK1 and CFTR gene mutations. *Gut, 59*(6), 800-807. doi:10.1136/gut.2009.191239

Miyamoto, H., Murakami, T., Tsuchida, K., Sugino, H., Miyake, H., & Tashiro, S. (2004). Tumor-stroma interaction of human pancreatic cancer: acquired resistance to anticancer drugs and proliferation regulation is dependent on extracellular matrix proteins. *Pancreas, 28*(1), 38-44.

Miyata, E., Masuya, M., Yoshida, S., Nakamura, S., Kato, K., Sugimoto, Y., Shibasaki, T., Yamamura, K., Ohishi, K., Nishii, K., Ishikawa, F., Shiku, H., & Katayama, N. (2008). Hematopoietic origin of hepatic stellate cells in the adult liver. *Blood, 111*(4), 2427-2435. doi:10.1182/blood-2007-07-101261

References

Mogilner, A., & Oster, G. (1996). Cell motility driven by actin polymerization. *Biophysical Journal, 71*(6), 3030-3045. doi:10.1016/s0006-3495(96)79496-1

Moore, M. J., Goldstein, D., Hamm, J., Figer, A., Hecht, J. R., Gallinger, S., Au, H. J., Murawa, P., Walde, D., Wolff, R. A., Campos, D., Lim, R., Ding, K., Clark, G., Voskoglou-Nomikos, T., Ptasynski, M., Parulekar, W., & National Cancer Institute of Canada Clinical Trials Group (2007). Erlotinib plus gemcitabine compared with gemcitabine alone in patients with advanced pancreatic cancer: a phase III trial of the National Cancer Institute of Canada Clinical Trials Group. *Journal of Clinical Oncology, 25*(15), 1960-1966. doi:10.1200/JCO.2006.07.9525

Moyano, J. V., Evans, J. R., Chen, F., Lu, M., Werner, M. E., Yehiely, F., Diaz, L. K., Turbin, D., Karaca, G., Wiley, E., Nielsen, T. O., Perou, C. M., & Cryns, V. L. (2006). AlphaB-crystallin is a novel oncoprotein that predicts poor clinical outcome in breast cancer. *Journal of Clinical Investigation, 116*(1), 261-270. doi:10.1172/jci25888

Nielsen, J. S., & McNagny, K. M. (2009). CD34 is a key regulator of hematopoietic stem cell trafficking to bone marrow and mast cell progenitor trafficking in the periphery. *Microcirculation, 16*(6), 487-496. doi:10.1080/10739680902941737

Noronha, M., Bordalo, O., & Dreiling, D. A. (1981). Alcohol and the pancreas. II. Pancreatic morphology of advanced alcoholic pancreatitis. *American Journal of Gastroenterology, 76*(2), 120-124.

Oberstein, P. E., & Olive, K. P. (2013). Pancreatic cancer: why is it so hard to treat? *Therapeutic Advances in Gastroenterology, 6*(4), 321-337. doi:10.1177/1756283X13478680

Okazaki, K., Uchida, K., Sumimoto, K., Mitsuyama, T., Ikeura, T., & Takaoka, M. (2014). Autoimmune pancreatitis: pathogenesis, latest developments and clinical guidance. *Therapeutic Advances in Chronic Disease, 5*(3), 104-111. doi:10.1177/2040622314527120

Olive, K. P., Jacobetz, M. A., Davidson, C. J., Gopinathan, A., McIntyre, D., Honess, D., Madhu, B., Goldgraben, M. A., Caldwell, M. E., Allard, D., Frese, K. K., Denicola, G., Feig, C., Combs, C., Winter, S. P., Ireland-Zecchini, H., Reichelt, S., Howat, W. J., Chang, A., Dhara, M., Wang, L., Rückert, F., Grützmann, R., Pilarsky, C., Izeradjene, K., Hingorani, S. R., Huang, P., Davies, S. E., Plunkett, W., Egorin, M., Hruban, R. H., Whitebread, N., McGovern, K., Adams, J., Iacobuzio-Donahue, C., Griffiths, J., & Tuveson, D. A. (2009). Inhibition of Hedgehog signaling enhances delivery of chemotherapy in a mouse model of pancreatic cancer. *Science, 324*(5933), 1457-1461. doi:10.1126/science.1171362

Omary, M. B., Lugea, A., Lowe, A. W., & Pandol, S. J. (2007). The pancreatic stellate cell: a star on the rise in pancreatic diseases. *Journal of Clinical Investigation, 117*(1), 50-59. doi:10.1172/JCI30082

Ozdemir, B. C., Pentcheva-Hoang, T., Carstens, J. L., Zheng, X., Wu, C. C., Simpson, T. R., Laklai, H., Sugimoto, H., Kahlert, C., Novitskiy, S. V., De Jesus-Acosta, A., Sharma, P., Heidari, P., Mahmood, U., Chin, L., Moses, H. L., Weaver, V. M., Maitra, A., Allison, J. P., LeBleu, V. S., & Kalluri, R. (2014). Depletion of carcinoma-associated fibroblasts and fibrosis induces immunosuppression and accelerates pancreas cancer with reduced survival. *Cancer Cell, 25*(6), 719-734. doi:10.1016/j.ccr.2014.04.005

Panicker, A. K., Buhusi, M., Thelen, K., & Maness, P. F. (2003). Cellular signalling mechanisms of neural cell adhesion molecules. *Frontiers in Bioscience, 8*, d900-911.

Paron, I., Berchtold, S., Vörös, J., Shamarla, M., Erkan, M., Höfler, H., & Esposito, I. (2011). Tenascin-C Enhances Pancreatic Cancer Cell Growth and Motility and Affects Cell Adhesion through Activation of the Integrin Pathway. *PLOS ONE, 6*(6). doi:10.1371/journal.pone.0021684

Paz, Z., & Shoenfeld, Y. (2010). Antifibrosis: to reverse the irreversible. *Clinical Reviews in Allergy & Immunology, 38*(2-3), 276-286. doi:10.1007/s12016-009-8157-7

Phillips, P. A., McCarroll, J. A., Park, S., Wu, M. J., Pirola, R., Korsten, M., Wilson, J. S., & Apte, M. V. (2003). Rat pancreatic stellate cells secrete matrix metalloproteinases: implications for extracellular matrix turnover. *Gut, 52*(2), 275-282.

Phillips, P. A., Yang, L., Shulkes, A., Vonlaufen, A., Poljak, A., Bustamante, S., Warren, A., Xu, Z., Guilhaus, M., Pirola, R., Apte, M. V., & Wilson, J. S. (2010). Pancreatic stellate cells produce acetylcholine and may play a role in pancreatic exocrine secretion. *Proceedings of the National*

Academy of Sciences of the United States of America, 107(40), 17397-17402. doi:10.1073/pnas.1000359107

Pollard, T. D., & Borisy, G. G. (2003). Cellular motility driven by assembly and disassembly of actin filaments. *Cell, 112*(4), 453-465.

Provenzano, P. P., Cuevas, C., Chang, A. E., Goel, V. K., Von Hoff, D. D., & Hingorani, S. R. (2012). Enzymatic targeting of the stroma ablates physical barriers to treatment of pancreatic ductal adenocarcinoma. *Cancer Cell, 21*(3), 418-429. doi:10.1016/j.ccr.2012.01.007

Rabizadeh, S., & Bredesen, D. E. (1994). Is p75NGFR involved in developmental neural cell death? *Developmental Neuroscience, 16*(3-4), 207-211.

Raimondi, S., Lowenfels, A. B., Morselli-Labate, A. M., Maisonneuve, P., & Pezzilli, R. (2010). Pancreatic cancer in chronic pancreatitis; aetiology, incidence, and early detection. *Best Practice & Research Clinical Gastroenterology, 24*(3), 349-358. doi:10.1016/j.bpg.2010.02.007

Ramadori, G., Veit, T., Schwogler, S., Dienes, H. P., Knittel, T., Rieder, H., & Meyer zum Buschenfelde, K. H. (1990). Expression of the gene of the alpha-smooth muscle-actin isoform in rat liver and in rat fat-storing (ITO) cells. *Virchows Archiv. B, Cell Pathology Including Molecular Pathology, 59*(6), 349-357.

Rhim, A. D., Oberstein, P. E., Thomas, D. H., Mirek, E. T., Palermo, C. F., Sastra, S. A., Dekleva, E. N., Saunders, T., Becerra, C. P., Tattersall, I. W., Westphalen, C. B., Kitajewski, J., Fernandez-Barrena, M. G., Fernandez-Zapico, M. E., Iacobuzio-Donahue, C., Olive, K. P., & Stanger, B. Z. (2014). Stromal elements act to restrain, rather than support, pancreatic ductal adenocarcinoma. *Cancer Cell, 25*(6), 735-747. doi:10.1016/j.ccr.2014.04.021

Rockey, D. C., Boyles, J. K., Gabbiani, G., & Friedman, S. L. (1992). Rat hepatic lipocytes express smooth muscle actin upon activation in vivo and in culture. *Journal of Submicroscopic Cytology and Pathology, 24*(2), 193-203.

Ronn, L. C., Hartz, B. P., & Bock, E. (1998). The neural cell adhesion molecule (NCAM) in development and plasticity of the nervous system. *Experimental Gerontology, 33*(7-8), 853-864.

Rosendahl, J., Bödeker, H., Mössner, J., & Teich, N. (2007). Hereditary chronic pancreatitis. *Orphanet Journal Of Rare Diseases, 2*. doi:10.1186/1750-1172-2-1

Rutishauser, U., Gall, W. E., & Edelman, G. M. (1978). Adhesion among neural cells of the chick embryo. IV. Role of the cell surface molecule CAM in the formation of neurite bundles in cultures of spinal ganglia. *Journal of Cell Biology, 79*(2 Pt 1), 382-393.

Rutishauser, U., Hoffman, S., & Edelman, G. M. (1982). Binding properties of a cell adhesion molecule from neural tissue. *Proceedings of the National Academy of Sciences of the United States of America, 79*(2), 685-689.

Sakamoto, Y., Kitajima, Y., Edakuni, G., Sasatomi, E., Mori, M., Kitahara, K., & Miyazaki, K. (2001). Expression of Trk tyrosine kinase receptor is a biologic marker for cell proliferation and perineural invasion of human pancreatic ductal adenocarcinoma. *Oncology Reports, 8*(3), 477-484.

Sarles, H. (1986). Etiopathogenesis and definition of chronic pancreatitis. *Digestive Diseases and Sciences, 31*(9 Suppl), 91S-107S.

Seaberg, R. M., Smukler, S. R., Kieffer, T. J., Enikolopov, G., Asghar, Z., Wheeler, M. B., Korbutt, G., & van der Kooy, D. (2004). Clonal identification of multipotent precursors from adult mouse pancreas that generate neural and pancreatic lineages. *Nature Biotechnology, 22*(9), 1115-1124. doi:10.1038/nbt1004

Sherman, M. H., Yu, R. T., Engle, D. D., Ding, N., Atkins, A. R., Tiriac, H., Collisson, E. A., Connor, F., Van Dyke, T., Kozlov, S., Martin, P., Tseng, T. W., Dawson, D. W., Donahue, T. R., Masamune, A., Shimosegawa, T., Apte, M. V., Wilson, J. S., Ng, B., Lau, S. L., Gunton, J. E., Wahl, G. M., Hunter, T., Drebin, J. A., O'Dwyer, P. J., Liddle, C., Tuveson, D. A., Downes, M., & Evans, R. M. (2014). Vitamin D receptor-mediated stromal reprogramming suppresses pancreatitis and enhances pancreatic cancer therapy. *Cell, 159*(1), 80-93. doi:10.1016/j.cell.2014.08.007

Sicklick, J. K., Choi, S. S., Bustamante, M., McCall, S. J., Pérez, E. H., Huang, J., Li, Y.-X., Rojkind, M., & Diehl, A. M. (2006). Evidence for epithelial-mesenchymal transitions in adult liver cells.

American Journal of Physiology - Gastrointestinal and Liver Physiology, 291(4), G575-583. doi:10.1152/ajpgi.00102.2006

Sidney, L. E., Branch, M. J., Dunphy, S. E., Dua, H. S., & Hopkinson, A. (2014). Concise review: evidence for CD34 as a common marker for diverse progenitors. *Stem Cells, 32*(6), 1380-1389. doi:10.1002/stem.1661

Siegel, R. L., Miller, K. D., & Jemal, A. (2016). Cancer statistics, 2016. *CA: A Cancer Journal for Clinicians, 66*(1), 7-30. doi:10.3322/caac.21332

Sparmann, G., Kruse, M. L., Hofmeister-Mielke, N., Koczan, D., Jaster, R., Liebe, S., Wolff, D., & Emmrich, J. (2010). Bone marrow-derived pancreatic stellate cells in rats. *Cell Research, 20*(3), 288-298. doi:10.1038/cr.2010.10

Stolzenberg-Solomon, R. Z., Cross, A. J., Silverman, D. T., Schairer, C., Thompson, F. E., Kipnis, V., Subar, A. F., Hollenbeck, A., Schatzkin, A., & Sinha, R. (2007). Meat and Meat-Mutagen Intake and Pancreatic Cancer Risk in the NIH-AARP Cohort. *Cancer Epidemiology, Biomarkers & Prevention, 16*(12), 2664-2675. doi:10.1158/1055-9965.EPI-07-0378

Sugimoto, H., Mundel, T. M., Kieran, M. W., & Kalluri, R. (2006). Identification of fibroblast heterogeneity in the tumor microenvironment. *Cancer Biology and Therapy, 5*(12), 1640-1646.

Suskind, D. L., & Muench, M. O. (2004). Searching for common stem cells of the hepatic and hematopoietic systems in the human fetal liver: CD34+ cytokeratin 7/8+ cells express markers for stellate cells. *Journal of Hepatology, 40*(2), 261-268.

Tezel, E., Kawase, Y., Takeda, S., Oshima, K., & Nakao, A. (2001). Expression of neural cell adhesion molecule in pancreatic cancer. *Pancreas, 22*(2), 122-125.

Theocharis, A. D., Tsara, M. E., Papageorgacopoulou, N., Karavias, D. D., & Theocharis, D. A. (2000). Pancreatic carcinoma is characterized by elevated content of hyaluronan and chondroitin sulfate with altered disaccharide composition. *Biochimica et Biophysica Acta, 1502*(2), 201-206.

Thiery, J. P., Brackenbury, R., Rutishauser, U., & Edelman, G. M. (1977). Adhesion among neural cells of the chick embryo. II. Purification and characterization of a cell adhesion molecule from neural retina. *Journal of Biological Chemistry, 252*(19), 6841-6845.

Toole, B. P., & Slomiany, M. G. (2008). Hyaluronan: a constitutive regulator of chemoresistance and malignancy in cancer cells. *Seminars in Cancer Biology, 18*(4), 244-250. doi:10.1016/j.semcancer.2008.03.009

Trim, N., Morgan, S., Evans, M., Issa, R., Fine, D., Afford, S., Wilkins, B., & Iredale, J. (2000). Hepatic stellate cells express the low affinity nerve growth factor receptor p75 and undergo apoptosis in response to nerve growth factor stimulation. *American Journal of Pathology, 156*(4), 1235-1243. doi:10.1016/s0002-9440(10)64994-2

Tuxhorn, J. A., Ayala, G. E., Smith, M. J., Smith, V. C., Dang, T. D., & Rowley, D. R. (2002). Reactive stroma in human prostate cancer: induction of myofibroblast phenotype and extracellular matrix remodeling. *Clinical Cancer Research, 8*(9), 2912-2923.

Ueha, S., Shand, F. H., & Matsushima, K. (2012). Cellular and molecular mechanisms of chronic inflammation-associated organ fibrosis. *Front Immunol, 3*, 71. doi:10.3389/fimmu.2012.00071

Uemori, T., Asada, K., Kato, I., and Harasawa, R. (1992). Amplification of the 16s-23s spacer region in ribosomal-RNA operons of mycoplasmas by the polymerase chain-reaction. *Systematic and Applied Microbiology, 15*, 181-186

Van Rijk, A. F., & Bloemendal, H. (2000). Alpha-B-crystallin in neuropathology. *Ophthalmologica, 214*(1), 7-12. doi:27468

Vaquero, E. C., Edderkaoui, M., Nam, K. J., Gukovsky, I., Pandol, S. J., & Gukovskaya, A. S. (2003). Extracellular matrix proteins protect pancreatic cancer cells from death via mitochondrial and nonmitochondrial pathways. *Gastroenterology, 125*(4), 1188-1202.

Vaquero, E. C., Edderkaoui, M., Pandol, S. J., Gukovsky, I., & Gukovskaya, A. S. (2004). Reactive oxygen species produced by NAD(P)H oxidase inhibit apoptosis in pancreatic cancer cells. *Journal of Biological Chemistry, 279*(33), 34643-34654. doi:10.1074/jbc.M400078200

References

Von Hoff, D. D., Ervin, T., Arena, F. P., Chiorean, E. G., Infante, J., Moore, M., Seay, T., Tjulandin, S. A., Ma, W. W., Saleh, M. N., Harris, M., Reni, M., Dowden, S., Laheru, D., Bahary, N., Ramanathan, R. K., Tabernero, J., Hidalgo, M., Goldstein, D., Van Cutsem, E., Wei, X., Iglesias, J., & Renschler, M. F. (2013). Increased survival in pancreatic cancer with nab-paclitaxel plus gemcitabine. *New England Journal of Medicine, 369*(18), 1691-1703. doi:10.1056/NEJMoa1304369

Vonlaufen, A., Joshi, S., Qu, C., Phillips, P. A., Xu, Z., Parker, N. R., Toi, C. S., Pirola, R. C., Wilson, J. S., Goldstein, D., & Apte, M. V. (2008). Pancreatic stellate cells: partners in crime with pancreatic cancer cells. *Cancer Research, 68*(7), 2085-2093. doi:10.1158/0008-5472.CAN-07-2477

Walker, R. A. (2001). The complexities of breast cancer desmoplasia. *Breast Cancer Research, 3*(3), 143-145. doi:10.1186/bcr287

Wang, L. M., Silva, M. A., D'Costa, Z., Bockelmann, R., Soonawalla, Z., Liu, S., O'Neill, E., Mukherjee, S., McKenna, W. G., Muschel, R., & Fokas, E. (2015). The prognostic role of desmoplastic stroma in pancreatic ductal adenocarcinoma. *Oncotarget, 7*(4), 4183-4194. doi:10.18632/oncotarget.6770

Wang, W., Zhao, H., Zhang, S., Kang, E., Chen, Y., Ni, C., Zhang, S., & Zhu, M. (2009). Patterns of expression and function of the p75(NGFR) protein in pancreatic cancer cells and tumours. *European Journal of Surgical Oncology, 35*(8), 826-832. doi:10.1016/j.ejso.2008.10.013

Watari, N., & Hotta, Y. (1982). Morphological studies on a vitamin A-storing cell and its complex with macrophage observed in mouse pancreatic tissues following excess vitamin A administration. *Okajimas Folia Anatomica Japonica, 58*(4-6), 837-858.

Whatcott, C. J., Diep, C. H., Jiang, P., Watanabe, A., LoBello, J., Sima, C., Hostetter, G., Shepard, H. M., Von Hoff, D. D., & Han, H. (2015). Desmoplasia in primary tumors and metastatic lesions of pancreatic cancer. *Clinical Cancer Research, 21*(15), 3561-3568. doi:10.1158/1078-0432.ccr-14-1051

World Health Organization (1990). Cancer pain relief and palliative care. Report of a WHO Expert Committee. *World Health Organisation Technical Report Series, 804*, 1-75.

Xu, Z., Vonlaufen, A., Phillips, P. A., Fiala-Beer, E., Zhang, X., Yang, L., Biankin, A. V., Goldstein, D., Pirola, R. C., Wilson, J. S., & Apte, M. V. (2010). Role of pancreatic stellate cells in pancreatic cancer metastasis. *American Journal of Pathology, 177*(5), 2585-2596. doi:10.2353/ajpath.2010.090899

Yadav, D., & Lowenfels, A. B. (2013). The epidemiology of pancreatitis and pancreatic cancer. *Gastroenterology, 144*(6), 1252-1261. doi:10.1053/j.gastro.2013.01.068

Yadav, D., & Whitcomb, D. C. (2010). The role of alcohol and smoking in pancreatitis. *Nature Reviews Gastroenterology & Hepatology, 7*(3), 131-145. doi:10.1038/nrgastro.2010.6

Yokoi, Y., Namihisa, T., Kuroda, H., Komatsu, I., Miyazaki, A., Watanabe, S., & Usui, K. (1984). Immunocytochemical detection of desmin in fat-storing cells (Ito cells). *Hepatology, 4*(4), 709-714.

Zhu, Z., Friess, H., diMola, F. F., Zimmermann, A., Graber, H. U., Korc, M., & Buchler, M. W. (1999). Nerve growth factor expression correlates with perineural invasion and pain in human pancreatic cancer. *Journal of Clinical Oncology, 17*(8), 2419-2428.

Zhu, Z. W., Friess, H., Wang, L., Bogardus, T., Korc, M., Kleeff, J., & Buchler, M. W. (2001). Nerve growth factor exerts differential effects on the growth of human pancreatic cancer cells. *Clinical Cancer Research, 7*(1), 105-112.

12 Acknowledgements